STATISTICAL ESTIMATION AND INFERENCE FOR THE ASSOCIATIONS OF MULTIVARIATE RECURRENT EVENT PROCESSES

by

Peilin Chen

A dissertation submitted to the faculty of
The University of North Carolina at Charlotte
in partial fulfillment of the requirements
for the degree of Doctor of Philosophy in
Applied Mathematics

Charlotte

2019

Approved by:

Dr. Yanqing Sun

Dr. Shaoyu Li

Dr. Qingning Zhou

Dr. Aidong Lu

ABSTRACT

PEILIN CHEN. Statistical Estimation and Inference for the Associations of Multivariate Recurrent Event Processes. (Under the direction of DR. YANQING SUN)

In this dissertation, we aim to develop a brand new method with a two-stage procedure to investigate the association between multivariate recurrent event processes.

First, under the assumption of independent censoring, we model each recurrent event process marginally through a mean rate model. There are two popular mean rate assumptions - multiplicative or additive to an unspecified baseline rate function. The robust semi-parametric approaches can be applied to estimate the covariate effects as well as the baseline rate function.

Second, inspired by Kendall's tau, we propose the rate ratio as an association measurement, which is the quotient of two conditional rates - the mean rate of two joint events over the marginal rates, both conditional on the covariates. Utilizing the information from the first stage, an unbiased and consistent estimator of the rate ratio is developed under the Generalized Estimation Equation method. The asymptotic properties of the rate ratio estimators are derived theoretically. Without modeling the joint events directly, the rate ratio can measure the association between two recurrent processes over time.

Since the rate ratio we proposed can be parametric, time and covariate dependent, it has good interpretability. We developed a formal hypothesis testing procedure to validate the parametric assumption of the rate ratio. Simulation studies show it is quite powerful under moderate to a strong association.

The proposed method is applied to the hemodialysis (HEMO) Study. Patients enrolled in HEMO study depend on blood dialysis or transplant surgery to continue their lives and experienced prevalent comorbidities such as diabetes, cardiovascular diseases, and infections. To increase the expected lifespan of patients, it is vital for us to understand the associations among these comorbidities. Our study finds that the dependence between cardiac and infectious hospitalization recurrences for patients in the HEMO study was not constant over time and was significantly positively related to the difference of recurring times. We also find a strong association between past-current cardiac hospitalizations: patients who have experienced cardiac hospitalizations have increased risk of cardiac hospitalizations than those who have not.

ACKNOWLEDGMENTS

I would love to express my sincere gratitude to my advisor Dr.Yanqing Sun, who not only guided me academically but also support me mentally. Her rigid statistical thoughts and passionate, hard-working spirit have highly impressed and influenced me.

Many thanks go to Dr. Shaoyu Li, Dr. Qingning Zhou, and Dr. Aidong Lu for their constructive and thoughtful suggestions as well as serving in the dissertation committee. I am very grateful for the support of all the honorable professors in the Department of Applied Mathematics and Statistics at UNC Charlotte, who provided me such an unforgettable study experience.

I would like to thank the National Institute of Diabetes and Digestive and Kidney Diseases (NIDDK) under National Institutes of Health (NIH) for providing the HEMO dataset. I also benefited from the inspiring discussion with Dr. Guofen Yan at University of Virginia School of Medicine about the HEMO data set. I would also like to thank Dr. Peter Gilbert at Fred Hutchinson Cancer Research Center and the University of Washington for motivating discussions on future applications to the Malaria vaccine study. This research was partially supported by the National Science Foundation grant DMS1513072 and NIAID NIH award number R37AI054165.

My dissertation cannot be completed without the support of my family. Especially my dear husband Alexander Hohl, who always encourages and supports me with his endless love.

TABLE OF CONTENTS

LIST OF FIGURES

LIST OF TABLES

CHAPTER 1: INTRODUCTION

This chapter aims to review related works and introduce the benefits and challenges of estimating the association between multivariate recurrent event processes. The structure of this chapter is as follows. In section 1.1 -1.2 we review the essential background for recurrent event data and popular approaches to estimate the mean event rate or the intensity of Hazard. Literature that focuses on modeling multivariate recurrent event data is discussed in Section 1.3.

1.1 Multivariate recurrent event data

Recurrent events involve repeat occurrences of the same type event over time, whereas a process that generates such data is called recurrent event process. Examples of recurrent events include multiple relapses from remission for leukemia patients, wildfires, and hurricanes. In Recent years, recurrent event data raises in many fields such as public health, business and industry, reliability, the social sciences, and insurance, and keep receiving fast growing attention. For instance, the tumor development time for 48 rats who were injected with a carcinogen represented Gail et al. (1980); the automobile warranty claims data for a specific car model considered by Lawless and Nadeau (1995).

Bivariate or multivariate recurrent event processes are often encountered in longitudinal data studies involving more than one type of event of interest. Unlike Life

Data which is valid to assume events are independent, recurrent event data are usually correlated because they represent the event time measured for the same subject over a time period.

1.2 Modeling recurrent event data

Many statistical methods focus on modeling the rate or intensity of the event recurrence. Aalen (1978) studied the properties of the Nelson-Aalen estimate in the poisson case and Nelson (1988, 1995) proposed the nonparametric estimation of the mean function for general processes. Studies based on poisson and related processes have also been discussed by Cheuvarte (1988), Lawless (1987a,b), Thall (1988), Thall and Lachin (1988), and Lawless and Nadeau (1995).

Early development was extended from survival analysis for the Cox Proportional hazards model (Cox, 1972). Aalen (1980) proposed semiparametric additive regression models for the rate function. Andersen and Gill (1982) introduced the semiparametric regression model for the rate functions and derived the asymptotic results based on the counting process theory.

Pepe and Cai (1993) considered robust methods for parametric or semeparametric regression analysis for the rate and mean functions. Lin et al. (2000) developed the asymptotic properties for the semiparametric regression analysis of Cox proportional mean functions whereas, Martinussen and Scheike (1999) and H Scheike (2002) provide more comprehensive discussion of semiparametric additivie models.

Mean rate models recently became more popular than the intensity based model because they are easier to interpret. Lin et al. (2000) compared the intensity and

rate based model. In their paper, $N^*(t)$ denotes the number of events occur over time $[0, t]$ and $Z(\cdot)$ is a p-dimensional covariate process, whereas $\mathcal{F}_t$ is the history of $\{N^*(s), Z(s) : 0 \leq s \leq t\}$ and $\lambda_Z(t)$ is the intensity of $N^*(t)$ associated with $\mathcal{F}_t$.

The Anderson -Gill intensity model

$$\lambda_Z(t) = e^{\beta_0^T Z(t)} \lambda_0(t) \tag{1.1}$$

is a special case under the assumptions that (a) $E[dN^*(t)|\mathcal{F}_t] = E[dN^*(t)|Z(t)]$ and (b) $E[dN^*(t)|Z(t)] = e^{\beta_0^T Z(t)} \lambda_0(t)dt$.

Lin (2000) proposed a mean rate model

$$E[dN^*(t)|Z(t)] = d\mu_Z(t) \tag{1.2}$$

without assumption (a), it is impractical to verify if the time-varying covariates adequately captured the dependence of the recurrent events. The regression coefficients in the mean event rate model nicely reflect covariate effects on the frequency.

Compared to the Anderson- Gill model (1.1), which is a special case of equation (1.2) by taking

$$d\mu_Z(t) = e^{\beta_0^T Z(t)}\, d\mu_0(t),$$

$$d\mu_0(t) = \lambda_0(t)\, dt,$$

model (1.2) is more versatile.

1.3 Modeling multivariate recurrent event

Here, we introduce the random effect model for multitype events here. for more details consult Cook and Lawless (2007). Let k index the subjects (or clusters) and j index the event type. The event rate at time t for events of type j conditional on subject and type-specific positive random effect r_{kj} is denoted by

$$\lambda_{kj}(t|\mathcal{F}_{kt}, r_{kj}) = \lim_{\Delta t \to 0^+} \frac{Pr(\Delta N_{kj}(t) = 1|\mathcal{F}_{kt}, r_{kj})}{\Delta t} \tag{1.3}$$

$j = 1, 2, ..., J,\ k = 1, 2, ..., K$ where r_{kj} denote the multivariate random effect. With multivariate random effects, it is often assumed that conditional on r_{kj} and $\mathcal{F}_{kt} = \{N_{kj}(s), Z_{kj} : 0 \leq s \leq t\}$, type i and type j event are independent if $i \neq j$, that is

$$\lambda_{kj}(t|\mathcal{F}_{kt}, r_{kj}) = r_{kj}\lambda_{kj}(t|\mathcal{F}_{kt}) \tag{1.4}$$

Random effect models are usually parameterized by assuming r_{kj} comes from an underlying distribution $G(r_k; \phi)$ so that $E(r_{kj}) = 1$, $\text{var}(r_{kj}) = \phi_j$ and $\text{cov}(r_{kj}, r_{ij}) = \phi_{ki}$. The corresponding likelihood conditional on r_{kj} is

$$\prod_{j=1}^{J} \Big\{ \prod_{l=1}^{n_{kj}} r_{kj}\lambda_{kj}(t_{kjl}|\mathcal{F}_{kt}) exp\Big(- r_{kj} \int_0^{\tau_k} \lambda_{kj}(u|\mathcal{F}_{kt})\, du\Big)\Big)\Big\}, \tag{1.5}$$

and the marginal likelihood for individual k as

$$\int \prod_{j=1}^{J} \Big\{ \prod_{l=1}^{n_{kj}} r_{kj}\lambda_{kj}(t_{kjl}|\mathcal{F}_{kt}) exp\Big(- r_{kj} \int_0^{\tau_k} \lambda_{kj}(u|\mathcal{F}_{kt})\, du\Big)\Big)\Big\} dG(r_k; \phi) \tag{1.6}$$

Analogous to the derivation above, we obtain mixed poisson models as well as their overall and marginal likelihood function by letting $\lambda_{kj}(t|\mathcal{F}_{kt}) = \lambda_{kj}(t)$. Related estimation approaches have been developed such as Abu-Libdeh et al. (1990),Lawless

and Nadeau (1995), Ng and Cook (1999) and Chen et.al (2005).

If the covariance or association parameters are not of interest, modeling multivariate recurrent events can be adapted from the analysis of univariate recurrent event process under the working independence assumption. Schaubel and Cai (2004, 2005) developed the estimation and inference for marginal analysis for the cox type model and H Scheike (2002) formulated a similar robust approach for the additive. Both of their work did not incorporate the association structure.

1.4 Study of associations

Association measurement such as Kendall's tau (Oakes, 1989), the correlation coefficient (Clayton, 1978), Cross Ratio (Anderson et al., 1992) and Odds Ratio (H Scheike and Sun, 2012) are designed for Life Time data. These methods only considered the first occurrence of each event type and are not suitable for censored recurrent event data. Most recently (Ning et al., 2015) proposed a time-dependent measure, termed the rate ratio as

$$\rho(s,t) = \frac{\lambda_{1|2}(s|t)}{\lambda_1(s)}, \quad s,t \geq 0, \tag{1.7}$$

where the conditional rate function is defined as

$$\lambda_{1|2}(s|t) = \lim_{\Delta \to 0^+} Pr\{N_1(s+\Delta) - N_1(s) > 0 | N_2(t+\Delta) - N_2(t) > 0\}/\Delta \tag{1.8}$$

to assess the local dependence between two types of recurrent event processes. A composite likelihood procedure was developed for model fitting and estimation. However, the composite likelihood-based method lacks a clear interpretation and is hard to

construct. It is not explicit how the method can be extended to a regression model of recurrent event processes for multiple types of events when the covariates are present. Here, we develop an alternative approach to model the rate ratio parametrically by a score function and provide a model checking procedure to test the parametric form of the rate ratio.

CHAPTER 2: CONDITIONAL RATE RATIO AS ASSOCIATION MEASURE FOR MULTIVARIATE RECURRENT EVENT PROCESSES

2.1 Preliminaries

Let $N^*_{kj}(t)$ be a counting process registering the number of event occurrences by time t for the jth subject in cluster k (or equivalently the type j event for subject k), for $j = 1, 2$ and $k = 1, ..., N$. Suppose $\left(N^*_{k1}(s), N^*_{k2}(t)\right)$ are i.i.d. and let $Z_{kj}(s), Z_{kj}(t)$ represents the associated covariate vector.

The event times for subjects within a cluster, which would be a family or a clinical center, or the sequentially observed times for a subject, are naturally correlated. Therefore we did not put any restraint here. The goal of this project is to characterize and model the association between the occurrences of events.

The marginal conditional rate function for $N^*_{kj}(t)$ is defined by

$$\mu_j(t|z_{kj}) = \lim_{dt\to 0^+} \frac{P\{\, dN^*_{kj}(t) \mid Z_{kj} = z_{kj}\}}{dt}, \quad \text{for} \quad j = 1, 2.$$

Let $\mu_{2|1}(s, t; z_{k1}, z_{k2}) = E\{dN^*_{k2}(t) = 1|dN^*_{k1}(s) = 1, Z_{k1} = z_{k1}, Z_{k2} = z_{k2}\}$. The conditional rate ratio is defined as

$$\rho(s, t; z_{k1}, z_{k2}) = \frac{\mu_{2|1}(s, t; z_{k1}, z_{k2})}{\mu_2(t; z_{k2})}, \qquad \text{for} \quad s, t \geq 0, \tag{2.1}$$

which is a measure of how the occurence of an event for subject 1 (or type 1 event) at time s modifies the likelihood of event occurrence for subject 2 in the same cluster

(or type 2 event of the same subject) at time t. It is natural to see that $\rho(s,t;z_{k1},z_{k2})$ measures the dependence of $\{N^*_{k1}(\cdot),N^*_{k2}(\cdot)\}$ at time (s,t). If the two processes are independent then $\rho(s,t;z_{k1},z_{k2})=1$.

Under the definition of the rate ratio,

$$\begin{aligned}
&E\{dN^*_{k1}(s)dN^*_{k2}(t)\ |Z_{k1}=z_{k1},Z_{k2}=z_{k2}\}\\
&=\rho(s,t;z_{k1},z_{k2})\mu_1(s;z_{k1})\mu_2(t;z_{k2})\,dsdt,\\
&=\rho(s,t;z_{k1},z_{k2})E\{dN^*_{k1}(s)\ |Z_{k1}=z_{k1}\}E\{dN^*_{k2}(t)\ |Z_{k2}=z_{k2}\},
\end{aligned}\tag{2.2}$$

where the marginal conditional mean rates $E\{dN^*_{k1}(s)|Z_{k1}=z_{k1}\}$ and $E\{dN^*_{k2}(t)|Z_{k2}=z_{k2}\}$ can be modeled, for example, by the semiparametric models such as the additive model of H Scheike (2002) or the multiplicative models of Lin et al. (2000). The association measure $\rho(s,t;z_{i1},z_{i2})$ can be modeled through parametric or semiparametric models. Consequently, a two-stage estimating procedure can be adopted.

2.2 Estimation and inference procedures

Let $Y_{kj}(t)=I(C_{kj}\geq t)$ be the at-risk process and $N_{kj}(t)=\int_0^t Y_{kj}(u)dN^*_{kj}(u)$ be the observed recurrent process. Let $\hat{\mu}_1(s;z_{k1})$ and $\hat{\mu}_2(t;z_{k2})$ be the estimates of the marginal rates $\mu_1(s;z_{k1})$ and $\mu_2(t;z_{k2})$, respectively, which is considered as the first-stage estimation. There are a number of options to estimate the conditional rate ratio $\rho(s,t;z_{k1},z_{k2})$ including nonparametric, parametric and semiparametric approaches, each with commonly known strengths and weaknesses. The nonparametric approach may suffer from the *curse-of-dimensionality* while the parametric models can be mis-specified. On the other hand, the association measure based on parametric models

can be more interpretable.

Suppose that $\rho(s,t,\theta;z_{k1},z_{k2})$, $\theta \in \Theta$, is a parametric model for $\rho(s,t;z_{k1},z_{k2})$, where Θ is a dimensional compact set. The estimating equation for θ can be constructed as

$$\begin{aligned}
&U(\theta,\hat{\mu}_1(\cdot;z_{k1}),\hat{\mu}_2(\cdot;z_{k2})) \\
&= \sum_{k=1}^{N}\int_0^\tau\int_0^\tau \frac{\partial\rho(s,t,\theta;z_{k1},z_{k2})}{\partial\theta}\Big\{\, dN_{k1}(s)\, dN_{k2}(t) \\
&\quad - \rho(s,t,\theta;z_{k1},z_{k2})Y_{k1}(s)\hat{\mu}_1(s;z_{k1})Y_{k2}(t)\hat{\mu}_2(t;z_{k2})\, ds\, dt\Big\}. \qquad (2.3)
\end{aligned}$$

Model checking is an essential part of the parametric approach. We proposed a goodness-of-fit procedure to test the parametric form of the rate ratio base on the supremum test statistic given by $T = \sup_{s,t\in[0,\tau]^2}\|V(s,t,\hat{\theta},\hat{\mu}_1(\cdot;z_{k1}),\hat{\mu}_2(\cdot;z_{k2}))\|$, where

$$\begin{aligned}
&V(s,t,\hat{\theta},\hat{\mu}_1(\cdot;z_{k1}),\hat{\mu}_2(\cdot;z_{k2})) \\
&= N^{-1/2}\sum_{k=1}^{N}\int_0^t\int_0^s W_n(u,v)\frac{\partial\rho(u,v,\theta;z_{k1},z_{k2})}{\partial\theta}\Big\{\, dN_{k1}(u)\, dN_{k2}(v) \\
&\quad - \rho(u,v,\theta;z_{k1},z_{k2})Y_{k1}(u)\hat{\mu}_1(u;z_{k1})\, Y_{k2}(v)\hat{\mu}_2(v;z_{k2})\, du\, dv\Big\}, \qquad (2.4)
\end{aligned}$$

$W_n(u,v)$ is prespecified weight function and $\|\cdot\|$ is the Euclidean norm. The critical values can be approximated by implementing the Gaussian multiplier method Gilbert et al. (2017)

CHAPTER 3: ESTIMATION AND INFERENCE OF THE RATE RATIO UNDER THE ADDITIVE MARGINAL MODEL

3.1 Estimation by a two-stage approach

We illustrate the two-stage approach described in Chapter 2 when the marginal conditional rate model is additive. Let $N^*_{kj}(t)$ follows the additive rates model

$$E[dN^*_{kj}(t)|Z_{kj}(t)] = d\mu_j(t|Z_{kj}(t)),$$

$$d\mu_j(t|Z_{kj}(t)) = d\mu_{0j}(t) + \beta_j^T Z_{kj}(t)\, dt, \quad k = 1, ..., N; j = 1, 2 \tag{3.1}$$

where $\mu_{0j}(t)$ is an unspecified baseline rate function and β_j an unknown p-dimensional vector. We consider the parametric approach by assuming $\rho(s, t, \theta; z_{k1}, z_{k2})$, where θ is the q-dimensional parameter of interest.

In the following sections, we first review the estimation procedure of β_j and $\mu_{0j}(t)$ from the additive marginal mean rate model by adapting the method proposed by H Scheike (2002). Then we develop the estimation procedures for parametric rate ratio and investigate its asymptotic properties. A goodness-of-fit procedure is also proposed to test the parametric assumption of the rate ratio. Lastly, we conduct simulations to validate the estimation and inference procedures, with the results presented at the end of this chapter.

3.1.1 Review of the estimation of the marginal model

We define a mean-zero stochastic process as

$$M_{kj}(t,\beta_j) = N_{kj}(t) - \int_0^t Y_{kj}(u)\{d\mu_{0j}(u) + \beta_j^T Z_{kj}(u)\,du\}. \tag{3.2}$$

Following the Generalized Estimating Equations proposed by (GEE; Liang and Zeger 1986), the estimating functions for $\mu_{0j}(t)$ and β_j are as

$$\sum_{k=1}^{N}\int_0^t Y_{kj}(u)\,dM_{kj}(u;\beta_j) = 0, \quad 0 \le t \le \tau. \tag{3.3}$$

$$\sum_{k=1}^{N}\int_0^\tau Y_{kj}(u)Z_{kj}(u)\,dM_{kj}(u;\beta_j) = 0. \tag{3.4}$$

respectively. By solving (3.3), we obtain the $\hat{\mu}_{0j}(t;\beta_j)$ as an estimate of $\mu_{0j}(t)$, where

$$\hat{\mu}_{0j}(t;\beta_j) = \int_0^t \frac{\sum_{k=1}^N[\,dN_{kj}(u) - Y_{kj}(u)\beta_j^T Z_{kj}(u)\,du]}{\sum_{k=1}^N Y_{kj}(u)}. \tag{3.5}$$

With some simple algebra, equation (3.4) is equivalent to

$$L_j(\beta_j) = \sum_{k=1}^{N}\int_0^\tau \{Z_{kj}(u) - \bar{Z}_j(u)\}\Big[\,dN_{kj}(u) - Y_{kj}(u)\beta_j^T Z_{kj}(u)\,du\Big],$$

where $\bar{Z}_j(t) = \frac{\sum_{k=1}^N Z_{kj}(t)Y_{kj}(t)}{\sum_{k=1}^N Y_{kj}(t)}$. Substituting $\hat{\mu}_{0j}(t;\beta_j)$ into equation (3.2) and solve equation (3.4) gives us the estimate of β_j as

$$\hat{\beta}_j = \Big[\sum_{k=1}^{N}\int_0^\tau Y_{kj}(u)\{Z_{kj}(u) - \bar{Z}_j(u)\}^{\otimes 2}\,du\Big]^{-1}\sum_{k=1}^{N}\int_0^\tau \{Z_{kj}(u) - \bar{Z}_j(u)\}\,dN_{kj}(u), \tag{3.6}$$

where $a^{\otimes 2} = aa^T$ for a vector a. Once $\hat{\beta}_j$ is obtained, $\mu_{0j}(t)$ can be estimated by $\hat{\mu}_{0j}(t;\hat{\beta}_j)$ from equation (3.5).

For convenience we summarize the estimation method of the additive marginal model developed by H Scheike (2002) here.

Theorem 3.1 (H Scheike (2002) Theorem A.2.) *Under the regularity (C.1.) - (C.5.),* $\hat{\beta}_j$ *converges almost surely to* β_j*, and has the following asymptotic approximation*

$$\sqrt{N}\{\hat{\beta}_j - \beta_j\} = A_j^{-1} N^{-1/2} \sum_{k=1}^{N} \xi_{kj} + o_p(1)$$

where $\xi_{kj} = \int_0^\tau \{Z_{kj}(u) - \bar{z}_j(u)\}\, dM_{kj}(u, \beta_j)$ *and* $\bar{z}_j(t) = \lim_{N\to\infty} \bar{Z}_j(t)$.

$\sqrt{N}(\hat{\beta}_j - \beta_j)$ *is asymptotically normal with mean zero and has the covariance matrix* $A_j^{-1}\Sigma_j A_j^{-1}$*, where*

$$A_j = E\{\int_0^\tau \{Z_{kj}(u) - \bar{z}_j(\beta_j, u)\}^{\otimes 2}\, du\},$$
$$\Sigma_j = E[\int_0^\tau \{Z_{1j}(u) - \bar{Z}_j(u)\} dM_{1j}(u, \beta_j) \int_0^\tau \{Z_{1j}(v) - \bar{Z}_j(v)\}\, dM_{1j}(v, \beta_j)].$$

The asymptotic covariance matrix can by consistently estimated by $\hat{A}_j^{-1}\hat{\Sigma}_j\hat{A}_j^{-1}$*, with*

$$\hat{A}_j = N^{-1} \sum_{k=1}^{N} \int_0^\tau \{Z_{kj}(u) - \bar{Z}_j(u)\}^{\otimes 2}\, du$$
$$\hat{\Sigma}_j = N^{-1} \sum_{k=1}^{N} \hat{\xi}_{kj}^{\otimes 2}$$
$$\hat{\xi}_{kj} = \int_0^\tau \{Z_{kj}(u) - \bar{Z}_j(u)\}\, d\hat{M}_{kj}(u; \hat{\beta}_j),$$
$$d\hat{M}_{kj}(t; \hat{\beta}_j) = dN_{kj}(t) - Y_{kj}(t)\{\, d\hat{\mu}_{0j}(t) + \hat{\beta}_j^T Z_{kj}(t)\, dt\}.$$

Theorem 3.2 *Under the regularity (C.1)-(C.5),* $\hat{\mu}_{0j}(t)$ *converges almost surely to* $\mu_{0j}(t)$ *uniformly in* $t \in [0, \tau]$. $\sqrt{N}\{\hat{\mu}_{0j}(t) - \mu_{0j}(t)\}$ *converges weakly to a mean-zero*

Gaussian process with covariance function

$$\Gamma_j(s,t) = E[\phi_{kj}(s)\phi_{kj}(t)], \tag{3.7}$$

where

$$\phi_{kj}(t) = \int_0^t \pi_j^{-1}(u) dM_{kj}(u;\beta_j) - H^T(t) A_j^{-1} \int_0^\tau \{Z_{kj}(u) - \bar{z}_j(u)\}\, dM_{kj}(u;\beta_j), \tag{3.8}$$

with $H(t) = \int_0^t \bar{z}_j(u)du$, $\bar{z}_j^T(t) = \lim_{N\to\infty} \bar{Z}_j^T(t)$ *and* $\pi_j(t) = N^{-1} \lim_{N\to\infty} \sum_{k=1}^N Y_{kj}(t)$.

The consistent estimates of $\Gamma(s,t)$ is $\hat{\Gamma}_j(s,t) = N^{-1}\sum_{k=1}^N \hat{\phi}_{kj}(s)\hat{\phi}_{kj}(t)$, where

$$\hat{\phi}_{kj}(t) = \int_0^t \hat{\pi}_j^{-1}(u)\, d\hat{M}_{kj}(u;\hat{\beta}_j) - \hat{H}^T(t)\hat{A}_j^{-1} \int_0^\tau \{Z_{kj}(u) - \bar{Z}_j(u)\}\, d\hat{M}_{kj}(u;\hat{\beta}_j),$$

with $\hat{\pi}_j(t) = N^{-1}\sum_{k=1}^N Y_{kj}(t)$ and $\hat{H}(t) = \int_0^t \bar{Z}_j(u)\, du$.

3.1.2 Estimation of the rate ratio

The rate ratio can be estimated by equation (2.3), the realization of which under model (3.1) is

$$U(\theta, \hat{\beta}_1, \hat{\beta}_2, \hat{\mu}_{01}(\cdot), \hat{\mu}_{02}(\cdot)) = \sum_{k=1}^N U_k(\theta, \hat{\beta}_1, \hat{\beta}_2, \hat{\mu}_{01}(\cdot), \hat{\mu}_{02}(\cdot)), \tag{3.9}$$

where

$$U_k(\theta, \hat{\beta}_1, \hat{\beta}_2, \hat{\mu}_{01}(\cdot), \hat{\mu}_{02}(\cdot)) = \int_0^\tau \int_0^\tau \frac{\partial \rho(s,t,\theta; Z_{k1}, Z_{k2})}{\partial \theta} \Big\{ dN_{k1}(s)\, dN_{k2}(t)$$
$$- \rho(s,t,\theta; Z_{k1}, Z_{k2}) Y_{k1}(s)[\, d\hat{\mu}_{01}(s) + \hat{\beta}_1^T Z_{k1}(s)\, ds] Y_{k2}(t)[\, d\hat{\mu}_{02}(t) + \hat{\beta}_2^T Z_{k2}(t)\, dt\,] \Big\}.$$

Denote $\hat{\theta}$ the solution to $U(\theta, \hat{\beta}_1, \hat{\beta}_2, \hat{\mu}_{01}(\cdot), \hat{\mu}_{02}(\cdot)) = 0$. We investigate the asymptotic properties of $U(\hat{\theta}, \hat{\beta}_1, \hat{\beta}_2, \hat{\mu}_{01}(\cdot), \hat{\mu}_{02}(\cdot))$ and $\hat{\theta}$ in Theorem 3.3 and 3.4 below.

Theorem 3.3 *$N^{-1/2}\{U(\theta,\hat{\beta}_1,\hat{\beta}_2,\hat{\mu}_{01}(\cdot),\hat{\mu}_{02}(\cdot))-U(\theta,\beta_1,\beta_2,\mu_{01}(\cdot),\mu_{02}(\cdot))\}$ converges to a mean-zero Gaussian process, with covariance*

$$\Omega=\lim_{N\to\infty}N^{-1}\sum_{k=1}^{N}\left\{h_{1,N}\xi_{k1}A_1^{-1}+g_{1,N,k}+h_{2,N}\xi_{k2}A_2^{-1}+g_{2,N,k}\right\}^{\otimes 2}.$$

The consistent estimate of Ω is

$$\hat{\Omega}=N^{-1}\sum_{k=1}^{N}\left\{\hat{h}_{1,N}\hat{\xi}_{k1}\hat{A}_1^{-1}+\hat{g}_{1,N,k}+\hat{h}_{2,N}\hat{\xi}_{k2}\hat{A}_2^{-1}+\hat{g}_{2,N,k}\right\}^{\otimes 2},$$

where $\hat{h}_{j,N}$, $\hat{\xi}_{kj}$, $\hat{g}_{j,N,k}(s,t)$ $(j=1,2)$ are shown in the appendix B.

Theorem 3.4 *$\sqrt{N}(\hat{\theta}-\theta)$ converges to a mean-zero Gaussian process and has the following approximation based on Taylor expansion that*

$$\sqrt{N}(\hat{\theta}-\theta)=N^{-1/2}\{\mathcal{I}(\theta)\}^{-1}\sum_{k=1}^{N}W_k(\theta)+o_p(1), \tag{3.10}$$

for which the formulae for $\mathcal{I}(\theta)$ and $W_k(\theta)$ are given in the appendix B.

The variance of $\sqrt{N}(\hat{\theta}-\theta)$ can be estimated by $\hat{\Phi}=N^{-1}(\hat{\mathcal{I}})^{-1}\sum_{k=1}^{N}(\hat{W}_k)^{\otimes 2}(\hat{\mathcal{I}}^T)^{-1}$, where $\hat{\mathcal{I}}$ and $\hat{W}_k$ are the empirical counterparts of $\mathcal{I}(\theta)$ and $W_k(\theta)$.

3.1.3 Simulation study

Before we conduct finite sample studies to investigate performance of the proposed estimation procedure, we want to show some examples that motivate us to model the rate ratio parametrically.

Proposition 1 *Under shared frailty model*

$$d\mu_j(t)=R_k\cdot\{d\mu_{0j}(t)+\beta_j^T Z_{kj}(t)\,dt\}, \tag{3.11}$$

where R_k is identically and independently distributed positive random variable, with $E(R_k)=\mu$ and $var(R_k)=\sigma^2$. The rate ratio only depends on the variance of frailty random variable and can be explicitly expressed as

$$\rho(s,t,\theta) = \rho = 1 + \frac{\sigma^2}{\mu^2}. \tag{3.12}$$

Proposition 2 *Let τ be the maximum observation time and c_0 lies in the middle of 0 and τ. Suppose the shared frailty mean rate model for $N^*_{kj}(t)$ is*

$$d\mu_j(t\,|Z_{kj}(t), R_k(t)) = R_k(t)\{d\mu_{0j}(t) + \beta_j^T Z_{kj}(t)\,dt\} \tag{3.13}$$

where $R_k(t) = I(t \le c_0)R_{k0} + I(t > c_0)R_{k1}$.

Before we exam the rate ratio in this time varying additive mean rate model, we introduce the shifted gamma distribution. Define the probability density function of the shifted Gamma(a,b,δ) as

$$f(x|a,b,\delta) = \frac{1}{\Gamma(a)b^a}(x-\delta)^{a-1}e^{\frac{-(x-\delta)}{b}}, x \in [\delta,\infty), \quad \delta \ge 0 \tag{3.14}$$

for $x \in [\delta,\infty)$, $\delta \ge 0$ and here $\Gamma(\cdot)$ denotes the Gamma function. Let X come from shifted Gamma(a,b,δ) then we have $E(X)=a\cdot b+\delta$ and $var(X)=a\cdot b^2$. As we can see when $\delta = 0$, the shifted Gamma distribution is reduced to the gamma distribution.

If R_{k0} and R_{k1} are independently from the corresponding shifted gamma distribution

(a_0, b_0, δ_0) and (a_1, b_1, δ_1), then the rate ratio is piecewise constant:

$$\rho(\theta, s \le c_0, t \le c_0) = 1 + \frac{a_0 b_0^2}{(a_0 b_0 + \delta_0)^2},$$
$$\rho(\theta, s > c_0, t > c_0) = 1 + \frac{a_1 b_1^2}{(a_1 b_1 + \delta_1)^2},$$
$$\rho(\theta, s \le c_0, t > c_0) = \rho(\theta, s > c_0, t \le c_0) = 1. \tag{3.15}$$

Proposition 3 *For $j = 1, 2$, denote $\tilde{\lambda}_j(t|z_j)$ the event rate of nonhomogeneous Possion Process $\tilde{N}_j(t)$. Let $N_0(t)$ be a nonhomogeneous Poisson process with event rate $\lambda_0(t|z_j)$. Assume that $\tilde{N}_j(t)$ and $N_0(t)$ be mutually independent, i.e. for any $u_1, u_2..., u_n$, the random vectors $\{\tilde{N}_1(u_1), \tilde{N}_1(u_1), , ..., \tilde{N}_1(u_n)\}$, $\{\tilde{N}_2(u_1), ..., \tilde{N}_2(u_n)\}$ and $\{N_0(u_1), ..., N_0(u_n)\}$ are independent to each other.*

Let $N_j(t) = \tilde{N}_j(t) + N_0(t)$ for $j = 1, 2$. Since $N_j(t)$ is the summation of two independent Poisson processes, $N_j(t)$ is also a Poisson process with rate $\lambda_j(t\,|z_j) = \tilde{\lambda_j}(t\,|z_j) + \lambda_0(t\,|z_j)$.

Let $\rho_0(s, t, \theta|z_1, z_2)$ and the $\rho(s, t, \theta|\, z_1, z_2)$ be the rate ratio of $\{N_0(s), N_0(t)\}$ and $\{N_1(s)\}, N_2(t)\}$ for $s, t \ge 0$, then we have $\rho(\theta, s, t|\, z_1, z_2)$

$$\rho(\theta, s, t; z_1, z_2) = 1 + \frac{\{\rho_0(\theta, s, t; z_1, z_2) - 1\}\lambda_0(s|z_1)\lambda_0(t|z_2)}{\lambda_1(s\,|z_1)\lambda_2(t\,|z_2)}. \tag{3.16}$$

The association is introduced by the shared counting process $N_0(s)$ and $N_0(t)$. If $\rho_0(\theta, s, t; z_1, z_2) = 1$ then $\rho(\theta, s, t; z_1, z_2) = 1$, thus if $\{N_0(s), N_0(t)\}$ is independent so is $\{N_1(s), N_2(t)\}$.

We conduct simulation studies to evaluate the finite sample properties based on the guidance of Proposition 1, 2 and 3. Let $\tau = 5$, C_{kj} follows a uniform distribution on [0,τ], and covariates Z_{kj} are from a uniform$[1, 2]$ for $j = 1, 2$. The observed events for the jth type in cluster k would be all the event times that are smaller than C_{kj}. We consider I, II, III scenarios where the rate ratio is constant, time varying, and covariate dependent. Scenario IV is an extension from II and III, with the rate ratio depending on event time and covariates.

(I) Constant $\rho(s, t, \theta) = \theta_0$

Recall the shared frailty model in equation (3.11)

$$d\mu_j(t\,|R_k, Z_{kj}(t)) = R_k \cdot \{\, d\mu_{0j}(t) + \beta_j Z_{kj}(t)\} \quad \text{for} \quad j = 1, 2.$$

Let R_k follows i.i.d Gamma(a, b) with $\mathrm{E}(R_k) = ab$ and $\mathrm{var}(R_k) = ab^2$. By proposition 1, $\rho(s, t, \theta) = \theta_0$ where $\theta_0 = 1 + ab^2/(ab)^2 = 1 + 1/a$.

Let $\beta_1 = 0.5$, $\beta_2 = 1$, $\mu_{01}(t) = \mu_{02}(t) = 0.25t, 0.5t, t$. The averaged observed type 1(2) events after right censoring are 2.50(4.37), 3.13(5.02) and 4.37(6.26) respectively. To variate the strength of the association, we take R_k from the pairs of (a, b) equal to (4, 0.25), (2, 0.5), (1.33, 0.75) and (1, 1) so that θ_0 = 1.25, 1.5, 1.75 and 2 correspondingly.

By taking the expectation of R_k in equation (3.11), the mean event rate still follows model (3.1). In the first-stage, $\hat{\beta}_j$, $\hat{\mu}_{0j}(t)$ are evaluated by equation (3.6) and (3.5). In general, the estimates of β_{0j} and $\mu_{0j}(t)$ agree with the discussions in literatures. We show part of the numerical results for the first-stage estimates in Table 1, from which

it is observed that $\hat{\beta}_1$ and $\hat{\beta}_2$ converges to the true values $\beta_1 = 0.5$ and $\beta_2 = 1$. The mean Estimated Standard Error of β_j (ESE) is very close to the Sample Standard Error of Estimates (SSE) and Empirical Coverage Probability (CP) is around to 0.95. We will skip the marginal model simulation result and focus on the estimation of the parameters in the rate ratio in the studies.

In the second-stage, $\hat{\beta}_j$, $\hat{\mu}_{0j}$ for $j = 1, 2$ are plugged into equation (3.9) and the root is derived by the Newton-Raphson method. Convergence is achieved at the ith iteration if $\frac{\theta^{(i)} - \theta^{(i-1)}}{\theta^{(i-1)}} < 10^{-5}$ or $i > 50$. In Table 2, the Bias is negligible for all the cases and the Standard Error of Estimates (SEE) is close to the Estimated Standard Error (ESE). The 95% coverage probability (CP) is also around 0.95. Both SEE and ESE decrease with a larger sample size. It is also observed that the SEE and ESE increase when the association between the two processes becomes stronger (i.e. θ_0 is larger) and such increment is slowly reduced by increasing the sample size. A possible interpretation is that for bivariate recurrent event processes, given the observed dataset with a fixed sample size, less information would be obtained if the two events are highly related. We might be able to adapt a weight function in the estimation equation (3.9) to improve the efficiency of this estimating procedure.

(II) Time dependent rate ratio $\rho(\theta, s, t) = 1 + \theta_0 \times (-0.15t + 0.9)(-0.15s + 0.9)$

For the j th individual in the kth cluster, let

$$N_{kj}(t) = \tilde{N}_{kj}(t) + N_{k0}(t), \quad \text{for} \quad j = 1, 2 \tag{3.17}$$

where $\{\tilde{N}_{k1}(\cdot), \tilde{N}_{k2}(\cdot), N_{k0}(\cdot)\}$ are independent Poisson process, conditional on co-

variates and frailty. Consider $E\{\, dN_{k0}(t) \,|\, z_j, R_k\} = R_k \cdot \lambda_{k0}(t|\, Z_{kj} = z_j)dt$, where $\lambda_{k0}(t|\, Z_{kj})\, dt = d\mu_{0j}(t) + \beta_{0j} Z_{kj}$, and R_k is i.i.d from a positive distribution with E(R_k)=μ_0 and var(R_k)=σ_0^2. By Proposition 1, the rate ratio of $\{N_{k0}(s), N_{k0}(t)\}$ is $\rho_0(s, t, \theta|z_1, z_2) = 1 + \sigma_0^2/\mu_0^2$.

Denote the mean rate for $\tilde{N}_{kj}(t)$ as $\tilde{\lambda}_{kj}(t|\, Z_{kj} = z_{kj})$ (for $j = 1, 2$ and $t \in (0, \tau)$) and assume $\tilde{\lambda}_{kj}(t|\, Z_{kj} = z_{kj}) = \{(0.15t + 0.9)^{-1} - 1\}\lambda_{k0}(t|\, Z_{kj} = z_{kj})$, By equation (3.17), the mean rate of $N_{kj}(t)$ is $\lambda_{kj}(t|z_{kj}) = (0.15t + 0.9)^{-1}\lambda_{k0}(t\,|z_{kj})$.

Following Proposition 3, the rate ratio of $\{N_{k1}(s), N_{k2}(t)\}$ can be expressed as

$$\rho(\theta, s, t) = 1 + \theta_0 \times (-0.15t + 0.9)(-0.15s + 0.9), \tag{3.18}$$

where $\theta_0 = \frac{\sigma_0^2}{\mu_0^2}$. Let R_k follows i.i.d Gamma(a, b) so that $\mu_0 = ab$ and $\sigma_0 = ab^2$. We take (a, b) as $(4, 0.25)$,$(2, 0.5)$, $(1, 1)$ and $(0.635, 1.6)$ and therefore the corresponding θ_0 are 0.25, 0.5, 1 and 1.6. To generate moderate and frequent event observations, we take $\beta_{01} = \beta_{02} = 0$ and set $\mu_{01}(t) = \mu_{02}(t)$ to be $0.25t$, $0.5t$, $0.75t$ and t, which gives us averaged events count as 2.13, 4.17, 5.21 and 6.39 respectively.

The Bias of the estimates (Bias), the Estimated Standard Error (ESE), the Sample Standard Error of Estimates (SSE) and 95% Empirical Coverage Probability (CP) are calculated from 1000 simulated datasets with sample size $N = 200, 500, 800$. The bias of θ_0 is low, the ESE is close to the SSE and the coverage probability is around 0.95. When the association between $N_{k1}(\cdot)$ and $N_{k2}(\cdot)$ become stronger, the ESE and SSE both increase, which is similar to the scenario I. For details, see Table 3.

(III) Covariate dependent rate ratio $\rho(\theta; Z_k) = \theta_1 I(Z_k = 1) + \theta_2 I(Z_k = 0)$

Let Z_k be a cluster level binary covariate. Assume the counting process $N^*_{kj}(t)$ follows the shared frailty model

$$E[dN^*_{kj}(t)|Z_k, R_k] = R_k\{\, d\mu_{0j}(t) + \beta_j Z_k(t)\, dt\},$$

where $\mathrm{E}[R_k|Z_k] = \mu(Z_k)$ and $\mathrm{var}[R_k|Z_k] = \sigma^2(Z_k)$. Following Proposition 1, we obtain

$$\rho(\theta; Z_k) = 1 + \frac{\sigma^2(Z_k)}{\mu^2(Z_k)}. \tag{3.19}$$

We take $\beta_1 = 0.5$, $\beta_2 = 1$, $\mu_{01}(t) = \mu_{02}(t) = 0.25t, 0.5t, 0.75t$. Z_k comes from Bernoulli($p = 0.5$), so that Z_k has equal chance to be 0 or 1. We generate R_k from Gamma$(4, 0.25)$ and Gamma$(1.33, 0.75)$ for $Z_k = 1$ and $Z_k = 0$ respectively.

In equation (3.19), $\rho(\theta; Z_k = 1) = 1.25$, $\rho(\theta; Z_k = 0) = 1.75$ and therefore we rewrite the rate ratio as

$$\rho(\theta; Z_k) = \theta_1 I(Z_k = 1) + \theta_2 I(Z_k = 0), \tag{3.20}$$

with $\theta_1 = 1.25$ and $\theta_2 = 1.75$. Under this setting, the averaged observed type 1(2) events after right censoring are 2.50(4.37), 3.13(5.02) and 4.37(6.26).

(IV) Time and covariate dependent rate ratio

Consider the bivariate counting processes $\{N_{k1}(\cdot), N_{k2}(\cdot)\}$ constructed by the summation of two independent Poisson processes $\widetilde{N}_{kj}(\cdot)$ and $N_{k0}(\cdot)$, as described in Proposition 3. Denote $\rho_0(\theta, s, t; z_1, z_2)$ and $\rho(\theta, s, t; z_1, z_2)$ be the rate ratio of $(N_{k0}(t), N_{k0}(s))$ and $(\{N_{k1}(s), N_{k2}(t)\})$ respectively. Following from Proposition 3, we have

$$\rho(\theta, s, t; z_1, z_2) = 1 + \frac{\{\rho_0(\theta, s, t; z_1, z_2) - 1\}\lambda_0(s; z_1)\lambda_0(t; z_2)}{\lambda_1(s\,; z_1)\lambda_2(t\,|z_2)},$$

where $\lambda_{k0}(s|z_1)\,ds$, $\lambda_j(s|z_1)\,ds$ are the conditional mean rate of $N_{k0}(s)$ and $N_{k1}(s)$, whereas $\lambda_{k0}(t|z_2)\,ds$, $\lambda_s(t|z_1)\,dt$ are that of $N_{k0}(t)$ and $N_{k2}(t)$.

Let $\lambda_{k0}(t|Z_k, R_k) = R_k(0.25+\beta_{0j}Z_k)$ and $\widetilde{\lambda}_{kj}(t) = 0.5t$, where R_k is generated from i.i.d Gamma(a, b) and Z_k is from Bernoulli(0.5). Consider (a, b) equal to (4, 0.25), (2, 0.5) and (1.33, 0.75) such that $\rho_0(\theta, s, t|z_1, z_2) = 1.25, 1.5$ and 1.75. Let $\beta_{01} = 0.1$, $\beta_{02} = 0.2$. The rate ratio of $N_{k1}(s)$ and $N_{k2}(t)$ is time-varying and dependent on the covariate Z_{kj}, where

$$\rho(\theta, s, t|Z_k) = 1 + \theta_1 \frac{(0.25 + 0.1Z_k)(0.25 + 0.2Z_k)}{(0.5t + 0.25 + 0.1Z_k)(0.5s + 0.25 + 0.2Z_k)}, \tag{3.21}$$

with $\theta_1 = \frac{\sigma^2}{\mu^2} = 0.25, 0.5, 0.75$ and 1.

To evaluate the influence of observed event frequency on the estimating procedure, we modified $\lambda_{k0}(t|Z_k, R_k) = R_k(0.5 + \beta_{0j}Z_k)$, whereas the rate ratio follows

$$\rho(\theta, s, t|Z_k) = 1 + \theta_2 \frac{(0.5 + 0.1Z_k)(0.5 + 0.2Z_k)}{(0.5t + 0.5 + 0.1Z_k)(0.5s + 0.5 + 0.2Z_k)}. \tag{3.22}$$

We obtained $\hat{\theta}_1$ and $\hat{\theta}_2$ from the two-stage estimation procedure. Table 5 has the simulation result, from which we observe the bias is going to zero and the ESE is getting close to SSE as sample size increase. The coverage probability is getting close to 0.95 for both θ_1 and θ_2. Each entry is based on 1000 simulated datasets.

Table 1: Scenario I - $\rho(s,t,\theta) = \theta_0$. Estimation of coefficients in the marginal additive model. The Bias, SEE(Standard Error of Estimates) ,ESE (Estimated Standard Errors) and the Empirical Coverage Probability of 95% confidence interval (CP) of (β_{01}, β_{02}). Each entry is based on 1000 simulations.

$\mu_{0j}(t)$	θ_0	N	Bias(β_{01}, β_{02})	SEE (β_{01}, β_{02})	ESE (β_{01}, β_{02})	CP(β_{01}, β_{02})
$0.75t$	1	200	(0.0097, 0.0127)	(0.1871, 0.2223)	(0.1902, 0.2335)	(0.9560, 0.9590)
		500	(0.0076, -0.0051)	(0.1183, 0.1464)	(0.1202, 0.1466)	(0.9500, 0.9500)
		800	(-0.0001, -0.0028)	(0.0944, 0.1159)	(0.0947, 0.1163)	(0.9540, 0.9460)
	1.25	200	(-0.0126, 0.0145)	(0.2938, 0.3876)	(0.2830, 0.3936)	(0.9450, 0.9580)
		500	(-0.0005, 0.0057)	(0.1746 0.2579)	(0.1803, 0.2497)	(0.9600, 0.9470)
		800	(0.0040, 0.0025)	(0.1478, 0.1976)	(0.1428, 0.1984)	(0.9450, 0.9540)
	1.5	200	(0.0106, 0.0110)	(0.3490, 0.5128)	(0.3524, 0.5073)	(0.9560, 0.9440)
		500	(0.0109, 0.0108)	(0.2337, 0.3232)	(0.2244, 0.3217)	(0.9440, 0.9610)
		800	(0.0039, 0.0254)	(0.1826, 0.263)1	(0.1773, 0.2550)	(0.9470, 0.9460)
	1.75	200	(0.0027, -0.0388)	(0.4227, 0.6018)	(0.4096, 0.5902)	(0.9540, 0.9490)
		500	(0.0067, -0.0002)	(0.2623, 0.3876)	(0.2597, 0.3790)	(0.9570, 0.9480)
		800	(-0.0019, 0.0056)	(0.2042, 0.2906)	(0.2072, 0.3024	(0.9470, 0.9580)
t	1	200	(0.0091, -0.0117)	(0.2041, 0.2467)	(0.2048, 0.2433)	(0.9500, 0.9580)
		500	(-0.0087, -0.0027)	(0.1265, 0.1538)	(0.1293, 0.1545)	(0.9480, 0.9530)
		800	(0.0050, -0.0011)	(0.1009, 0.1246)	(0.1022, 0.1223)	(0.9500, 0.9600)
	1.25	200	(-0.0110, -0.0028)	(0.3289, 0.4274)	(0.3202, 0.4282)	(0.9410, 0.9560)
		500	(-0.0039, -0.0064)	(0.2022, 0.2755)	(0.2037, 0.2730)	(0.9460, 0.9550)
		800	(-0.0013, 0.0005)	(0.1656, 0.2209)	(0.1611, 0.2164)	(0.9460, 0.9530)
	1.5	200	(0.0295, -0.0237)	(0.4212, 0.5470)	(0.4010, 0.5476)	(0.9520, 0.9530)
		500	(0.0150, 0.0041)	(0.2649, 0.3599)	(0.2566, 0.3519)	(0.9510, 0.9450)
		800	(-0.0039, -0.0123)	(0.2067, 0.2745)	(0.2029, 0.2793)	(0.9540, 0.9580)
	1.75	200	(0.0181, 0.0012)	(0.4745, 0.6696)	(0.4692, 0.6541)	(0.9480, 0.9500)
		500	(0.0093, 0.0208)	(0.3089, 0.4311)	(0.3007, 0.4203)	(0.9500, 0.9450)
		800	(0.0005, -0.0082)	(0.2418, 0.3357)	(0.2381, 0.3333)	(0.9570, 0.9530)

Table 2: Scenario I - Estimation of $\rho(s,t,\theta)=\theta_0$. Bias, SEE(Standard Error of Estimates) , ESE(Estimated Standard Error), CP (95% Coverage Probability) lists. Each entry is based on 1000 simulated datasets. The marginal models are additive and association come from the shared random effect.

$\mu_{0j}(t)$	θ_0	N	Bias	SEE	ESE	CP	$\mu_{0j}(t)$	θ_0	N	Bias	SEE	ESE	CP
$0.25t$	1.25	200	-0.0031	0.0845	0.0818	0.9350	$0.75t$	1.25	200	-0.0011	0.0770	0.0726	0.9330
		500	0.0005	0.0567	0.0536	0.9420			500	-0.0011	0.0520	0.0476	0.9300
		800	0.0001	0.0432	0.0428	0.9520			800	-0.0001	0.0395	0.0385	0.9420
	1.50	200	-0.0131	0.1392	0.1248	0.8960		1.50	200	-0.0079	0.1280	0.1179	0.8970
		500	-0.0024	0.0896	0.0849	0.9200			500	-0.0025	0.0851	0.0791	0.9290
		800	-0.0045	0.0672	0.068	0.9500			800	-0.0041	0.0667	0.0636	0.9310
	1.75	200	-0.0160	0.1926	0.1715	0.8930		1.75	200	-0.0126	0.1978	0.1659	0.8850
		500	0.0006	0.1311	0.1212	0.9130			500	-0.0082	0.1212	0.1121	0.9160
		800	-0.0049	0.1031	0.0962	0.9290			800	.-0.0018	0.0954	0.0914	0.9260
$0.5t$	1.25	200	-0.0016	0.0858	0.0762	0.9090	t	1.25	200	-0.0057	0.0747	0.0699	0.9230
		500	-0.0019	0.0517	0.0500	0.9370			500	0.0003	0.0472	0.0465	0.9410
		800	-0.0009	0.0402	0.0402	0.9460			800	-0.0012	0.0379	0.0374	0.9460
	1.5	200	-0.0138	0.1361	0.1192	0.8830		1.50	200	-0.0125	0.1235	0.1127	0.9130
		500	0.0002	0.0862	0.0827	0.9310			500	-0.0026	0.0847	0.0777	0.9050
		800	-0.0014	0.0672	0.0652	0.9290			800	-0.0052	0.0658	0.0621	0.9210
	1.75	200	-0.0101	0.1916	0.1656	0.8840		1.75	200	-0.0154	0.1742	0.1577	0.8840
		500	0.0015	0.1224	0.1172	0.9160			500	0.0031	0.1207	0.1135	0.9250
		800	-0.0047	0.1019	0.0933	0.9270			800	0.0018	0.0980	0.0912	0.9300

Table 3: Scenario II - Estimation of $\rho(s,t,\theta) = 1 + \theta_0(-0.15t + 0.9)(-0.15s + 0.9)$. Bias, SEE (Standard Error of Estimates), ESE (Estimated Standard Error), CP of the parameter θ_0 in $\rho(s,t,\theta)$. Each entry is based on 1000 simulations with correctly specified marginals and rate ratio form.

$\mu_{0j}(t)$	θ_0	N	Bias	SEE	ESE	CP	$\mu_{0j}(t)$	θ_0	N	Bias	SEE	ESE	CP
$0.5t$	0.25	200	0.0114	0.1793	0.1697	0.9410	t	0.25	200	-0.0073	0.1205	0.1207	0.9450
		500	0.0002	0.1134	0.1089	0.9440			500	0.0029	0.0760	0.0781	0.9520
		800	0.0001	0.0891	0.0860	0.9520			800	0.0007	0.0613	0.0620	0.9490
	0.50	200	-0.0053	0.2325	0.2162	0.9260		0.5	200	-0.0047	0.1832	0.1698	0.9160
		500	-0.0038	0.1427	0.1406	0.9310			500	-0.0036	0.1124	0.1099	0.9310
		800	-0.0026	0.1156	0.1118	0.9360			800	-0.0038	0.0904	0.0881	0.9290
	1	200	-0.0096	0.3406	0.3295	0.9170		1	200	-0.0193	0.2988	0.2811	0.8960
		500	-0.0066	0.2120	0.2180	0.9370			500	-0.0048	0.1779	0.1890	0.9490
		800	0.0007	0.1697	0.1765	0.9440			800	-0.0031	0.1472	0.1518	0.9420
	1.6	200	-0.0112	0.4884	0.4857	0.9150		1.6	200	-0.0101	0.4317	0.4388	0.9060
		500	-0.0120	0.3338	0.3325	0.9140			500	-0.0065	0.3049	0.3030	0.9130
		800	-0.0073	0.2697	0.2685	0.9240			800	-0.0085	0.2427	0.2452	0.9370
	2	200	-0.0324	0.6739	0.6011	0.8740		2	200	-0.0270	0.6112	0.5526	0.8780
		500	-0.0166	0.4226	0.4164	0.9040			500	-0.0249	0.3853	0.3821	0.9100
		800	-0.0059	0.3300	0.3431	0.9300			800	-0.0053	0.3039	0.3198	0.9390

Table 4: Scenario III - Estimation of θ's in $\rho(\theta; Z_k) = \theta_1 I(Z_k = 1) + \theta_2 I(Z_k = 0)$, with true value $\theta_1 = 1.25$ and $\theta_2 = 1.75$. Summary of Bias, SEE (Standard Error of Estimates), ESE (Estimated Standard Error), CP. Each entry is based on 1000 simulations with correctly specified marginals and rate ratio form.

		θ_1				θ_2			
$\mu_{0j}(t)$	N	Bias	SEE	ESE	CP	Bias	SSE	ESE	CP
$0.25t$	200	-0.0094	0.1284	0.1177	0.9250	-0.0012	0.4543	0.3610	0.8860
	500	-0.0046	0.0817	0.0776	0.9280	-0.0033	0.2675	0.2476	0.9190
	800	-0.0028	0.0653	0.0626	0.9430	-0.0043	0.2218	0.2016	0.9130
	1100	0.0010	0.0561	0.0545	0.9510	0.0151	0.1906	0.1798	0.9380
$0.50t$	200	-0.0055	0.1193	0.1075	0.9190	-0.0160	0.3267	0.2703	0.8720
	500	-0.0046	0.0765	0.0715	0.9320	-0.0226	0.2118	0.1873	0.8950
	800	-0.0013	0.0597	0.0583	0.9530	-0.0081	0.1674	0.1542	0.9180
	1100	-0.0003	0.0494	0.0502	0.9640	-0.0066	0.1408	0.1355	0.9240
$0.75t$	500	-0.0103	0.1131	0.1011	0.8960	-0.0182	0.2826	0.2469	0.8820
	500	-0.0020	0.0722	0.0689	0.9340	-0.0095	0.1933	0.1706	0.9110
	800	-0.0009	0.0564	0.0552	0.9370	-0.0037	0.1512	0.1401	0.9200
	1100	-0.0020	0.0486	0.0470	0.9420	0.0033	0.1251	0.1231	0.9330

Table 5: Scenario IV - estimates θ_1, θ_2 in the underline models where $\rho(\theta, s, t; Z_k) = 1 + \theta_1 \frac{(0.25+0.1Z_k)(0.25+0.2Z_k)}{(0.5t+0.25+0.1Z_k)(0.5s+0.25+0.2Z_k)}$ and $\rho(\theta, s, t; Z_k) = 1 + \theta_2 \frac{(0.5+0.1Z_k)(0.5+0.2Z_k)}{(0.5t+0.5+0.1Z_k)(0.5s+0.5+0.2Z_k)}$. Summary of Bias, SEE (Standard Error of Estimates), ESE (Estimated Standard Error), CP of θ where each entry is based on 1000 simulations. The averaged observed events for type1 (2) event is 2.44(2.56)

θ_1	N	Bias	SEE	ESE	CP	θ_2	Bias	SEE	ESE	CP
0.25	200	-0.0017	0.4030	0.4401	0.9580	0.25	-0.0027	0.2143	0.2513	0.9700
	500	-0.0221	0.2529	0.2840	0.9650		0.0005	0.1320	0.1625	0.9810
	800	0.0014	0.1916	0.2255	0.9770		-0.0020	0.1078	0.1287	0.9790
	1100	0.0038	0.1728	0.1933	0.9720		-0.0001	0.0897	0.1104	0.9820
0.50	200	-0.0177	0.4404	0.4948	0.9730	0.50	-0.0202	0.2703	0.3050	0.9560
	500	-0.0178	0.2843	0.3201	0.9570		-0.0047	0.1703	0.2001	0.9670
	800	-0.0001	0.2235	0.2570	0.9750		-0.0001	0.1337	0.1605	0.9820
	1100	0.0026	0.2003	0.2197	0.9660		0.0014	0.1123	0.1378	0.9850
0.75	200	-0.0154	0.5316	0.5598	0.9510	0.75	-0.0438	0.3170	0.3607	0.9470
	500	-0.0031	0.3184	0.3641	0.9680		-0.0079	0.2029	0.2443	0.9750
	800	-0.0105	0.2513	0.2899	0.9720		0.0030	0.1554	0.1952	0.9830
	1100	-0.0050	0.2156	0.2496	0.9720		-0.0029	0.1385	0.1671	0.9720
1.00	200	0.0008	0.5731	0.6270	0.9630	1.00	-0.0282	0.3863	0.4341	0.9530
	500	0.0002	0.3891	0.4154	0.9590		-0.0047	0.2473	0.2920	0.9590
	800	-0.0007	0.2939	0.3308	0.9730		-0.0019	0.1955	0.2331	0.9740
	1100	0.0010	0.2584	0.2834	0.9620		-0.0107	0.1614	0.1985	0.9740

3.2 Hypothesis testing of the rate ratio

Although the parametric rate ratio model has better interpretability than nonparametric ones, it might suffer from model misspecification and induce model bias. In this section, we aim at providing a goodness-of-fit procedure to test the parametric assumption of the rate ratio, i.e. $H_0 : \rho(s,t,\theta;z_1,z_2) = \theta_0$, under the additive marginal mean rate model. A finite sample study is also conducted to check the performance of the goodness-of-fit procedure.

3.2.1 Procedure description

The residual process followed by equation (2.4) under model (3.1) is defined as

$$V\big(s,t,\hat{\theta},\hat{\mu}_1(\cdot;z_{k1}),\hat{\mu}_2(\cdot;z_{k2})\big) = N^{-1/2}\sum_{k=1}^{N} V_k\big(s,t,\hat{\theta},\hat{\mu}_1(\cdot;z_{k1}),\hat{\mu}_2(\cdot;z_{k2})\big) \tag{3.23}$$

with

$$\begin{aligned}
&V_k\big(s,t,\hat{\theta},\hat{\mu}_1(\cdot;z_{k1}),\hat{\mu}_2(\cdot;z_{k2})\big)\\
&= \int_0^t\int_0^s W_N(u,v)\frac{\partial\rho(u,v,\theta)}{\partial\theta}\Big|_{\theta=\hat{\theta}}\Big\{\, dN_{k1}(u)dN_{k2}(v)\\
&\quad - \rho(u,v,\hat{\theta})Y_{k1}(u)\{d\hat{\mu}_{01}(u) + \hat{\beta}_1^T Z_{k1}(u)\,du\}Y_{k2}(v)\{d\hat{\mu}_{02}(v) + \hat{\beta}_2^T Z_{k2}(v)\,dv\}\Big\},
\end{aligned} \tag{3.24}$$

where $W_N(u,v)$ is a prespecified weight, and for simplicity we let $W_N(u,v) = 1$. With correctly specified marginal mean rate and $\rho(s,t,\theta;z_{k1},z_{k2})$, one would expect the value of equation (3.23) to fluctuate around zero at the any $(s,t) \in [0,\tau]^2$.

Let $T = \sup_{s,t\in[0,\tau]^2} \parallel V(s,t,\hat{\theta},\hat{\mu}_1(\cdot;z_{k1}),\hat{\mu}_2(\cdot;z_{k2})) \parallel$ be the supremum test statistic which measures the maximum observed residuals across the observable periods of type

1(2) events. A reasonable small T value is expected from a good fitting. Since the underlying distribution of T is intractable, we apply the Gaussian multiplier method to approximate its empirical distribution.

The Gaussian multiplier method.

The first order Taylor expansion of equation (3.23) w.r.t θ is

$$\begin{aligned} & V\Big(s,t,\hat{\theta},\hat{\mu}_1(\cdot;z_{k1}),\hat{\mu}_2(\cdot;z_{k2})\Big) \\ & = V\Big(s,t,\theta,\hat{\mu}_1(\cdot;z_{k1}),\hat{\mu}_2(\cdot;z_{k2})\Big) + N^{-1/2}\frac{\partial V\Big(s,t,\theta,\hat{\mu}_1(\cdot;z_{k1}),\hat{\mu}_2(\cdot;z_{k2})\Big)}{\partial\theta}N^{1/2}(\hat{\theta}-\theta) \\ & \quad + o_p(1), \end{aligned} \tag{3.25}$$

which can be further decomposed as

$$\begin{aligned} & V\Big(s,t,\hat{\theta},\hat{\mu}_1(\cdot;z_{k1}),\hat{\mu}_2(\cdot;z_{k2})\Big) \\ & = N^{-1/2}\textstyle\sum_{k=1}^{N}\Big\{V_k\Big(s,t,\theta,\mu_1(\cdot;z_{k1}),\mu_2(\cdot;z_{k2})\Big) \\ & \quad + \Upsilon_{k1}(s,t,\theta)+\Upsilon_{k2}(s,t,\theta)+\zeta_{k1}(s,t,\theta)+\zeta_{k2}(s,t,\theta)\Big\}+o_p(1), \end{aligned} \tag{3.26}$$

with details shown in Appendix C.

Let $T^* = \sup_{s,t\in[0,\tau]^2} \parallel V^*(s,t) \parallel$ and

$$\begin{aligned} & V^*(s,t,\hat{\theta}) \\ & = N^{-1/2}\sum_{k=1}^{N}\Big\{V_k(s,t,\hat{\theta},\hat{\mu}_1(\cdot;z_{k1}),\hat{\mu}_2(\cdot;z_{k2})) \\ & \quad +\hat{\Upsilon}_{k1}(s,t,\hat{\theta})+\hat{\zeta}_{k1}(s,t,\hat{\theta})+\hat{\Upsilon}_{k2}(s,t,\hat{\theta})+\hat{\zeta}_{k2}(s,t,\hat{\theta})\Big\}G_k, \end{aligned} \tag{3.27}$$

where G_k is i.i.d standard normal random number. $V\Big(s,t,\hat{\theta},\hat{\mu}_1(\cdot;z_{k1}),\hat{\mu}_2(\cdot;z_{k2})\Big)$ in equation (3.27) converges to a mean zero Gaussian process, which is approximated

by $V^*(s,t,\hat{\theta})$. and hence the T has empirical distribution T^*.

The Gaussian multiplier resampling method is summarized in Algorithm 1. In one simulation, a Gaussian random vector $\{G_1, G_2, ..., G_N\}$ is generated and $V^*(s,t,\hat{\theta})$ is calculated from equation (3.27). By taking the maximum of $V^*(s,t,\hat{\theta})$ across all the equally distanced grids, we have one sample from the T^* distribution. Repeating this simulation procedure 1000 times allows us to obtain 1000 samples and therefore the empirical distribution of T^*. On the other hand, the supremum test statistic T can be obtained by taking the maximum of equation (3.23). We consider the 95th percentile among the 1000 realizations of T^* as the critical value (C_{95}) and would reject H_0 if $T > C_{95}$.

3.2.2 Simulation studies

In this section, we conduct simulation studies to investigate the performance of the proposed goodness-of-fit procedure.

For bivariate counting processes, firstly, we detect the existence of dependency. The null model is that the bivariate counting processes are indepdendent and the constant rate ratio model is treated as its alternative. Secondly, we test the hypotheses $H_0 : \rho(s,t,\theta;z_1,z_2) = \theta_0$ vs $H_a : \rho(s,t,theta;z_1,z_2) \neq \theta_0$. The model under H_0 is generated from the shared frailty model whereas we consider piecewise constant (PWC), time dependent (TD), time and covariate dependent (TCD) models as H_a models. The size and power of the test are also computed via Gaussian multiplier method.

3.2.2.1 Testing for independence

The first hypothesis of interest is whether $\{N_{k1}(\cdot)\}$ and $\{N_{k2}(\cdot)\}$ are independent, which is equivalent to test $H_0 : \rho = 1 \quad \text{vs} \quad H_a : \rho \neq 1$. To investigate the size, events data are generated from an additive marginal model

$$d\mu_j(t; Z_{kj}(t)) = d\mu_{0j}(t) + \beta_j Z_{kj}(t).$$

Let $\tau = 5$, $\beta_{01} = 0.5$, $\beta_{02} = 1$, C_{kj} follows Uniform$[0, \tau]$ and covariates Z_{k1}, Z_{k2} are from a uniform distribution on $[1, 2]$. We take $\mu_{0j}(t) = 0.25t$, $0.5t$, $0.75t$, and t which gives the average observed events counts range from 2.50 to 6.26. Datasets under $H_a : \rho(\theta, s, t) = \theta_0$ are generated from the shared frailty model

$$d\mu_j(t; Z_{kj}(t), R_k) = R_k\{d\mu_{0j}(t) + \beta_j Z_{kj}(t)\},$$

where R_k from Gamma(a, b) with $(a, b) = (4, 0.25)$, $(2, 0.5)$, $(1.33, 0.75)$, $(1, 1)$. Thus θ_0 in H_a are equal to $1.25, 1.5, 1.75, 2$. We compare the supreme test statistic under $\rho(\theta, s, t) = \theta_0$ to the corresponding value obtained by assuming $\rho = 1$ and regard the rejection rate among 1000 simulations as the power of the test.

We only consider the case when $\mu_{0j} = 0.25t$, since it has the smallest number of observed events and other cases would have even more rejection, i.e. higher power. The empirical size (power) calculated as the rejection rate from 1000 simulated datasets under $H_0 : \rho = 1$ ($H_a : \rho(s, t, \theta; z_1, z_2) = \theta_0$).

Table 8 shows that the proposed testing procedure has size around its nominee value (5%). The test procedure is powerful at detecting the non-independent case

with probability above 99%.

3.2.2.2 Testing for parametric form with constant rate ratio

We are also interested in testing the parametric assumption of the rate ratio, i.e. $H_0 : \rho(\theta, s, t) = \theta_0$. The H_0 model is the shared frailty model in equation (3.11),

$$\text{shared frailty: } E[dN^*_{kj}(u)|R_k, Z_{kj}(u)] = R_k\{d\mu_{0j}(u) + \beta_j^T Z_{kj}(u)\, du\}$$

from which $\rho(s, t, \theta) = \theta_0$ where $\theta_0 = 1 + \sigma^2/\mu^2$, $\mathrm{E}[R_k] = \mu$ and $\mathrm{var}[R_k] = \sigma^2$.

From the first section in Table 9, we see the empirical size of the test under null model is bounded by its nominee value 0.05. Thus the hypothesis testing can control the probability of mistakenly reject $H_0 : \rho(s, t, \theta) = \theta_0$ under 0.05.

To investigate the power of the test, we propose three alternative models to introduce the time varying and covariate dependency cases: the piecewise constant rate ratio model(PWC), the time dependent rate ratio model(TD Model) and the covariate dependent rate ratio model(CD model). Alternative models and the corresponding performance are illustrated in the following sections.

(I) The piecewise constant rate ratio model - PWC Model

Described in equation (3.28), the random effect is time varying, which is a natural generalization of the shared frailty model

$$\text{PWC: } d\mu_j(t\,|R_k(t), Z_{kj}(t)) = R_k(t)\{d\mu_{0j}(t) + \beta_j^T Z_{kj}(t)\, dt\}. \tag{3.28}$$

For simplicity, we consider $R_k(t)$ come from different distributions only when t falls in non-overlapping intervals.

Let $\tau = 5$, $R_k(t) = I(t < 2.5)R_{k0} + I(t > 2.5)R_{k1}$, where R_{k0} and R_{k1} are independently from the shifted Gamma(a_0, b_0, δ_0) and Gamma(a_1, b_1, δ_1) respectively. The shifted Gamma Distribution with (a, b, δ) as shape, scale and shift parameters is introduced here to avoid rare event observations. We take $\mu_{01}(u) = \mu_{02}(u) = 0.125u^2$, $\beta_1 = 0.5$, $\beta_2 = 1$, and $Z_{k1}(u), Z_{k2}(u)$ from uniform$[1, 2]$.

Table 6 summarizes the parameter settings and the corresponding rate ratio value. We see the variation of the association is increasing from PWC_1 to PWC_4 and one can visualize the trend in Figure 1 as well.

To evaluate the power of the test, first, we generate 1000 datasets and within each simulation, the rate ratio $\rho(\theta, s, t)$ is estimated under H_0. The residual process and supreme statistic T are computed and a rejection is made when $T > C_{95}$, where C_{95} is the 95% percentile of Gaussian Multiplier samplers. The overall rejection rate among the 1000 datasets is considered as the empirical power of the hypothesis test. From Table 9, the power increases with the sample size and it is more likely to detect the divergence from H_0 when the association become stronger.

(II) Time dependent rate ratio model - TD model

Assuming $\{N_{k1}(s), N_{k2}(t)\}$ follows the bivariate counting processes below

$$\begin{aligned} N_{k1}(s) &= \widetilde{N}_{k1}(s) + N_{k0}(s), \\ N_{k2}(t) &= \widetilde{N}_{k2}(t) + N_{k0}(t), \end{aligned} \tag{3.29}$$

where $\widetilde{N}_{k1}(\cdot)$, $\widetilde{N}_{k2}(\cdot)$ and $N_{k0}(\cdot)$ follow Poisson Processes and are also mutually independent.

Let $\lambda_{k0}(t|Z_{kj}, R_k)\,dt$ be the event rate of $N_{k0}(t)$ and $\lambda_{k0}(t|Z_{kj}, R_k) = R_k(d\mu_{0j}(t) + \beta_{0j}Z_{kj}(t)$, where R_k is the frailty variable with mean μ and variance σ^2. For $j = 1, 2$ and $t \in (0, \tau)$, let $\widetilde{\lambda}_{kj}(t|Z_{kj}(t)) = \{(-0.15s + 0.9)^{-1} - 1\}\lambda_{k0}(t|Z_{kj}(t))$ Following simulation settings in equation 3.18 to generate data that share the rate ratio as

$$\text{TD model: } \rho(\theta, s, t) = 1 + \theta_0 \times (-0.15s + 0.9)(-0.15t + 0.9). \tag{3.30}$$

where $\theta_0 = \frac{\sigma^2}{\mu^2}$ reflects the time varying component in $\rho(\theta, s, t)$ proportionally. To capture different time varying levels, we take R_k from a shifted gamma distribution, with parameters $(a, b, \delta) = (0.25, 2, 0.5)$,$(0.2, 3, 0.4)$ $(0.25, 3, 0.25)$ and $(0.2, 4, 0.2)$ so that $\mu = 1$ and $\sigma^2 = 1$, 1.8, 2.25 and 3.2. Let $\beta_{01} = \beta_{02} = 0$, $\tau = 5$, C_{kj} be uniform on $(0, \tau)$, and Z_{k1}, Z_{k2} are i.i.d uniform$(1, 2)$. Simulation settings are summarized in Table 7 and Figure 2.

The variation of $\rho(\theta, s, t)$ is scaling up from TD_1 to TD_4, so does the empirical power of the test shown in Table 9. From our observation, the proposed model checking procedure performs well with a large sample size, especially when the rate ratio is very time dependent.

(III) Time and covariates dependent rate ratio model -TCD Model

Under the same framework of the TD Model, assume $N_{k0}(t)$ and $\widetilde{N}_{kj}(t)$ are Poisson processes with rate conditional on covariates and unobservable frailty R_k as $\lambda_{k0}(t|Z_{kj}, R_k) = R_k\{0.25 + \beta_{0j}Z_{kj}\}$ and $\widetilde{\lambda}_{kj}(t) = t$ respectively. The conditional rate of $N_{kj}(t)$ equals to $\lambda_{kj}(t|Z_{kj}, R_k)$ where $\lambda_{kj}(t|Z_{kj}, R_k) = t + \{0.25 + \beta_{0j}Z_{kj}\}$.

Let $\beta_{01} = 0.5$, $\beta_{02} = 1$, Z_{kj} follow uniform$(1, 2)$. Take R_k as i.i.d Gamma$(1/v, v)$

with $v = 0.5, 0.8, 1, 2$ so that $\mathrm{E}(R_k) = 1$ and $\mathrm{var}(R_k) = 0.5, 0.8, 1, 2$. Denoted by $\rho(\theta, s, t; Z_{k1}, Z_{k2})$ the rate ratio of $\{N_{k1}(s), N_{k2}(t)\}$, where

$$\rho(\theta, s, t; Z_{k1}, Z_{k2}) = 1 + \theta \frac{(0.25 + 0.5Z_{k1})(0.25 + Z_{k2})}{(t + 0.25 + 0.5Z_{k1})(s + 0.25 + Z_{k2})}. \tag{3.31}$$

is obtained by Proposition 3, with true θ equal to 0.5, 0.8, 1 and 2.

The average rejection of $H_0 : \rho(s, t, \theta) = \theta_0$ under equation (3.31) among 1000 are summarized in Table 9. The test is powerful at detecting violation of H_0 and the rejection rate of the test is consistently increase when the sample size changed from 200 to 800.

Algorithm 1 Gaussian Multiplier Method

For dataset $m = 1, 2, ..., \mathcal{M}$

1. Let $\mathcal{M}$ the total number of simulated datasets, consider $\mathcal{M} = 1000$;
2. For a given dataset, calculate T by equation (3.2.1);
   - set $i = 1$;
   - while $i <= 1000$, we generate a vector composed by i.i.d Standard Gaussian random numbers, so that each row is an N dimensional vector: $G_i = \{G_{i1}, G_{i2}, G_{i3}, ..., G_{iN}\}$
   - applying (3.27) to calculate $\{V_i^*(s,t)\}$ and obtain T_i^*.
   - $i = i + 1$;
3. Denote the 95th percentile of $\{T_1^*, T_2^*, ..., T_{1000}^*\}$ to be C_{95}. We would reject H_0 if $T > C_{95}$ and fail to reject H_0 if $T < C_{95}$.
4. Calculate the percentage of rejections in a total of $\mathcal{M}$ datasets to find the size or the power of test statistic.

Table 6: Summary of simulation settings under the piecewise constant rate ratio model with the corresponding ρ values followed from Proposition 2.

Settings	PWC_1	PWC_2	PWC_3	PWC_4
$R_{k0}: \ (a_0, b_0, \delta_0)$	(0.25,1,0.75)	(0.5,1,0.5)	(0.25,2,0.5)	(0.25,2,0.5)
$R_{k1}: \ (a_1, b_1, \delta_1)$	(0.25,1,0.75)	(0.25,1,0.75)	(0.5,1,0.5)	(0.25,1,0.75)
$\rho(s < 2.5, t < 2.5)$	1.25	1.5	2	2
$\rho(s > 2.5, t < 2.5)$	1	1	1	1
$\rho(s > 2.5, t > 2.5)$	1.25	1.25	1.5	1.25

Figure 1: Visualization of piecewise constant $\rho(s, t, \theta)$ (PWC) under the additive marginal. The variation of $\rho(s, t)$ between different pieces is growing from PWC_1 to PWC_4.

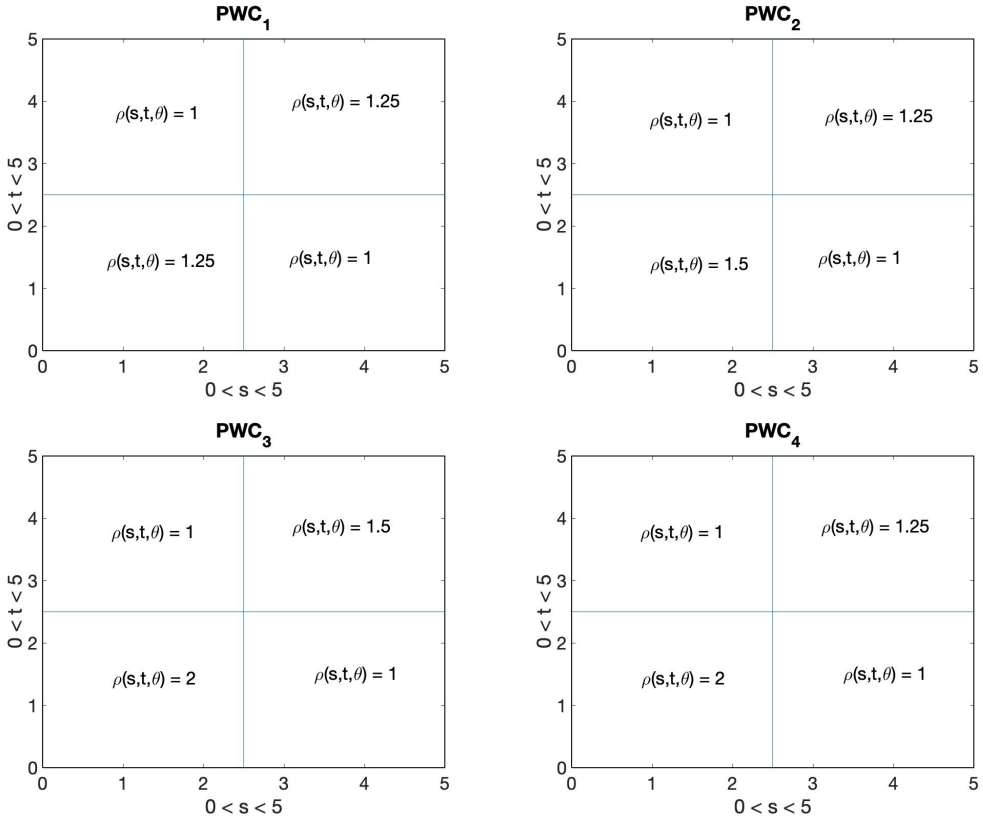

Table 7: Simulation settings of the time varying rate ratio (TD models). From TD1 to TD4, the value of σ^2/μ^2 is increasing and so is the association between the bivariate recurrent event processes.

Settings	TD_1	TD_2	TD_3	TD_4
(μ, σ^2)	(1, 1)	(1, 1.8)	(1, 2.25)	(1, 3.2)
$\frac{\sigma^2}{\mu^2}$	1	1.8	2.25	3.2

Figure 2: The contour plot of the rate ratio $\rho(s,t)$ under the additive marginal mean rate models. The x-axis and y-axis represents the observation time for type1 and type2 events. From upper left to lower right, the heterogeneity of $\rho(s,t)$ is increased.

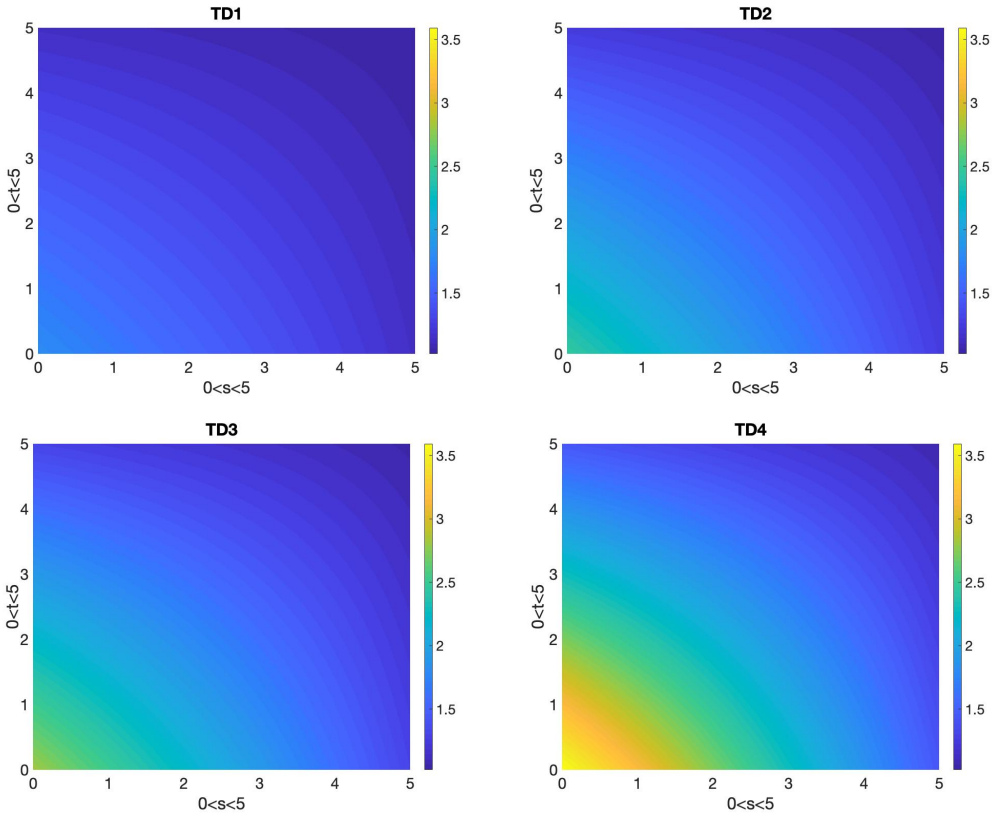

Table 8: Observed sizes and powers of the test statistic T via the proposed model-checking procedure under $H_0 : \rho(s,t,\theta) = 1$ vs $H_a : \rho(s,t,\theta) = \theta_0$ and $\theta_0 > 1$, at significance level 0.05. The numbers in the parentheses represent the count for type 1 and type 2 event across the observation period. Each entry is calculated based on 1000 Gaussian multiplier samples with 1000 replicates.

		Size		
event count	ρ	N=200	N=500	N=800
(2.50, 4.37)	1	0.043	0.052	0.051
(3.13, 5.02)	1	0.051	0.057	0.051
(3.76, 5.64)	1	0.043	0.053	0.041
(4.37, 6.26)	1	0.045	0.049	0.054
		Power		
	θ_0	N=200	N=500	N=800
(2.50, 4.37)	1.25	0.995	1.000	1.000
	1.5	1.000	1.000	1.000
	1.75	1.000	1.000	1.000
	2	1.000	1.000	1.000

Table 9: Observed sizes and powers of the test statistic T for the proposed model-checking procedure under $H_0 : \rho(\theta, s, t) = \theta_0$ (i.e. constant) vs $H_a : (\theta, s, t) \neq \theta_0$, at 0.05 significance level. Each entry is calculated based on 1000 Gaussian multiplier samples with 1000 replicates.

		Size			
event count	N	$\theta_0 = 1.25$	$\theta_0 = 1.5$	$\theta_0 = 2$	$\theta_0 = 2.25$
	200	0.038	0.038	0.031	0.038
(3.50, 4.67)	500	0.057	0.037	0.032	0.040
	800	0.042	0.042	0.051	0.046
		Power			
		PWC_1	PWC_2	PWC_3	PWC_4
	200	0.173	0.579	0.638	0.755
(2.91, 4.80)	500	0.421	0.912	0.958	0.983
	800	0.622	0.979	0.990	0.999
		TD_1	TD_2	TD_3	TD_4
	200	0.197	0.231	0.311	0.307
(4.27, 4.27)	500	0.556	0.621	0.760	0.738
	800	0.773	0.821	0.887	0.894
		TCD_1	TCD_2	TCD_3	TCD_4
	200	0.250	0.336	0.405	0.455
(6.67, 8.54)	500	0.514	0.678	0.756	0.823
	800	0.735	0.900	0.917	0.933

CHAPTER 4: ESTIMATION AND INFERENCE OF THE RATE RATIO UNDER THE MULTIPLICATIVE MARGINAL MODEL

4.1 Estimation by a two-stage approach

Additive and multiplicative mean rate models postulate a different relationship between the underline counting process and the covariates. The multiplicative model, also known as Cox model is popular due to its easy implementation and clear interpretation of the covariate effect. In this chapter, we develop the estimation procedure for the rate ratio under the multiplicative marginal event rate model.

Lin et al. (2000) proposed the mean rate of the counting process $N^*_{kj}(t)$ as

$$E[dN^*_{kj}(t)|Z_{kj}(t)] = d\mu_j(t; Z_{kj}(t)),$$
$$d\mu_j(t; Z_{kj}(t)) = e^{\beta_j^T Z_{kj}(t)}\, d\mu_{0j}(t), \tag{4.1}$$

where β_j is a p-dimensional vector, $\mu_{0j}(t)$ is an unspecified baseline rate at time t. Assume $\rho(s, t, \theta; z_{k1}, z_{k2})$ is the rate ratio of $N^*_{k1}(t)$ and $N^*_{k2}(s)$. θ is the dependence parameter which can be approximated by solving the estimation equation (2.3), with the $\hat{\mu}_j(t)$ estimated by the method proposed by Lin et al. (2000). We adjust some notations from Chapter 3 with a superscription c (Cox-type) to represent estimators derived from model (4.1).

4.1.1 Review the estimation of the marginal model

Adapting from the approach of Lin et al. (2000), for type j event we define

$$
\begin{aligned}
d\bar{N}_{\cdot j}(t) &= \sum_{k=1}^{N} dN_{kj}(t), \\
M_{kj}^{c}(t) &= N_{kj}(t) - \int_0^t Y_{kj}(u) e^{\beta_j^T Z_{kj}(u)}\, d\mu_{01}(u), \\
S_j^d(t,\beta) &= N^{-1} \sum_{k=1}^{N} Y_{kj}(t) Z_{kj}^{\otimes d}(t) e^{\beta^T Z_{kj}(t)}, \qquad d = 0,1,2
\end{aligned} \tag{4.2}
$$

where $a^{\otimes 0} = 1$, $a^{\otimes 1} = a$, and $a^{\otimes 2} = aa^T$. Let $\tilde{Z}_j(t,\beta) = S_j^1(t,\beta)/S_j^0(t,\beta)$; $\tilde{z}_j(t,\beta)$, $s_j^d(t,\beta)$ be the limit of $\tilde{Z}_j(\beta,t)$ and $S_j^d(t,\beta)$ as $N \to \infty$ respectively.

Denote $\tilde{\beta}_j$ the solution to $L_j^c(\beta,\tau) = 0$, where $L_j^c(\beta,\tau) = \sum_{k=1}^{N} \int_0^\tau \{Z_{kj}(u) - \tilde{Z}_j(u,\beta)\} dN_{kj}(u)$ is the partial likelihood score function.

Under certain regularity conditions, $\tilde{\beta}_j$ converges almost surely to β_j and $\sqrt{n}(\tilde{\beta}_j - \beta_j)$ has weak convergence to a zero-mean normal random vector with covariance matrix $\Gamma_j \equiv (A_j^c)^{-1}\Sigma_j^c(A_j^c)^{-1}$. When $\tilde{\beta}_j$ is available, the baseline function $\mu_{0j}(t)$ can be consistently estimated by the Aalen-Breslow type estimator

$$
\tilde{\mu}_{0j}(t,\tilde{\beta}_j) = \int_0^t \frac{d\bar{N}_j(u)}{N S_j^0(u,\tilde{\beta}_j)}, \quad t \in [0,\tau]. \tag{4.3}
$$

We investigate the asymptotic properties of $\hat{\theta}$ under the assumption that the distribution functions of the C_{kj} are independent from covariates and the counting process. We recall Theorem 4.1, Theorem 4.2 due to Lin et al. (2000).

Theorem 4.1 (Lin et al. (2000) A.1.) *For $j = 1,2$, $\tilde{\beta}_j$ converges almost surely to β_j and $\sqrt{N}(\tilde{\beta}_j - \beta_j)$ is asymptotically normal with covariance matrix $(A_j^c)^{-1}\Sigma_j^c(A_j^c)^{-1}$,*

where

$$A_j^c = E\Big[\int_0^\tau \{Z_{1j}(u) - \tilde{z}_j(u,\beta_j)\}^{\otimes 2} Y_{1j}(u) e^{\beta_j^T Z_{1j}(u)}\, d\mu_{0j}(u)\Big],$$
$$\Sigma_j^c = E\Big[\int_0^\tau \{Z_{1j}(u) - \tilde{z}_j(u,\beta_j)\} dM_{1j}^c(u) \int_0^\tau \{Z_{1j}(v) - \tilde{z}_j(v,\beta_j)\} dM_{1j}^c(v)\Big]. \quad (4.4)$$

The asymptotic approximation of $\tilde{\beta}_j$ *is*

$$\sqrt{N}(\tilde{\beta}_j - \beta_j) = (A_j^c)^{-1} N^{-1/2} \sum_{k=1}^N \int_0^\tau \{Z_{kj}(u) - \tilde{z}_{kj}(u,\tilde{\beta}_j)\}\, dM_{kj}^c(u,\beta_j) + o_p(1), \quad (4.5)$$

from which the covariance matrix can be consistently estimated by $\tilde{A}_j^{-1}\tilde{\Sigma}_j\tilde{A}_j^{-1}$*, where*

$$\tilde{A}_j = N^{-1}\sum_{k=1}^N \int_0^\tau \{Z_{kj}(u) - \tilde{Z}_{kj}(u,\tilde{\beta}_j)\}^{\otimes 2} Y_{kj}(u) e^{\tilde{\beta}_j^T Z_{kj}(u)}\, d\tilde{\mu}_{0j}(u),$$
$$\tilde{\Sigma}_j = N^{-1}\sum_{k=1}^N \tilde{\xi}_{kj}^{\otimes 2},$$
$$\tilde{\xi}_{kj} = \int_0^\tau \{Z_{kj}(u) - \tilde{Z}_{kj}(u,\tilde{\beta}_j)\}\, d\tilde{M}_{kj}(u),$$
$$\tilde{M}_{kj}(t) = N_{kj}(t) - \int_0^t Y_{kj}(u) e^{\tilde{\beta}_j^T Z_{kj}(u)} d\tilde{\mu}_{0j}(u).$$

Theorem 4.2 (Lin et al. (2000) A.3.) *For* $j = 1, 2$*,* $\tilde{\mu}_{0j}(t) \equiv \tilde{\mu}_{0j}(t, \tilde{\beta}_j)$ *converges almost surely to* $\mu_{0j}(t)$ *in* $t \in [0, \tau]$*, and* $\sqrt{N}\{\tilde{\mu}_{0j}(t) - \mu_{0j}(t)\}$ *converges weakly to a Gaussian process with mean zero and covariance function given by*

$$\Gamma_j^c(s,t) = E[\phi_{kj}^c(s)\phi_{kj}^c(t)] \quad at \quad (s,t),$$

where

$$\phi_{kj}^c(t) = \int_0^t \frac{dM_{kj}^c(u;\beta_j)}{s_j^0(u,\beta_j)} - H^T(t;\beta_j)(A_j^c)^{-1} \int_0^\tau \{Z_{kj}(u) - \tilde{z}_{kj}(u,\beta_j)\}\, dM_{kj}^c(u), \quad (4.6)$$

and

$$H(t;\beta_j) = \int_0^t \tilde{z}_j(u,\beta_j) d\mu_{0j}(u) \tag{4.7}$$

The covariance function $\Gamma_j^c(s,t)$ *can be consistently estimated by*

$$\tilde{\Gamma}_j(s,t) = N^{-1} \sum_{k=1}^{N} \tilde{\phi}_{kj}(s)\tilde{\phi}_{kj}(t) \tag{4.8}$$

where

$$\tilde{\phi}_{kj}(t) = \int_0^t \frac{d\tilde{M}_{kj}(u)}{S_j^0(u,\tilde{\beta}_j)} - \tilde{H}^T(t;\tilde{\beta}_j)\tilde{A}_j^{-1} \int_0^\tau \{Z_{kj}(u) - \tilde{Z}_{kj}(u,\tilde{\beta}_j)\}\, d\tilde{M}_{kj}(u)$$

and

$$\tilde{H}(t;\tilde{\beta}_j) = \int_0^t \tilde{Z}_j^T(u,\tilde{\beta}_j) \frac{d\bar{N}_j(u)}{NS_j^0(u,\tilde{\beta}_j)}.$$

4.1.2 Estimation of the rate ratio

In the second stage, the dependence parameter can be estimated by the root to the following estimation equation

$$U^c\Big(\theta, \beta_1, \mu_{01}(\cdot), \beta_2, \mu_{02}(\cdot)\Big) = \sum_{k=1}^{N} U_k^c\Big(\theta, \beta_1, \mu_{01}(\cdot), \beta_2, \mu_{02}(\cdot)\Big), \tag{4.9}$$

where

$$\begin{aligned}
&U_k^c\Big(\theta, \beta_1, \mu_{01}(\cdot), \beta_2, \mu_{02}(\cdot)\Big) \\
&= \int_0^\tau \int_0^\tau \frac{\partial \rho(\theta, s, t; Z_{k1}(s), Z_{k2}(t)}{\partial \theta} \cdot \Big\{ dN_{k1}(s)\, dN_{k2}(t) \\
&\quad - \rho(\theta, s, t; Z_{k1}(s), Z_{k2}(t)) Y_{k1}(s) e^{\beta_1^T Z_{k1}(s)}\, d\mu_{01}(s) Y_{k2}(t) e^{\beta_2^T Z_{k2}(t)}\, d\mu_{02}(t) \Big\}.
\end{aligned} \tag{4.10}$$

with β_1, β_2, $\mu_{01}(\cdot)$, $\mu_{02}(\cdot)$ replaced by estimator $\tilde{\beta}_1$, $\tilde{\beta}_2$, $\tilde{\mu}_{01}(\cdot)$, $\tilde{\mu}_{02}(\cdot)$ from the first stage.

The resulting estimator $\tilde{\theta}$ does not have an explicit form. We adapt the asymptotic properties of $\tilde{\beta}_j$ and $\tilde{\mu}_{0j}(\cdot)$ from Theorem 4.1 and Theorem 4.2 to show the weak covergence of $\tilde{\theta}$.

Theorem 4.3 $N^{-1/2}\Big\{U^c\Big(\theta, \tilde{\beta}_1, \tilde{\mu}_{01}(\cdot), \tilde{\beta}_2, \tilde{\mu}_{02}(\cdot)\Big) - U^c\Big(\theta, \beta_1, \mu_{01}(\cdot), \beta_2, \mu_{02}(\cdot)\Big)\Big\}$ *follows a mean-zero Gaussian process and has the following approximation*

$$
\begin{aligned}
&N^{-1/2}\{U^c(\theta, \tilde{\beta}_1, d\tilde{\mu}_{01}(\cdot), \tilde{\beta}_2, d\tilde{\mu}_{02}(\cdot)) - U^c(\theta, \beta_1, d\mu_{01}(\cdot), \beta_2, d\mu_{02}(\cdot))\} \\
&= N^{-1/2}\sum_{k=1}^{N}\Big\{h^c_{1,N}(A_1)^{-1}\xi^c_{k1} + g^c_{1,N,k} + h^c_{2,N}(A_2)^{-1}\xi_{k2} + g^c_{2,N,k}\Big\} + o_p(N^{-1/2}), \quad (4.11)
\end{aligned}
$$

where

$$
\begin{aligned}
q^c_l(\theta, s, t) &= -\rho(\theta, s, t)\frac{\partial \rho(\theta, s, t)}{\partial \theta} Y_{l1}(s) e^{\beta_1^T Z_{l1}(s)} Y_{l2}(t) e^{\beta_2^T Z_{l2}(t)}, \\
h^c_{1,N} &= N^{-1}\sum_{l=1}^{N}\int_0^\tau \int_0^\tau q^c_l(\theta, s, t) Z^T_{l1}(s)\, d\mu_{01}(s) d\mu_{02}(t), \\
h^c_{2,N} &= N^{-1}\sum_{l=1}^{N}\int_0^\tau \int_0^\tau q^c_l(\theta, s, t) Z^T_{l2}(t)\, d\mu_{02}(t) d\mu_{01}(s), \\
g^c_{1,N,k} &= N^{-1}\sum_{l=1}^{N}\int_0^\tau \int_0^\tau q^c_l(\theta, s, t)\, d\mu_{02}(t)\, d\phi^c_{k1}(s), \\
g^c_{2,N,k} &= N^{-1}\sum_{l=1}^{N}\int_0^\tau \int_0^\tau q^c_l(\theta, s, t)\, d\mu_{01}(s)\, d\phi^c_{k2}(t). \quad (4.12)
\end{aligned}
$$

The right hand side in equation (4.11) can be estimated by

$$
N^{-1/2}\sum_{k=1}^{N}\Big\{\tilde{h}_{1,N}\tilde{A}_1^{-1}\tilde{\xi}_{k1} + \tilde{g}_{1,N,k} + \tilde{h}_{2,N}\tilde{A}_2^{-1}\tilde{\xi}_{k2} + \tilde{g}_{2,N,k}\Big\},
$$

where $\tilde{h}_{1,N}$, $\tilde{\xi}_{k1}$, $\tilde{h}_{2,N}$, $\tilde{\xi}_{k2}$, $\tilde{g}_{1,N,k}$, $\tilde{g}_{2,N,k}$ *are obtained by plugging* $\tilde{\beta}_j$, $\tilde{\theta}$, $\tilde{\mu}_{0j}(\cdot)$ *and*

$\tilde{\phi}_{kj}(t)$ into equation (4.12).

Theorem 4.4 *We show in the Appendix that $\sqrt{N}(\tilde{\theta}-\theta)$ is asymptotically normal and has the following i.i.d. approximation:*

$$\begin{aligned}&\sqrt{N}(\tilde{\theta}-\theta)\\&= N^{-1/2}\{\mathcal{I}^c(\theta,\beta_1,\mu_{01}(\cdot),\beta_2,\mu_{02}(\cdot))\}^{-1}\sum_{k=1}^{N} W_k^c(\theta,\beta_1,\mu_{01}(\cdot),\beta_2,\mu_{02}(\cdot)) + o_p(1)\end{aligned} \quad (4.13)$$

where

$$\mathcal{I}^c(\theta,\beta_1,\mu_{01}(\cdot),\beta_2,\mu_{02}(\cdot)) = -N^{-1}\sum_{k=1}^{N}\left\{\frac{\partial U_k^c(\theta,\beta_1,\mu_{01}(\cdot),\beta_2,\mu_{02}(\cdot))}{\partial\theta}\right\}^T, \quad (4.14)$$

and

$$\begin{aligned}&W_k^c(\theta,\beta_1,\mu_{01}(\cdot),\beta_2,\mu_{02}(\cdot))\\&= U_k^c(\theta,\beta_1,\mu_{01}(\cdot),\beta_2,\mu_{02}(\cdot)) + \left\{h_{1,N}^c(A_1^c)^{-1}\xi_{k1}^c + g_{1,N,k}^c + h_{2,N}^c(A_2^c)^{-1}\xi_{k2}^c + g_{2,N,k}^c\right\}.\end{aligned} \quad (4.15)$$

By the central limit theorem $\sqrt{N}(\tilde{\theta}-\theta)$ is asymptotically normal with mean 0 and variance which can be estimated by $\tilde{\Phi} = N^{-1}(\tilde{\mathcal{I}})^{-1}(\sum_{k=1}^{N}\tilde{W}_k^{\otimes 2})(\tilde{\mathcal{I}}^T)^{-1}$, where $\tilde{\mathcal{I}}$ and $\tilde{W}_k$ are the empirical counterparts of

$$\mathcal{I}^c(\theta,\beta_1,\mu_{01}(\cdot),\beta_2,\mu_{02}(\cdot))$$

$$W_k^c(\theta,\beta_1,\mu_{01}(\cdot),\beta_2,\mu_{02}(\cdot))$$

respectively, obtained by substituting $\tilde{\theta}$, $\tilde{\beta}_1$, $\tilde{\mu}_{01}(\cdot)$, $\tilde{\beta}_1$, $\tilde{\mu}_{02}(\cdot)$ into equation (4.14) and (4.15).

4.1.3 Simulation studies

To evaluate the performance of the proposed method, we conduct a finite sample simulation study with some shared settings. The end of study time is set as $\tau = 4$, censoring time follows uniform$(3, 4)$, and covariates $\{Z_{kj}\}$ for the two types of disease are generated from uniform$(1, 2)$.

(I) Constant rate ratio $\rho = \theta_0$

Under the shared random effect model, $E[dN^*_{kj}(t)|R_k, Z_{kj}(t)] = R_k\{e^{\beta_j^T Z_{kj}(t)}\, d\mu_{0j}(t)\}$, where $\{R_k\}$ is the cluster level random effect, and are assumed to be i.i.d from a positive distribution with mean $E(R_k) = 1$ and variance $\text{var}(R_k) = \sigma^2$. Proved in Proposition1 that the rate Ratio is reduced to $\rho(\theta) = 1 + \sigma^2$, which only related to the variance of random effect R_k.

Let $\beta_1 = 0.2$ $\beta_2 = 0.4$. Take $\mu_{01}(t) = \mu_{02}(t) = 0.125t^2$, $0.25t^2$, $0.375t^2$, and $0.5t^2$ such that the averaged observed type 1(2) events after right censoring are 2.06(2.84), 4.18(5.67), 6.25(8.48), 8.3(11.3) respectively. R_k are independently simulated from a Gamma distribution with mean 1 and variance $\sigma^2 = 0.25, 0.5, 0.75$, which leads to $\rho = 1.25, 1.5, 1.75$.

In the first-stage, we estimate β_1, β_2 based marginal mean rate model (4.1). From the result in Table 10, $\hat{\beta}_1$ and $\hat{\beta}_2$ converges to true the values $\beta_1 = 0.2$ and $\beta_2 = 0.4$, and the ESE (Estimated Standard Error) is close to SEE (Standard Error of Estimates). The empirical coverage probability is close to its 95% nominee value.

In the second-stage, we substitute $\tilde{\beta}_1, \tilde{\beta}_2, \tilde{\mu}_{01}(\cdot), \tilde{\mu}_{02}(\cdot)$ into the estimation equation (4.9) and obtain $\tilde{\theta}$ by solving $U(\theta, \tilde{\beta}_1, \tilde{\mu}_{01}(\cdot), \tilde{\beta}_2, \tilde{\mu}_{02}(\cdot)) = 0$. The average Bias, SEE

(Standard Error of Estimates), ESE (Estimated Standard Error), CP (coverage probability of the 95% confidence interval) of ρ are summarized in Table 11, where each entry based on 1000 replicates.

$\tilde{\rho}$ is unbiased and the estimated standard error can be reduced by increasing the sample size. Similar to the estimation result shown in table 3, the standard error is underestimated which cause the coverage probability consistently slightly smaller than 95%, especially when the ρ increases. One possible explanation is that the information gains from increasing the sample size is offset by the stronger association between two recurrent event processes. An extreme condition is that the two processes are identical, then we are actually observing and utilizing the information for a single process and therefore the rate ratio would be underestimated.

(II) Time varying rate ratio $\rho(\theta, s, t) = 1 + \theta_0(-0.15s + 0.9)(-0.15t + 0.9)$

Assume the counting process for j th type event in cluster K at time u as

$$N_{kj}(t) = \tilde{N}_{kj}(t) + N_{k0}(t), \quad \text{for} \quad j = 1, 2$$

where $\{\tilde{N}_{kj}(t)\}$, and $\{N_{k0}(t)\}$ are mutually independent. Denote $\rho_0(\theta, s, t)$ be the rate ratio of $N_{k0}(s)$ and $N_{k0}(t)$. By proposition 3, we have the rate ratio of $\{N_{k1}(s), N_{k2}(t)\}$ as

$$\rho(\theta, s, t\,|z_1(s), z_2(t)) = 1 + \{\rho_0(\theta, s, t) - 1\}\frac{\lambda_{k0}(s|z_1(s))\lambda_{k0}(t|z_2(t))}{\lambda_{k1}(s|z_1(s))\lambda_{k2}(t|z_2(t))},$$

where $E\{dN_{k0}(s)|z_1\} = \lambda_{k0}(s|z_1(s))\,ds$, $E\{dN_{k1}(s)|z_1(s)\} = \lambda_{k1}(s|z_1(s))\,ds$, while $E\{dN_{k2}(t)|z_2(t)\} = \lambda_{k2}(t|z_2(t))\,dt$. It is straight forward to show $\lambda_{k1}(s\,|z_1(s)) = \lambda_{k0}(s\,|z_1(s)) + \tilde{\lambda}_{k1}(s|z_1(s))$, with $\tilde{\lambda}_{k1}(s|z_1(s))$ be the mean event rate for counting

process $\tilde{N}_{k1}(s)$. The same logic applies to type 2 event.

for $s, t \in [0, \tau]$, we take $\tilde{\lambda}_{k1}(s|z_1) = \{(-0.15s+0.9)^{-1}-1\}\lambda_{k0}(s|z_1)$ and $\tilde{\lambda}_{k1}(t|z_2) = \{(-0.15t+0.9)^{-1}-1\}\lambda_{k0}(t|z_2)$.

To specify the $\rho_0(\theta, s, t)$, we consider

$$E[dN^*_{k0}(s)|R_k, Z_{k1}] = R_k \cdot \{e^{\beta_1^T Z_{k1}}\, d\mu_{01}(s)\},$$

$$E[dN^*_{k0}(t)|R_k, Z_{k2}] = R_k \cdot \{e^{\beta_2^T Z_{k2}}\, d\mu_{02}(t)\},$$

where R_k is the cluster level random effect which is i.i.d from a positive distribution. We take Z_{kj} from i.i.d U[1,2] and set $\beta_1 = \beta_2 = 0$. R_k are generated from Gamma distribution with E(R_k) =1 and var(R_k) =0.25, 0.5, 1, 1.5,and 2, which yields $\rho_0(\theta, s, t)$ =1.25,1.5,2 and 2.5. The rate ratio $\rho(\theta, s, t)$ can be represented as

$$\rho(\theta, s, t) = 1 + \theta_0(-0.15s + 0.9)(-0.15t + 0.9), \tag{4.16}$$

with the parameter θ_0 equal to 0.25, 0.5, 1 and 1.5.

A simulation study for the rate ratio with sample size $K = 200, 500, 800$ is summarized in Table 12, with each entry based on 1000 simulations. The estimator is unbiased and the estimated standard error is very close to its true value, with coverage probability around 95%. The SSE and ESE is decreasing while increasing the sample size showing that the estimation procedure is more efficient with a large sample size. We observe consistently higher standard error when the association between bivariate recurrent processes increases.

(III) Covariate dependent rate ratio $\rho(\theta; Z_k) = \theta_1 I(Z_k = 1) + \theta_2 I(Z_k = 0)$

Let $Z_{kj} = Z_k$ denote the cluster level covariates. Assume the shared frailty model

$$E[dN^*_{kj}(t)|Z_k, R_k] = R_k \cdot e^{\beta_{0j} Z_k(t)}\, d\mu_{0j}(t) \tag{4.17}$$

where $E[R_k|Z_k] = \mu(Z_k)$ and $\text{var}[R_k|Z_k] = \sigma^2(Z_k)$. Following Proposition 1, $\rho(s,t,\theta) = 1 + \frac{\sigma^2(Z_k)}{\mu^2(Z_k)}$. Denoted by the θ_1 and θ_2 the value of $\rho(s,t,\theta)$ when $Z_k = 1, 0$, i.e.

$$\rho(s,t,\theta) = \theta_1 I(Z_k = 1) + \theta_2 I(Z_k = 0). \tag{4.18}$$

Let $\beta_{01} = 0.2$, $\beta_{02}(t) = 0.4$. We consider $\mu_{0j}(t) = 0.125t^2, 0.25t^2$ for moderately observed event process, whereas $\mu_{0j}(t) = 0.375t^2$ and $0.5t^2$ stand for more frequently observed ones. Z_k from Bernoulli($p = 0.5$) and R_k from Gamma($1/v_k, v_k$) so that $E(R_k)$=1 and $\text{var}(R_k) = v_k$. Let $\theta_1 = 1.25$ and $\theta_2 = 1.75$ represent the weak and the strong association, which are generated by taking $v_k = 0.25$ for $Z_k = 1$, and v_k =0.75 while $Z_k = 0$.

Simulation result for sample size 200, 500, 800 and 1100, each with 1000 replicates are shown in Table 13. The estimator is unbiased and the ESE is close to SEE. The coverage probability is approaching to 0.95 when the sample size increases from 200 to 1100. The ESE and SEE of θ_2 are consistently larger than that of θ_1, even through both are reduced in a larger sample size.

(IV) Time and covariate dependent rate ratio

For $j = 1, 2$, we construct a bivariate counting process N_{kj} with $N_{kj}(t) = \widetilde{N}_{kj}(t) +$

$N_{k0}(t)$. Let

$$E\{dN_{k0}(t)|Z_{kj}, R_k\} = \lambda_{k0}(t|Z_{kj}, R_k)\, dt$$

$$E\{d\widetilde{N}_{kj}(t)|Z_{kj}, R_k\} = \widetilde{\lambda}_{kj}(t)\, dt$$

where $\lambda_{k0}(t|Z_{kj}, R_k) = R_k e^{\beta_{0j} Z_{kj}} 0.25t$ and $\widetilde{\lambda}_{kj}(t) = 0.25$.

We take R_k from i.i.d Gamma(a, b) with (a, b) equal to (4, 0.25), (2, 0.5), (1.33, 0.75) and (1, 1) such that $\rho_0(\theta, s, t) = 1.25, 1.5,\ 1.75$ and 2. Let Z_k is from Bernoulli(0.5), $\beta_{01} = 0.1$ and $\beta_{02} = 0.2$. By Proposition 3, the rate ratio of $N_{k1}(s)$ and $N_{k2}(t)$ is time-varying and dependent on the covariate Z_{kj} which is denoted by

$$\rho(\theta, s, t|Z_{k1}, Z_{k2}) = 1 + \theta_1 \frac{(0.25t\, e^{0.1Z_{k1}})(0.25s\, e^{0.2Z_{k2}})}{(0.25 + 0.25t\, e^{0.1Z_{k1}})(0.25 + 0.25s\, e^{0.2Z_{k2}})}, \tag{4.19}$$

where $\theta = \rho_0(\theta, s, t) - 1 = 0.25, 0.5, 0.75$ and 1.

To evaluate the performance difference between moderate and high frequency event processes, we consider $\lambda_{k0}(t|Z_{kj}, R_k) = R_k \cdot 0.5 e^{\beta_{0j} Z_{kj}}$. While keeping other settings the same, the event process $N_{kj}(t)$ would expect to have more observations than the previous setting and following equation (4.19) we have

$$\rho(\theta, s, t|Z_k) = 1 + \theta_2 \frac{(0.5t\, e^{0.1Z_{k1}})(0.5s\, e^{0.2Z_{k2}})}{(0.25 + 0.5t\, e^{0.1Z_{k2}})(0.25 + 0.5s\, e^{0.2Z_{k2}})}. \tag{4.20}$$

The simulation result from Table 14 shows that the estimating procedure works well for both settings. The bias is going to zero and the ESE is getting close to SSE as sample size increase. The coverage probability is getting around 95% for both θ_1 and θ_2.

Table 10: Scenario I: Numerical results for (β_1, β_2) with true value equals $(0.2, 0.4)$. Bias, SEE (Standard Error of Estimates), ESE (Estimated Standard Error), CP summarized for (β_1, β_2). Each entry is based on 1000 simulated datasets under shared random effect model with multiplicative marginals.

$\mu_j(t)$	θ_0	N	bias of $(\hat{\beta}_1, \hat{\beta}_2)$	SEE $(\hat{\beta}_1, \hat{\beta}_2)$	ESE$(\hat{\beta}_1, \hat{\beta}_2)$	CP
$0.25t^2$	1.25	200	(-0.0063, 0.0019)	(0.1679, 0.1569)	(0.1710,0.1600)	(0.9620, 0.9550)
		500	(0.0042, 0.0021)	(0.1080, 0.1037)	(0.1088, 0.1021)	(0.9480, 0.9490)
		800	(0.0032, -0.0046)	(0.0871, 0.0822)	(0.0861, 0.0807)	(0.9480, 0.9420)
	1.5	200	(0.0061, 0.0092)	(0.2139, 0.2072)	(0.2107, 0.2028)	(0.9460, 0.9410)
		500	(-0.0075, 0.0092)	(0.1335, 0.1320)	(0.1341, 0.1286)	(0.9470, 0.9470)
		800	(0.0029, 0.0059)	(0.1100, 0.1050)	(0.1061, 0.1020)	(0.9410, 0.9430)
	1.75	200	(-0.0199, 0.0017)	(0.2457, 0.2394)	(0.2428, 0.2365)	(0.9430, 0.9500)
		500	(-0.0066, 0.0016)	(0.1589, 0.1529)	(0.1545, 0.1507)	(0.9390, 0.9480)
		800	(-0.0066, 0.0011)	(0.1236, 0.1192)	(0.1227, 0.1190)	(0.9500, 0.9560)
$0.375t^2$	1.25	200	(0.0068, -0.0028)	(0.1565, 0.1571)	(0.1571, 0.1506)	(0.9540, 0.9420)
		500	(-0.0039, 0.0042)	(0.0990, 0.0959)	(0.0996, 0.0950)	(0.9450, 0.9480)
		800	(-0.0004, 0.0013)	(0.0816, 0.0751)	(0.0790, 0.0751)	(0.9470, 0.9550)
	1.5	200	(0.0071, 0.0017)	(0.2106, 0.1958)	(0.1987, 0.1936)	(0.9350, 0.9500)
		500	(0.0012, 0.0011)	(0.1237, 0.1316)	(0.1267, 0.1228)	(0.9600, 0.9460)
		800	(0.0023, -0.0018)	(0.1041, 0.0966)	(0.1005, 0.0975)	(0.9450, 0.9600)
	1.75	200	(-0.0046, 0.0038)	(0.2314, 0.2376)	(0.2318, 0.2279)	(0.9510, 0.9320)
		500	(-0.0051, 0.0033)	(0.1499, 0.1514)	(0.1482, 0.1456)	(0.9460, 0.9370)
		800	(-0.0002, -0.0054)	(0.1213, 0.1199)	(0.1174, 0.1156)	(0.9460, 0.9480)

Table 11: Scenario I - Estimation of θ_0 in $\rho(s,t,\theta) = \theta_0$. Bias, SEE (Standard Error of Estimates), ESE (Estimated Standard Error), CP are summarized. Each entry is based on 1000 replicates under shared random effect model with multiplicative marginals.

$\mu_{0j}(t)$	θ_0	N	Bias	SEE	ESE	CP	$\mu_{0j}(t)$	θ_0	N	Bias	SEE	ESE	CP
$0.125t^2$	1.25	200	-0.0041	0.0911	0.0878	0.9210	$0.375t^2$	1.25	200	-0.0010	0.0411	0.0386	0.9180
		500	0.0004	0.0588	0.0572	0.9420			500	-0.0003	0.0257	0.0252	0.9380
		800	-0.0002	0.0444	0.0450	0.9530			800	-0.0002	0.0206	0.0199	0.9400
	1.50	200	-0.0055	0.1273	0.1199	0.9190		1.50	200	-0.0045	0.0742	0.0702	0.9130
		500	-0.0046	0.0816	0.0789	0.9290			500	-0.0031	0.0493	0.0459	0.9170
		800	-0.0028	0.0646	0.0630	0.9380			800	-0.0010	0.0388	0.0370	0.9260
	1.75	200	-0.0082	0.1593	0.1556	0.9170		1.75	200	-0.0094	0.1081	0.1025	0.9050
		500	-0.0007	0.1109	0.1042	0.9260			500	-0.0051	0.0733	0.0697	0.9270
		800	-0.0056	0.0838	0.0825	0.9410			800	-0.0014	0.0572	0.0560	0.9350
$0.25t^2$	1.25	200	-0.0022	0.0443	0.0432	0.9220	$0.5t^2$	1.25	200	-0.0006	0.0370	0.0362	0.9300
		500	-0.0005	0.0285	0.0278	0.9370			500	-0.0004	0.0235	0.0234	0.9480
		800	-0.0009	0.0228	0.0223	0.9440			800	-0.0010	0.0192	0.0186	0.9450
	1.50	200	0.0002	0.0850	0.0759	0.9100		1.50	200	-0.0040	0.0725	0.0673	0.9230
		500	-0.0015	0.0512	0.0492	0.9440			500	-0.0015	0.0454	0.0446	0.9250
		800	-0.0008	0.0382	0.0391	0.9480			800	0.0013	0.0376	0.0362	0.9320
	1.75	200	-0.0082	0.1212	0.1078	0.8970		1.75	200	-0.0057	0.1088	0.1020	0.9170
		500	-0.0063	0.0743	0.0715	0.9230			500	0.0005	0.0715	0.0686	0.9320
		800	-0.0020	0.0613	0.0589	0.9340			800	0.0008	0.0554	0.0556	0.9370

Table 12: Scenario II - Estimation of θ_0 in $\rho(s,t,\theta) = 1+\theta_0(-0.15t+0.9)(-0.15s+0.9)$. The summary of Bias, SEE (Standard Error of Estimates), ESE(Estimated Standard Error) and CP (Coverage Probability). The marginal model is multiplicative and the parametric form of $\rho(s,t,\theta)$ is correctly specified. Each entry is based on 1000 simulations.

$\mu_{0j}(t)$	θ_0	N	Bias	SEE	ESE	CP	$\mu_{0j}(t)$	θ_0	N	Bias	SEE	ESE	CP
$0.125t^2$	0.25	200	-0.0042	0.1168	0.1140	0.9370	$0.375t^2$	0.25	200	-0.0032	0.0580	0.0579	0.9450
		500	0.0013	0.0745	0.0731	0.9480			500	0.0000	0.0395	0.0375	0.9260
		800	0.0000	0.0605	0.0581	0.9370			800	-0.0010	0.0299	0.0298	0.9570
	0.50	200	-0.0055	0.1527	0.1445	0.9280		0.50	200	-0.0038	0.0921	0.0891	0.9260
		500	0.0012	0.0967	0.0940	0.9450			500	-0.0038	0.0591	0.0587	0.9310
		800	-0.0029	0.0756	0.0745	0.9430			800	-0.0003	0.0494	0.0473	0.9340
	1	200	-0.0006	0.2424	0.2224	0.9050		1	200	-0.0182	0.1821	0.1673	0.8860
		500	-0.0045	0.1482	0.1478	0.9350			500	-0.0051	0.1143	0.1123	0.9330
		800	0.0033	0.1212	0.1185	0.9260			800	-0.0032	0.0922	0.0904	0.9310
$0.25t^2$	0.25	200	-0.0009	0.0713	0.0717	0.9370	$0.5t^2$	0.25	200	0.0004	0.0524	0.0515	0.9380
		500	-0.0012	0.0454	0.0462	0.9530			500	-0.0011	0.0342	0.0331	0.9360
		800	-0.0012	0.0370	0.0368	0.9420			800	0.0004	0.0266	0.0264	0.9410
	0.50	200	-0.0042	0.1075	0.1040	0.9320		0.50	200	-0.0082	0.0890	0.0835	0.9120
		500	-0.0005	0.0683	0.0678	0.9390			500	-0.0001	0.0556	0.0553	0.9380
		800	-0.0027	0.0564	0.0538	0.9390			800	-0.0009	0.0437	0.0438	0.9500
	1	200	-0.0170	0.1893	0.1781	0.8960		1	200	-0.0058	0.1789	0.1624	0.8860
		500	0.0008	0.1201	0.1208	0.9350			500	-0.0037	0.1173	0.1091	0.9240
		800	-0.0068	0.1040	0.0963	0.9210			800	-0.0043	0.0895	0.0863	0.9190

Table 13: Scenario III - Bias, SEE (Standard Error of Estimates), ESE (Estimated Standard Error), CP of θ in $\rho(\theta; Z_k) = \theta_1 I(Z_k = 1) + \theta_2 I(Z_k = 0)$, with true value $\theta_1 = 1.25$ and $\theta_2 = 1.75$. Each entry is based on 1000 simulations.

		θ_1				θ_2			
$\mu_{0j}(t)$	N	Bias	SEE	ESE	CP	Bias	SSE	ESE	CP
$0.125t^2$	200	-0.0045	0.0885	0.0843	0.9200	-0.0164	0.2187	0.1880	0.8950
	500	-0.0020	0.0590	0.0557	0.9420	-0.0139	0.1352	0.1266	0.9120
	800	0.0007	0.0447	0.0444	0.9530	-0.0033	0.1069	0.1039	0.9320
	1100	0.0006	0.0378	0.0382	0.9560	0.0007	0.0950	0.0899	0.9400
$0.25t^2$	200	-0.0040	0.0639	0.0608	0.9170	-0.0174	0.1691	0.1527	0.8770
	500	0.0010	0.0440	0.0401	0.9270	-0.0007	0.1149	0.1061	0.9210
	800	-0.0009	0.0326	0.0319	0.9410	-0.0007	0.0934	0.0860	0.9150
	1100	-0.0009	0.0278	0.0278	0.9490	-0.0032	0.0826	0.0737	0.9240
$0.375t^2$	200	-0.0039	0.0563	0.0532	0.9150	-0.0129	0.1622	0.1434	0.8900
	500	-0.0029	0.0364	0.0347	0.9250	-0.0050	0.1048	0.0983	0.9280
	800	0.0002	0.0292	0.0283	0.9310	-0.0022	0.0846	0.0804	0.9310
	1100	0.0011	0.0258	0.0245	0.9380	-0.0019	0.0713	0.0698	0.9390
$0.5t^2$	200	-0.0035	0.0530	0.0499	0.9150	-0.0142	0.1643	0.1399	0.8820
	500	-0.0025	0.0335	0.0326	0.9360	-0.0014	0.1041	0.0959	0.9310
	800	-0.0007	0.0268	0.0263	0.9490	-0.0029	0.0853	0.0784	0.9190
	1100	-0.0003	0.0229	0.0227	0.9470	-0.0012	0.0693	0.0668	0.9250

Table 14: Scenario IV - estimates θ_1, θ_2 in the underline models where $\rho(\theta, s, t; Z_k) = 1 + \theta_1 \frac{(0.25te^{0.1Z_{k1}})(0.25se^{0.2Z_{k2}})}{(0.25+0.25te^{0.1Z_{k1}})(0.25+0.25se^{0.2Z_{k2}})}$ and $\rho(\theta, s, t; Z_k) = 1 + \theta_2 \frac{(0.5te^{0.1Z_{k1}})(0.5se^{0.2Z_{k2}})}{(0.25+0.5te^{0.1Z_{k1}})(0.25+0.5se^{0.2Z_{k2}})}$. With the true values of θ_1, θ_2 equal to 0.25, 0.5, 0.75 and 1.00. Summary of Bias, SEE (Standard Error of Estimates), ESE (Estimated Standard Error), CP of θ where each entry is based on 1000 simulations. The averaged observed events for type 1(2) event is 2.44(2.56)

θ_1	N	Bias	SEE	ESE	CP	θ_2	Bias	SEE	ESE	CP
0.25	200	-0.0020	0.0804	0.0798	0.9420	0.25	-0.0036	0.0523	0.0498	0.9280
	500	0.0012	0.0508	0.0518	0.9550		0.0000	0.0335	0.0328	0.9360
	800	0.0009	0.0420	0.0411	0.9490		-0.0002	0.0275	0.0260	0.9390
	1100	-0.0006	0.0345	0.0350	0.9500		0.0010	0.0232	0.0224	0.9490
0.50	200	-0.0012	0.1237	0.1130	0.9170	0.50	-0.0015	0.0908	0.0835	0.9220
	500	0.0004	0.0763	0.0735	0.9260		-0.0059	0.0551	0.0531	0.9170
	800	-0.0007	0.0617	0.0590	0.9400		0.0008	0.0448	0.0436	0.9370
	1100	0.0000	0.0488	0.0503	0.9420		-0.0020	0.0377	0.0370	0.9320
0.75	200	-0.0094	0.1584	0.1471	0.9090	0.75	-0.0097	0.1286	0.1149	0.8800
	500	0.0004	0.1067	0.0993	0.9240		-0.0033	0.0841	0.0793	0.9070
	800	-0.0002	0.0275	0.0260	0.9390		-0.0020	0.0612	0.0628	0.9400
	1100	0.0010	0.0232	0.0224	0.9490		-0.0030	0.0524	0.0539	0.9430
1.00	200	-0.0015	0.0908	0.0835	0.9220	1.00	-0.0035	0.1797	0.1587	0.8730
	500	-0.0059	0.0551	0.0531	0.9170		0.0011	0.1079	0.1056	0.9280
	800	0.0008	0.0448	0.0436	0.9370		-0.0028	0.0833	0.0827	0.9330
	1100	-0.0020	0.0377	0.0370	0.9320		-0.0074	0.0771	0.0719	0.9190

4.2 Hypothesis testing of the rate ratio

4.2.1 Procedure description

For the case that the marginal mean rate model is additive, we developed a supreme test statistic to check the null hypothesis $\rho(s,t,\theta)=\theta_0$. We apply the same procedure and illustrate the test statistic below for hypothesis testing purposes. Define the residual process under the multiplicative marginal mean rate model as

$$V^c(s,t,\tilde{\theta},\hat{\mu}_1(\cdot;z_{k1}),\hat{\mu}_2(\cdot;z_{k2}))=N^{-1/2}\sum_{k=1}^{N}V_k^c(s,t,\tilde{\theta},\hat{\mu}_1(\cdot;z_{k1}),\hat{\mu}_2(\cdot;z_{k2})), \tag{4.21}$$

where

$$\begin{aligned}&V_k^c(s,t,\tilde{\theta},\hat{\mu}_1(\cdot;z_{k1}),\hat{\mu}_2(\cdot;z_{k2}))=\\&\int_0^t\int_0^s w(u,v)\frac{\partial\rho(u,v,\theta)}{\partial\theta}\Big|_{\theta=\tilde{\theta}}\Big\{\,dN_{k1}(u)dN_{k2}(v)\\&-\rho(u,v,\tilde{\theta})Y_{k1}(u)d\mu_{01}(u)e^{\beta_1^TZ_{k1}(u)}\cdot Y_{k2}(v)d\mu_{02}(v)e^{\beta_2^TZ_{k2}(v)}\Big\}.\end{aligned} \tag{4.22}$$

We define a Supreme test statistic

$$T=\sup_{s,t\in[0,\tau]}\parallel V^c(s,t,\tilde{\theta},\hat{\mu}_1(\cdot;z_{k1}),\hat{\mu}_2(\cdot;z_{k2}))\parallel. \tag{4.23}$$

Similarly, to access the empirical distribution of T, firstly we approximate it by the first-order Taylor expansion,

$$\begin{aligned}&V^c(s,t,\tilde{\theta},\hat{\mu}_1(\cdot;z_{k1}),\hat{\mu}_2(\cdot;z_{k2}))\\&=V^c(s,t,\theta,\hat{\mu}_1(\cdot;z_{k1}),\hat{\mu}_2(\cdot;z_{k2}))+N^{-1/2}\frac{\partial V^c(s,t,\theta,\hat{\mu}_1(\cdot;z_{k1}),\hat{\mu}_2(\cdot;z_{k2}))}{\partial\theta}N^{1/2}(\tilde{\theta}-\theta)\\&\quad+o_p(1),\end{aligned} \tag{4.24}$$

where

$$V^c\big(s,t,\theta,\hat{\mu}_1(\cdot;z_{k1}),\hat{\mu}_2(\cdot;z_{k2})\big)$$
$$= N^{-1/2}\sum_{k=1}^{N}\Big\{V_k^c\big(s,t,\theta,\mu_1(\cdot;z_{k1}),\mu_2(\cdot;z_{k2})\big)+\Upsilon_{k1}^c(s,t)+\Upsilon_{k2}^c(s,t)\Big\}+o_p(1),$$

and

$$N^{-1/2}\frac{\partial V^c\big(s,t,\theta,\hat{\mu}_1(\cdot;z_{k1}),\hat{\mu}_2(\cdot;z_{k2})\big)}{\partial\theta}N^{1/2}(\tilde{\theta}-\theta)$$
$$= N^{-1/2}\big\{\zeta_{k1}^c(s,t,\theta)+\zeta_{k2}^c(s,t,\theta)\big\}+o_p(1). \tag{4.25}$$

Therefore equation (4.24) can be written as

$$V^c\big(s,t,\tilde{\theta},\hat{\mu}_1(\cdot;z_{k1}),\hat{\mu}_2(\cdot;z_{k2})\big)$$
$$= N^{-1/2}\sum_{k=1}^{N}\Big\{V_k^c\big(s,t,\theta,\mu_1(\cdot;z_{k1}),\mu_2(\cdot;z_{k2})\big)+\Upsilon_{k1}^c(s,t)+\Upsilon_{k2}^c(s,t)$$
$$+\zeta_{k1}^c(s,t,\theta)+\zeta_{k2}^c(s,t,\theta)\Big\}+o_p(1) \tag{4.26}$$

Next, we apply the Gaussian multiplier method by multiplying random numbers G_k from normal distribution, so that

$$V^*(s,t,\tilde{\theta})$$
$$= N^{-1/2}\sum_{k=1}^{N}\Big\{V_k^c\big(s,t,\theta,\mu_1(\cdot;z_{k1}),\mu_2(\cdot;z_{k2})\big)$$
$$+\hat{\Upsilon}_{k1}^c(s,t,\hat{\theta})+\hat{\Upsilon}_{k2}^c(s,t,\hat{\theta})+\hat{\zeta}_{k1}^c(s,t)+\hat{\zeta}_{k2}^c(s,t)\Big\}\cdot G_k \tag{4.27}$$

By taking the supremum of $V^*(s,t,\tilde{\theta})$ among mesh grids of (s,t), we obtain T^* from the empirical distribution of $\sup_{s,t\in[0,\tau]^2}\parallel V^*(s,t,\tilde{\theta})\parallel$. Repeating above the process 1000 times enables us to have enough observations and we would reject the

$H_0 : \rho(s,t,\theta) = \theta_0$ when T^* excesses the 95th percentile of the observations.

4.2.2 Simulation studies

Here, we hope to answer two questions: (1)Are the two event processes independent? (2) If not, is the association constant? Firstly, to detect the dependency, we consider the independent bivariate counting processes as the null model and the constant rate ratio as alternative model. Secondly, we propose the constant rate ratio model as the null and Piecewise Constant (PWC), Time Dependent (TD), Time and Covariate Dependent (TCD) models as the corresponding alternatives.

To investigate the performance of the model checking procedure, finite sample studies are conducted, with multiplicative mean rate marginal model. The size and power of the hypothesis test are also computed via Gaussian Multiplier Method.

4.2.2.1 Test for constant association with multiplicative marginal models

We consider the shared frailty model below as the null model

$$E[dN^*_{k1}(s)|R_k, Z_{k1}(s)] = R_k e^{\beta_1^T Z_{k1}(s)}\, d\mu_{01}(s),$$

$$E[dN^*_{k2}(t)|R_k, Z_{k2}(t)] = R_k e^{\beta_2^T Z_{k2}(t)}\, d\mu_{02}(t),$$

where R_k is independent and comes from a Gamma Distribution. Following from Proposition 1, under the null model, we have $\rho(\theta, s, t) = 1 + \sigma^2/\mu^2$ where σ^2 and μ^2 represent E(R_k) and var(R_k). Let $\beta_{01} = 0.2$, $\beta_{02} = 0.4$, $\tau = 4$ and the censoring time follow uniform$(3, 4)$. We take baseline rate $\mu_{01}(t) = \mu_{02}(t)$ and set the values equal to $0.25t^2, 0.375t^2, 0.5t^2$ to represent moderately or more frequently observed events. The event count after censoring ranges from 4.18 to 11.30. To accommodate the

association strength, we generate R_k from Gamma distribution with $\mathrm{E}(R_k) = 1$ and $\mathrm{var}(R_k) = 0.25, 0.5, 0.75, 1$ so that $\rho = 1.25, 1.5, 1.75$ and 2 respectively.

As we can see, the null model corresponds to $H_0 : \rho(\theta, s, t) = \theta$. Implementing the Gaussian Multiplier method enables us to approach the empirical distribution of the supreme residuals under the H_0. Therefore the rejection rate under the H_0 can be used as an empirical size of the test and should be around its nominee value. The simulation result summarized in Table 16 shows the test has size below or around 0.05 consistently which agrees with the theoretical value.

Similar to the illustration in section 3.2.2.2, we propose the PWC, TD and TCD model as alternative models to exam the power of the testing procedure. The adjustment is concerned with the marginal mean rate, which should be multiplicative in the following sections.

(I) The piecewise constant rate ratio model - PWC model

Assume $\tau = 4$ and analogous to equation (3.28),the counting process $N^*_{kj}(t)$ is from

$$E[dN^*_{kj}(t)|R_k(t), Z_{kj}(t)] = R_k(t)\{d\mu_{0j}(t)e^{\beta_j^T Z_{kj}(t)}\}. \tag{4.28}$$

where $R_k(t) = I(t < 2)R_{k0} + I(t > 2)R_{k1}$ is time varying frailty. Let $\beta_{01} = 0.2$, $\beta_{02} = 0.4$, C_{kj} be uniform on $(3, 4)$ and Z_{kj} follows Uniform$(0, 1)$. To modify the events observed before censoring, we take $\mu_{0j}(t)$ equal to $0.125t^2$, $0.25t^2$, $0.375t^2$, $0.5t^2$. Consider R_{k0} and R_{k1} are independently generated from Gamma(a_0, b_0) and Gamma(a_1, b_1), where the choice of parameters represent the value of the piecewise rate ratio. The simulation settings are summarized in the Table 15 and Figure 3.

PWC models are alternatives to the null model and therefore the residuals calculated under H_0 should depart far away from zero. We would expect the supreme test statistic to go beyond threshold with high likelihood and a high rejection rate is an indicator of the power. 17 shows the proposed procedure can correctly detect non constant rate ratio at or above 95% of the cases when sample size is large ($N = 800$) and the accuracy is improved by increasing the sample size.

(II) Time dependent rate ratio - TD model

Consider the Bivariate Counting Process described by equation (3.29). Assume the Poisson process $N_{k0}(t)$ has conditional mean rate

$$E[dN_{k0}(t)|Z_{kj}(t), R_k] = \lambda_{k0}(t|Z_{kj}(t), R_k)\, dt$$

and

$$\lambda_{k0}(t|Z_{kj}(t), R_k)\, dt = R_k \cdot d\mu_{0j}(t) e^{\beta_{0j} Z_{kj}(t)}, \tag{4.29}$$

with R_k is the cluster level random effect. Let the conditional mean rate of Poisson process be $\widetilde{\lambda}_{kj}(t|Z_{kj}(t))$ and by assigning an appropriate value, we can generate the counting processes $N_{k1}(t)$ and $N_{k2}(s)$ with rate ratio

$$\rho(\theta, s, t) = 1 + \theta(-0.15s + 0.9)(-0.15t + 0.9).$$

where $\theta = \frac{\sigma^2}{\mu^2}$. To consider rare, moderate and high time dependent association, we generate $\theta = 0.5, 1, 1.5, 2$ by taking R_k from Gamma distribution, where the shape and scale parameter pairs in the Gamma Distribution are $(2, 0.5)$, $(1, 1)$, $(0.67, 1.5)$ and $(0.5, 2)$. The color plots for the four settings are also illustrated by Figure 4.

The goodness of fit procedure is more likely to detect non-constant rate ratio for a more varying scenario or a larger sample case. It is observed in Table 18 that the time dependent rate ratio and piecewise constant rate ratio model have similar simulation performance.

(III) Time and covariate dependent model - TCD model

The time and covariate dependent rate ratio can be derived by comparing to section 3.2.2.2. Assume the Poisson process $N_{k0}(t)$ has marginal conditional rate $\lambda_0(t)$ where $\lambda_0(t|Z_{kj}(t), R_k)\, dt, = R_k \cdot d\mu_{0j}(t) e^{\beta_{0j} Z_{kj}(t)}$ with R_k the random frailty. By Proposition 1, $\rho(\theta, s, t; z_1, z_2) = 1 + \sigma^2/\mu^2$, where σ^2 and μ represent the variance and mean of R_k. Let the Poisson process $\widetilde{N}_{kj}(t)$ has rate $\widetilde{\lambda}_{kj}$ =1. Following Proposition 3, the rate ratio of $\{N_{k1}(s), N_{k2}(t)\}$ is equivalent to

$$\rho(\theta, s, t; z_1, z_2) = 1 + \theta \frac{\lambda_0(s|z_1)\lambda_0(t|z_2)}{(1 + \lambda_0(s|z_1))(1 + \lambda_0(t|z_2))},$$

where $\theta = \sigma^2/\mu^2$.

To generate $\theta = 0.25, 0.5, 1, 2$, we consider R_k be from Gamma distribution with $\mu = 1$ and $\sigma^2 = 0.25$, 0.5, 1, 2. Let $\tau = 4$, $\beta_{01} = 0.1$, $\beta_{02} = 0.2$ and $\mu_{0j}(t) = 0.125t^2$, $0.25t^2$, $0.375t^2$, $0.5t^2$ for $j = 1$ or 2. Take the censoring time and covariates from uniform distribution on (3, 4) and (1, 2) respectively. The rate ratio is in form of

$$\rho(\theta, s, t; z_1, z_2) = 1 + \theta \frac{\lambda_0(s|z_1)\lambda_0(t|z_2)}{(1 + \lambda_0(s|z_1))(1 + \lambda_0(t|z_2))},$$

Table 19 summarizes of the simulation result for the above settings, from which similar patterns of PWC and TD models are shown. In general the test performs well and can distinguish the null model and alternative models with high precision,

especially when the sample size is large or the variability of association is increasing.

Table 15: Summary of simulation settings under the PWC model with the corresponding θ values followed from Proposition 2. The marginal model is multiplicative.

Settings	PWC_1	PWC_2	PWC_3	PWC_4
$R_{k0}: \ (a_0, b_0)$	(4, 0.25)	(4, 0.25)	(2, 0.5)	(4, 0.25)
$R_{k1}: \ (a_1, b_1)$	(2, 0.5)	(1.33,0.75)	(1, 1)	(1, 1)
$\rho(s<2, t<2)$	1.25	1.25	1.5	1.25
$\rho(s>2, t<2)$	1	1	1	1
$\rho(s>2, t>2)$	1.5	1.75	2	2

Figure 3: Visualization of piecewise constant $\rho(s, t, \theta)$ (PWC) under the multiplicative marginal mean rate models. The variation of $\rho(s, t)$ between different pieces is growing from PWC_1 to PWC_4.

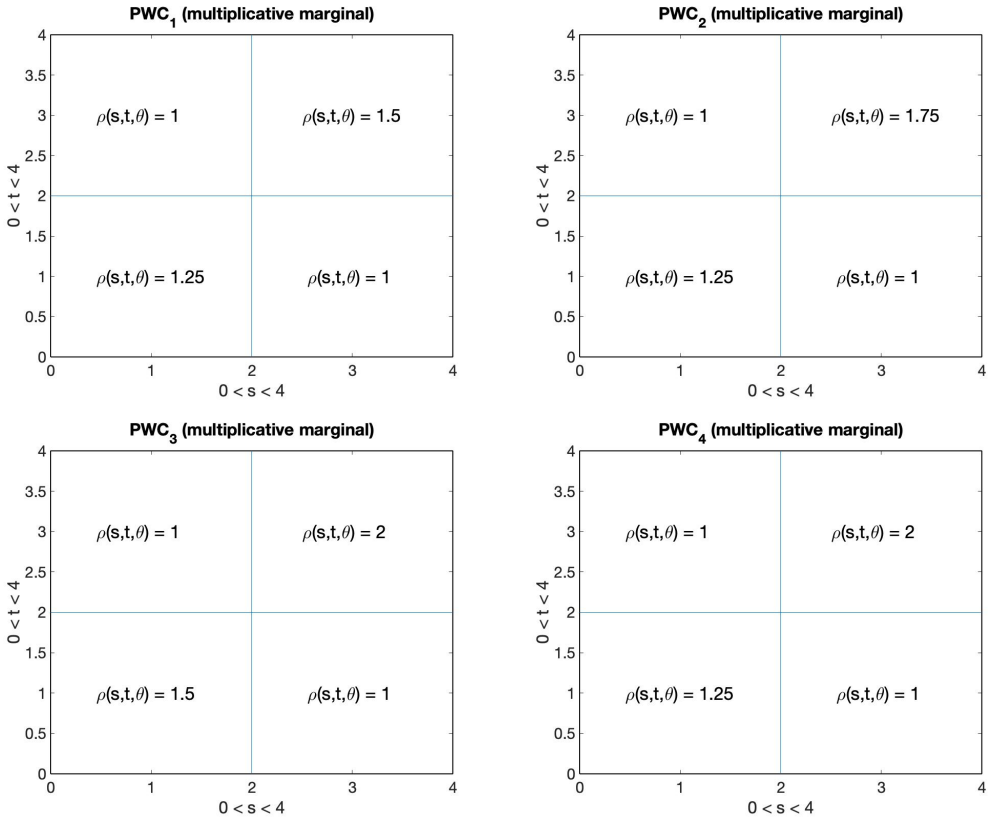

Figure 4: The contour plot of the rate ratio $\rho(s,t)$ under the multiplicative marginal models. The x-axis and y-axis represent the observation time for type1 and type2 events. From upper left to lower right, the heterogeneity of $\rho(s,t)$ is increased.

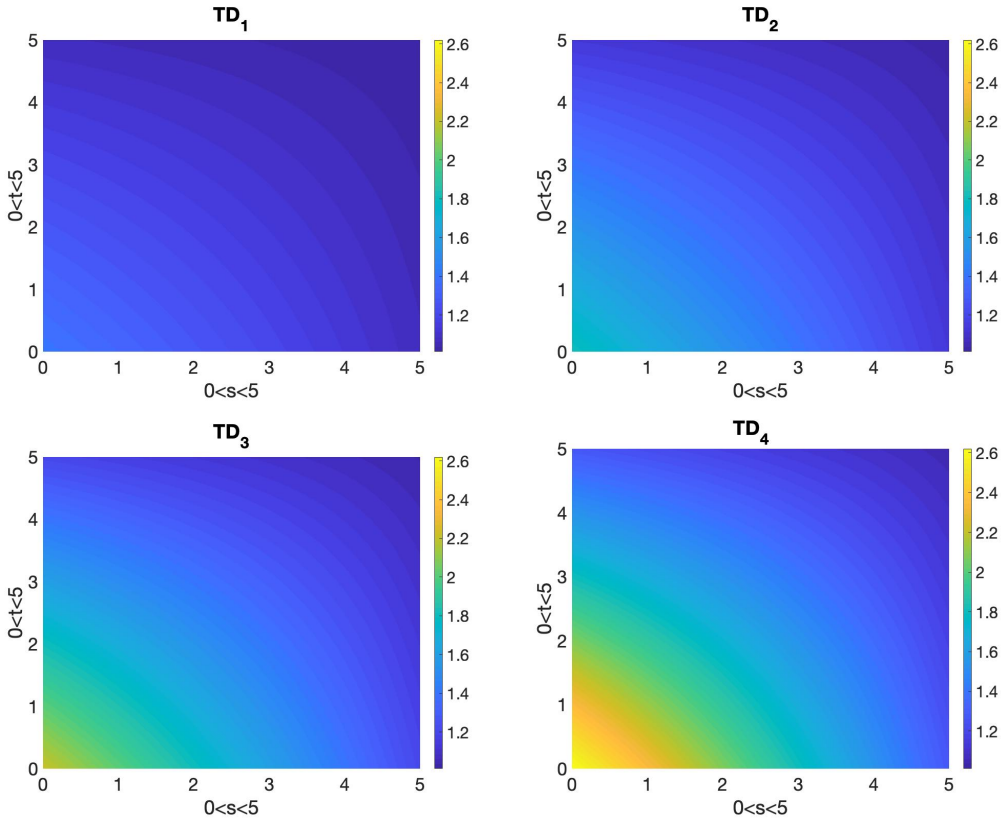

Table 16: Observed size of the test statistic T for the proposed model-checking procedure under $H_0 : \rho(\theta, s, t) = \theta_0$ vs $Ha : \rho(\theta, s, t) \neq \theta_0$, at significance level 0.05. The numbers in the parentheses represent the average observed count of type 1 and type 2 event after censoring. Each entry is calculated based on 1000 Gaussian multiplier samples and 1000 replicates.

		Size				
event counts	$\mu_{0j}(t)$	N	$\theta_0 = 1.25$	$\theta_0 = 1.5$	$\theta_0 = 1.75$	$\theta_0 = 2$
(4.18,5.67)	$0.25t^2$	200	0.041	0.025	0.037	0.034
		500	0.038	0.042	0.033	0.033
(6.25, 8.48)	$0.375t^2$	200	0.042	0.035	0.030	0.021
		500	0.040	0.037	0.039	0.037
(8.34, 11.30)	$0.5t^2$	200	0.040	0.037	0.003	0.030
		500	0.043	0.043	0.032	0.037

Table 17: Power of $H_0 : \rho(\theta, s, t) = \theta_0$ vs $Ha : \rho(\theta, s, t) \neq \theta_0$. The H_a model has piecewise constant rate ratio (PWC model). Each entry is calculated based on 1000 Gaussian multiplier samples with 1000 replicates.

		Power				
event counts	$\mu_{0j}(t)$	N	PWC_1	PWC_2	PWC_3	PWC_4
(2.09, 2.83)	$0.125t^2$	200	0.443	0.882	0.777	0.942
		500	0.934	0.999	0.994	0.999
		800	0.995	1.000	1.000	1.000
(4.16, 5.65)	$0.25t^2$	200	0.867	0.977	0.951	0.987
		500	0.998	1.000	1.000	0.999
		800	1.000	1.000	1.000	1.000
(6.25, 8.48)	$0.375t^2$	200	0.955	0.993	0.968	0.991
		500	1.000	1.000	1.000	1.000
		800	1.000	1.000	1.000	1.000
(8.34, 11.32)	$0.5t^2$	200	0.985	0.994	0.986	0.995
		500	1.000	1.000	0.999	1.000
		800	1.000	1.000	1.000	1.000

Table 18: Power of $H_0 : \rho(\theta, s, t) = \theta_0$ vs $Ha : \rho(\theta, s, t) \neq \theta_0$. The H_a model is time and dependent (TD). Each entry is calculated based on 1000 Gaussian multiplier samples with 1000 replicates.

		Power			
$\mu_{0j}(t)$	N	TD_1	TD_2	TD_3	TD_4
$0.125t^2$	200	0.129	0.252	0.308	0.355
	500	0.295	0.560	0.706	0.782
	800	0.463	0.817	0.906	0.932
$0.25t^2$	200	0.238	0.415	0.524	0.556
	500	0.587	0.862	0.929	0.940
	800	0.768	0.974	0.990	0.986
$0.375t^2$	200	0.337	0.518	0.598	0.675
	500	0.748	0.933	0.961	0.947
	800	0.931	0.991	0.994	0.995
$0.5t^2$	200	0.433	0.578	0.691	0.674
	500	0.826	0.949	0.962	0.968

Table 19: Power of $H_0 : \rho(\theta, s, t) = \theta_0$ vs $Ha : \rho(\theta, s, t) \neq \theta_0$. The H_a model is time and covariate dependent (TCD). Each entry is calculated based on 1000 Gaussian multiplier samples and 1000 replicates.

		Power			
$\mu_{0j}(t)$	N	TCD_1	TCD2	TCD3	TCD4
$0.125t^2$	200	0.102	0.226	0.453	0.706
	500	0.208	0.520	0.916	0.991
$0.25t^2$	200	0.175	0.417	0.704	0.798
	500	0.508	0.923	0.988	0.977
$0.375t^2$	200	0.246	0.480	0.701	0.727
	500	0.650	0.946	0.983	0.963
$0.5t^2$	200	0.210	0.437	0.566	0.631
	500	0.658	0.952	0.972	0.949

CHAPTER 5: DATA APPLICATION

5.1 The hemodialysis (HEMO) study

5.1.1 Study design

The HEMO study was a 2-by-2 prospective, randomized, multicenter clinical trial of dialysis prescriptions for patients at end-stage renal disease (Greene et al., 2000). The HEMO study design has 2 levels of dose: standard dose and high dose (equilibrated Kt/V levels of 1.05 and 1.45, respectively), and two membrane types: low-flux dialyzers (mean β_2-microglobulin clearance of <10 ml/min) and high-flux dialyzers (mean β_2-microglobulin >20 ml/min). The study randomized 1846 patients between March 1995 and October 2000; follow-up continued until December 31, 2001.The maximum follow-up period for individual patients was between 0.9 and 6.6 years, depending on the randomization date. Fifteen clinical centers, with a total of 72 dialysis facilities were involved in this study. 926 patients enrolled in the standard ktv group, while 920 patients were in the high dose group. In terms of flux types, there were 925 patients in low-flux and another 921 were assigned in high-flux group. The patient enrollment is summarized in Table 20.

5.1.2 Hospitalization review

The primary outcome of the study was all-cause mortality. Since Cardiac disease is the leading cause of death among dialysis patients, and infections are one of the main concerns, various predefined hospitalizations and death due to cardiac or infectious causes (Cheung et al., 2004; Rocco et al., 2002) are considered as the secondary outcomes. The HEMO study recorded hospitalizations due to cardiac causes, which included angina, myocardial infarction (MI), congestive heart failure(CHF), arrhythmias and other heart diseases (valvular diseases, pericarditis, and endocarditis). Hospitalization due to infectious causes includes Bacteremia-sepsis infection (BACTSEP), or Soft tissue-cellulitis infection(TISSUE). Each hospitalization or death could potentially be attributed to one or multiple causes.

A total of 1503 patients experienced 7832 hospitalizations during the study period, 6 hospitalizations occurred before the randomization of the HEMO study and were removed. The cleaned data set has 7826 eligible hospitalization records for 1502 patients. 343 of them were censored because they either transferred to non-trial clinical centers, received kidney transplantation, died or because the study ended.

The hospitalization classifications from clinical centers are summarized in Table 21. The label 'Any Cardiac' consists of hospitalization caused by Angina, Arrhythmia, Arrhythmias, CHF, MI, or other heart diseases and the next five labels are broken down by specific causes. 22.51% (1762 of 7826) of all hospitalizations were identified as Any Cardiac, whereas 22.23% (1740 of 7826) are classified as Any infection, leaving 55.24% classified as noncardiac and non-infection. Among Cardiac diseases, Ar-

rhythmia and CHF attribute to the most classified hospitalizations, whereas Angina, Arrhythmia, and CHF are common among patients (more than 23%).

Hospitalizations with missing causes are excluded since they only comprise less than 1% of the composite cardiac and infection hospitalizations. We show baseline characteristics of the study cohort in Table 22 and Figure 5. The age of patients ranged from 18 to 80, with a median 61, mean 58.21 and the standard deviation 13.66. The prior years of dialysis before entering the HEMO study varies a lot: mean duration is 3.78, standard deviation is 4.37, the shortest duration is 0.19 year (about 69 days) while the longest is 31.27 years. Half of the patients have been on dialysis for less than 2.2 years.Kaysen (2003) found that serum albumin is lower than normal range among dialysis patients and resistant to therapy since the simultaneous occurrence of decreased protein intake and inflammation prevent these homeostatic compensations to reduced nitrogen and energy intake from occurring. The baseline albumin of the study cohort ranges from 2.55 to 4.90, with 3.60 as the mean level and 0.3569 as the standard error.

To better understand the patient demography factors and their impact on hospitalization, we summarized the average frequency of cardiac and infectious hospitalizations in Table 23, Figure 6 and Figure 7. The qualitative covariates are sex, race, diabetes status, Ktv dose, flux level and ICED score, the last one of which is the index of comorbidity where a higher value indicates a more severe degree. Females, nonblack, diabetic patients or those with more severe comorbidities have more averaged cardiac hospitalizations. Patients receiving high-flux dialyzer or high dose Ktv treatment have higher cardiac hospitalization rates. In terms of infectious hospital-

izations, females, black or diabetic patients, or those who had standard Ktv dose or low-flux dialyzer have more frequent admissions.

Table 20: A 2 by 2 balanced factor design. 1846 patients randomized into the combination of two flux levels and ktv doses.

	low-flux	high-flux	total
standard-ktv	467	459	926
high-ktv	458	462	920
total	925	921	1846

Table 21: Clinical center classifications of hospitalizations due to cardiovascular and infections. Total hospitalization N=7826 cases confirmed or missing (N/A).

clinical center classification	classified hospitalization	N/A hospitalization	Patients (%)
Any Cardiac	1762	17	808 (53.79%)
Angina	360	4	427 (28.43%)
Arrhythmia	657	5	360 (23.97%)
CHF (congestion heart failure)	722	10	418 (27.83%)
MI (myocardial infarction)	256	8	201 (13.38%)
Other heart diseases	207	9	161 (10.72%)
Any infection	1740	1	834 (55.52%)
Bacteremia or sepsis infection (BACT-SEP)	811	1	516 (34.35%)
Soft tissue, cellulitis infection (Tissue-Infection)	1298	1	693 (46.14%)

Table 22: Baseline characteristics of the study cohort (N=1502).

Factors	Mean	Sd	Min	25th	Median	75th	Max
Age (years)	58.21	13.66	18	49	61	69	80
Duration (years)	3.78	4.37	0.19	0.95	2.20	4.75	31.27
BALB (albumin, g/dL)	3.61	0.36	2.55	3.37	3.60	3.85	4.90
Follow-up (years)	2.82	1.79	0.022	1.30	2.50	4.22	6.64

Figure 5: Visualizing the baseline characteristics of the study cohort (N=1502).

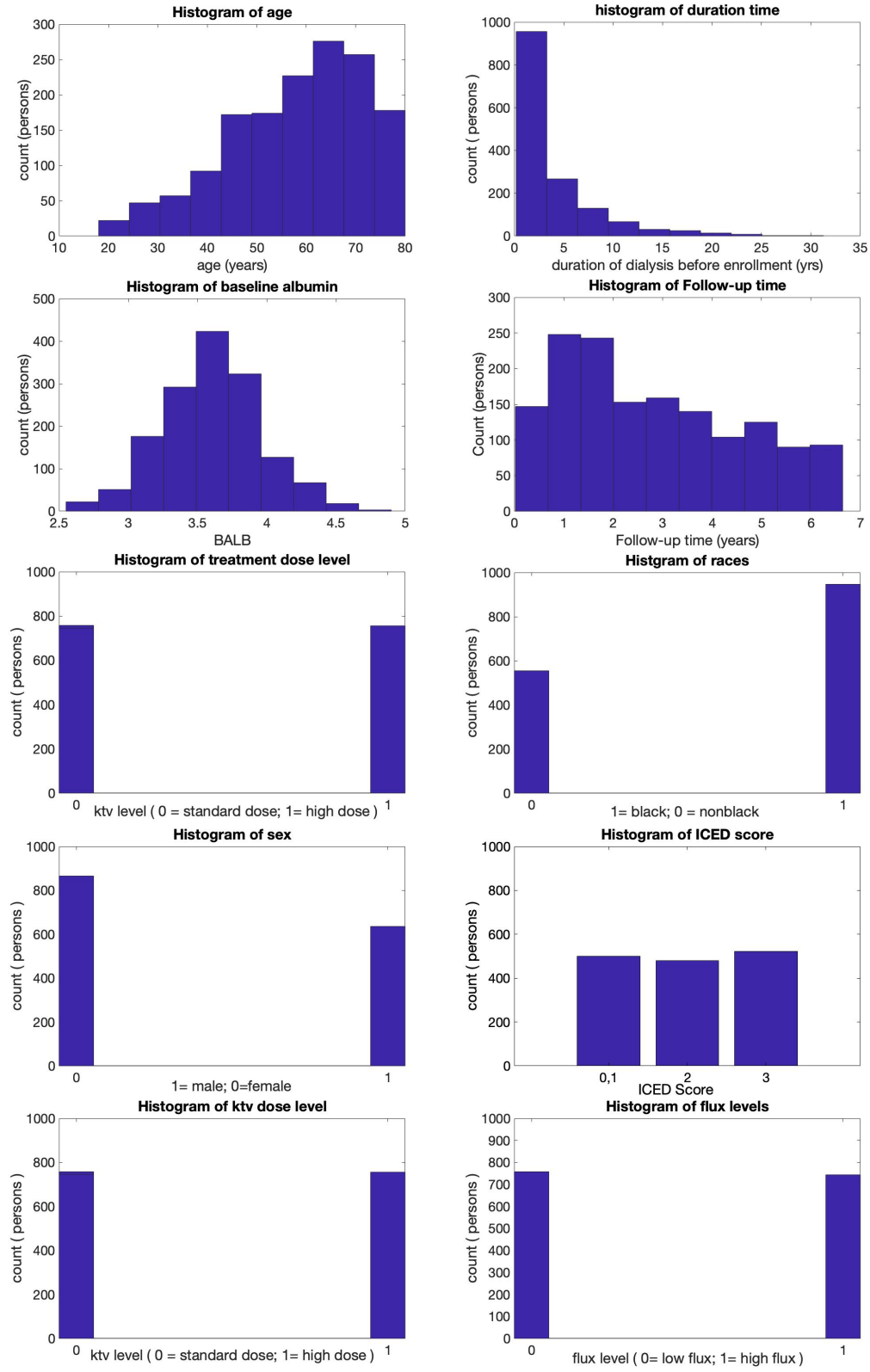

Table 23: Mean hospitalization frequency of the study cohort (N=1502).

Factors	level	%Patients	Cardiac	Infectious
Sex	male=1	42.34%	1.12	1.11
	female=0	57.66%	1.21	1.19
Race	black=1	63.05%	1.16	1.19
	nonblack=0	36.95%	1.20	1.11
Diabetic	Yes=1	46.80%	1.25	1.34
	No=0	53.20%	1.11	1.00
Ktv dose	standard=0	49.67%	1.14	1.19
	high=1	50.33%	1.21	1.12
Flux level	low=0	50.47%	1.15	1.17
	high=1	49.53%	1.20	1.14
ICED	score =0,1	33.36%	0.90	0.93
	score =2	31.89%	1.43	1.23
	score =3	34.75%	1.21	1.32

Figure 6: Mean hospitalizations caused by cardiac diseases (angina, arrhythmias, congestive heart failure (CHF), myocardial infarction (MI) and other cardiovascular diseases). Grouped by diabetes status, race, sex, ICED scores, Ktv doses, and flux types.

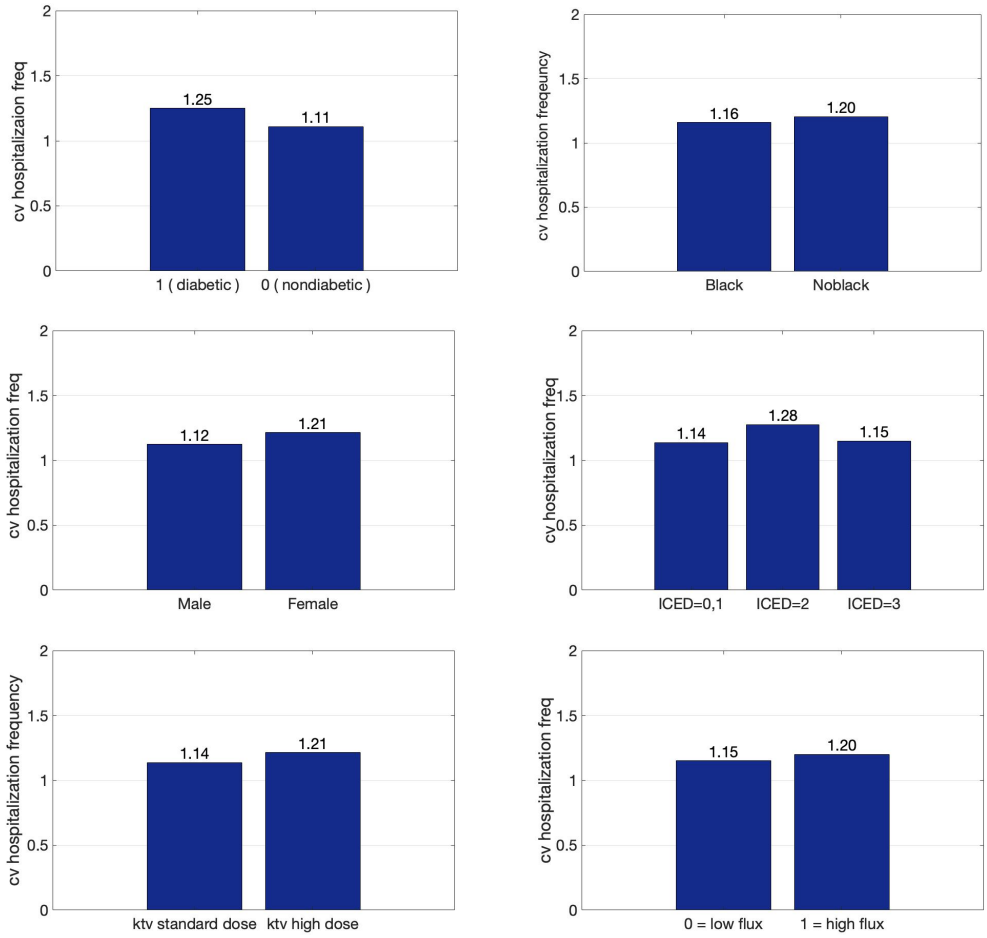

Figure 7: Mean hospitalizations caused by infections (including Bacteremia-sepsis infection (BACT-SEP), or Soft tissue-cellulitis (Tissue) infection). Grouped by diabetes status, race, sex, ICED scores, Ktv doses, and flux types.

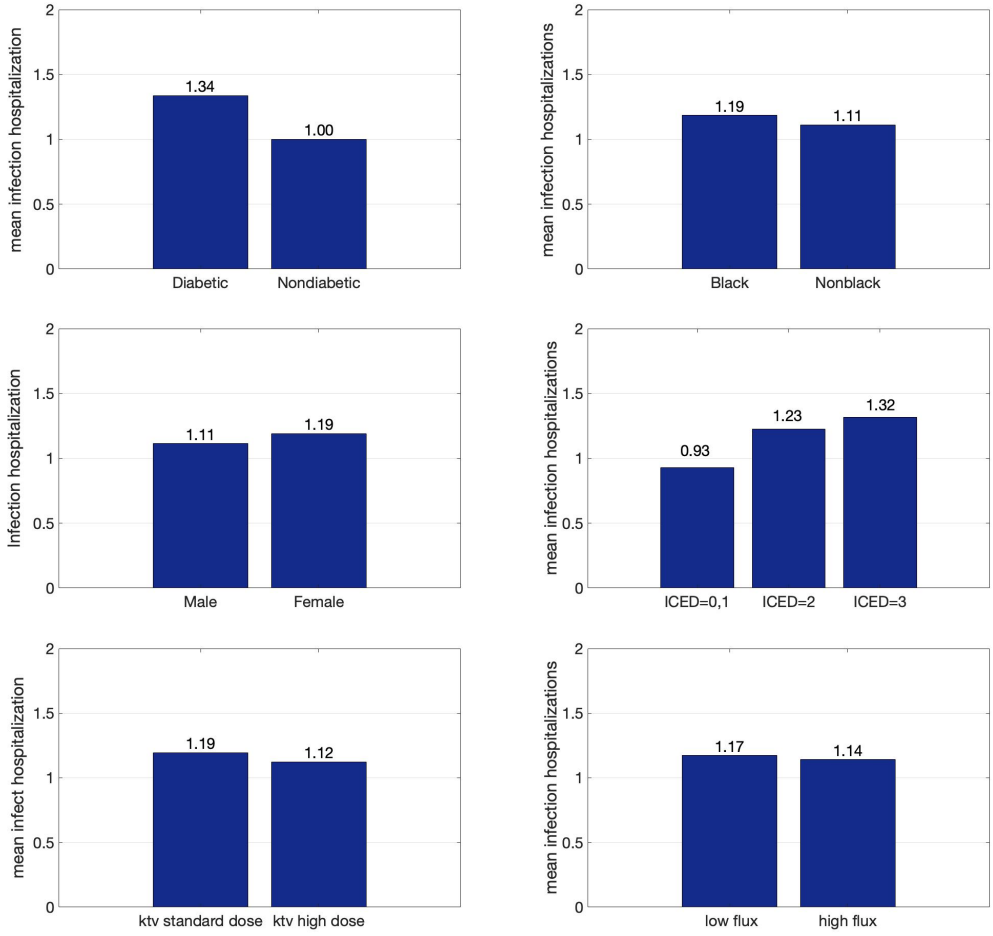

5.2 Application 1: the rate ratio between composite cardiac and infection hospitalizations

In Table 21, 808 patients experienced 1762 composite cardiac (Angina, Arrhythmia, CHF, MI or other heart diseases) hospitalizations, which is similar to hospitalizations caused by infections. Cardiovascular diseases and infections are common among dialysis patients and we are interested to investigate their associations. The rate ratio we proposed, by definition, can compare the rate of cardiac hospitalizations conditional on infections information to the mean rate of cardiac hospitalizations alone. It enables us to know if and how the occurrence of infections would impact on the rate of cardiac hospitalizations.

In this data application, the bivariate counting processes are composite cardiac and infectious hospitalizations. To estimate the rate ratio, we first model the mean rate of cardiac and infectious hospitalizations separately by the additive model, i.e.

$$E[dN_1(s)|Z_1] = d\mu_1(s) + \beta_1 Z_1,$$

$$E[dN_2(t)|Z_2] = d\mu_2(t) + \beta_2 Z_2,$$

where Z_1 and $Z2$ are covariates which include age, duration, sex, race, diabetes status, ktv dose, flux, and ICED score. Table 23 indicates dummy variables for these qualitative covariates, except the ICED score, which is represented by ICED_2 and ICED_3. ICED_2=1 if ICED score is 2 whereas ICED_3=1 if the score is 3. Cases for ICED score equal 0 and 1 are represented by letting both ICED_2 and ICED_3 both be 0. The marginal additive means rate model for cardiac and infectious hospitalization are fit-

ted separately (Table 24). For cardiac hospitalizations, the significant covariates are BALB, Black, age, $ICED_2$ and $ICED_3$. Estimation results show on average a lower event rate for black patients or those who have a higher BALB value, whereas aged patients or those with more severe comorbidity status have an elevated rate. For infectious hospitalizations, being diabetic or having severe comorbidities($ICED_2$, $ICED_3$) is related to higher infections rate significantly, while the rate is lower for black patients or those have higher value of BALB. We also found that the treatments are not significant for both cardiac and infectious hospitalizations. Thus, patients who took high dose ktv or high-flux dialyzer did not have significantly different hospitalizations rates than those receiving a standard dose or low-flux dialyzer.

In the second stage, we first investigate the global association by the constant rate ratio model,

$$\rho(s, t, \theta) = \theta_0. \tag{5.1}$$

Results are summarized in Table 25,where the estimated rate ratio is 1.0293 and the 95% confidence interval (0.9464, 1.1122) which contains value 1. It suggests a multiplicative increase of 1.0293 risks in cardiac hospitalization for patients experienced infections than those who did not; however, the increase of risk is not significant.

Since the rate ratio is the ratio of two event rates, which is nonnegative, we propose the second model.

$$log\{\rho(s, t, \theta)\} = \theta_0 \tag{5.2}$$

where θ_0 is the parameter of interest. The estimation result in Table 25 suggested

the risk in cardiac occurrence does not significantly elevate for patients who had infections, comparing to those who had no infections. We check the assumption of global dependence structure, i.e $H_0 : \rho(s,t,\theta) = \theta_0$ vs $H_a : \rho(s,t,\theta) \neq \theta_0$ via the supreme test statistic. The p-value calculated by Gaussian multiplier methods is 0.004, which indicate a strong support to H_0.

BALB, Black, ICED_2 and ICED_3 are significant risk factors to the mean rate of cardiac, as well as the infectious hospitalizations (Table 24). We are interested in quantifying the impact of risk factors on the association between cardiac and infectious hospitalizations. Here we propose a third model

$$log\{\rho(s,t,\theta;Z_k)\} = \theta_0 + \theta_1 \text{BALB} + \theta_2 \text{Black} + \theta_3 \text{ICED}_2 + \theta_4 \text{ICED}_3 \tag{5.3}$$

which describes the logarithm of rate ratio by the linear combination of significant risk factors in the marginal mean rate models. The estimated result shows none of BALB, Black, ICED_2 and ICED_3 are significantly contributing to the rate ratio because the 95% confidence intervals all include value 0.

Instead of describing the rate ratio by a constant or linear model with covariates, cardiac and infectious hospitalizations might be dependent on event times. We apply the piecewise constant model by dichotomizing the time scales of the cardiac or infectious hospitalizations at the median follow up time - 2.5 years (see Table 22),

$$log\{\rho(s,t,\theta)\} = \theta_0 + \theta_1 I(s < 2.5) + \theta_2 I(t < 2.5) + \theta_3 I(s < 2.5, t < 2.5). \tag{5.4}$$

In the interpretation section of Table 25, the rate ratio of early recurrence of cardiac and infectious hospitalizations is, $\exp(\theta_0+\theta_1+\theta_2+\theta_3) = 1.2015$ with a 95% confidence

interval $(1.0718, 1.3312)$ which indicates a multiplicative increase of 1.2015 in the risk of early cardiac hospitalizations conditional on early infections. If cardiac events occurred at early follow-up time, the risk of having infections later is reduced since the rate ratio $\exp(\theta_0 + \theta_1) = 0.7652$ and the confidence interval is between 0.6093 and 0.9211. Likewise, $\exp(\theta_0 + \theta_3) = 0.7384$ with a 95% confidence interval $(0.1714, 1.3054)$ suggests no elevated risk of later time cardiac events if patients had experienced infections at early time. However, we find that cardiac and infectious events are strongly positively associated at a later follow-up period, with rate ratio $\exp(\theta_0) = 1.2402$ and a confidence interval $(1.0459, 1.4345)$.

From the fitting result of model (5.4), the cardiac and infectious events occurred at the same time period (both earlier than median follow-up or later than that point) are strongly associated. This motivates us to consider the log-distance rate ratio model below

$$log\{\rho(s, t, \theta)\} = \theta_0 + \theta_1 |s - t|, \tag{5.5}$$

where the rate ratio is varying continuously with the difference of recurrence times. The result of model (5.5) in Table 25 indicates that the longer the time between cardiac and infectious hospitalization recurrence, the weaker the dependence. The log-distance assumption can be supported by a scatter plot of cardiac and infectious hospitalization times. For instance, patient A had cardiac hospitalizations at $s = (1.79, 5.48, 5.56)$ and infections at $t = (4.75, 4.82)$. Therefore there are 6 unique pairs of cardiac-infectious admission times during the follow-up period, which is shown in Figure 8 plot (a). Patients B, C, and D are included in the plot (b) and we find

the observations are clustered around the diagonal line - 12 dots lie within 0.5-year distance, 19 within 1 year, 20 within 1.5 years and 24 within 2 years. The density of joint events can be calculated using the event number over the length of the time interval, according to which the density within dashed lines of the plot (c), (d), (e) and (f) are 12, 9.5, 6.7 and 6 respectively. Similar pattern is observed for all patients (N=1502), with details in Figure 9.

Table 24: Additive marginal mean rate models for cardiac and infectious hospitalizations are fitted separately. At $\alpha = 0.05$, BALB, Black, $ICED_2$ and $ICED_3$ are significant for both cardia and infectious events.

Factor	est	se	95% lwr	95% upr	Z-value	p-value
Any cardiac						
BALB	-0.2392	0.1151	-0.4647	-0.0136	-2.0786	0.0377
Black	-0.0972	0.0381	-0.1719	-0.0225	-2.5495	0.0108
diabetic	0.0202	0.0412	-0.0605	0.1008	0.4899	0.6248
age	0.4478	0.0752	0.3004	0.5952	5.9535	< 0.001
$ICED_2$	0.1792	0.0441	0.0928	0.2656	4.0659	< 0.001
$ICED_3$	0.1362	0.0399	0.0579	0.2144	3.4095	< 0.001
ktv	0.0126	0.0336	-0.0534	0.0785	0.3739	0.7084
flux	-0.0339	0.0346	-0.1017	0.0338	-0.9816	0.3261
sex	0.0040	0.0369	-0.0683	0.0763	0.1077	0.9142
duration(yrs)	-0.0483	0.1015	-0.2473	0.1507	-0.4754	0.6347
Any infection:						
BALB	-0.6445	0.1098	-0.8598	-0.4293	-5.8688	< 0.001
Black	-0.0753	0.0316	-0.1371	-0.0134	-2.3849	0.0171
diabetic	0.1296	0.0343	0.0624	0.1967	3.7823	< 0.001
age	0.0031	0.0721	-0.1382	0.1444	0.0435	0.9653
$ICED_2$	0.1133	0.0360	0.0427	0.1839	3.1435	< 0.001
$ICED_3$	0.1623	0.0376	0.0887	0.2359	4.3210	< 0.001
ktv	-0.0294	0.0294	-0.0870	0.0281	-1.0030	0.3158
flux	-0.0313	0.0295	-0.0892	0.0265	-1.0610	0.2887
sex	0.0199	0.0302	-0.0393	0.0791	0.6587	0.5105
duration (yrs)	0.1055	0.1066	-0.1034	0.3144	0.9900	0.3222

Table 25: Estimation: The estimate, standard error and the 95% confidence interval of parameters in the proposed rate ratio models. Interpretation: under the assumptions specified in equation 5.4, rate ratio is piecewise constant; the estimate of $\exp\{\theta\}$, its standard error, and the 95% confidence interval.

		Estimation			
model	θ	estimate	standard error	95%lwr	95%upr
(5.1)	θ_0	1.0293	0.0423	0.9464	1.1122
(5.2)	θ_0	0.0289	0.0435	-0.0564	0.1142
(5.3)	θ_0	-0.4020	0.1839	-0.7624	-0.0416
	θ_1	0.4953	0.3444	-0.1797	1.1702
	θ_2	0.1539	0.0953	-0.0329	0.3408
	θ_3	0.1844	0.1057	-0.0227	0.3914
	θ_4	0.1029	0.1054	-0.1036	0.3094
(5.4)	θ_0	0.2153	0.0799	0.0586	0.3720
	θ_1	-0.4829	0.1119	-0.7022	-0.2636
	θ_2	-0.5186	0.1179	-0.7498	-0.2875
	θ_3	0.9698	0.1599	0.6563	1.2833
(5.5)	θ_0	0.5944	0.0780	0.4415	0.7473
	θ_1	-0.4963	0.1013	-0.6948	-0.2977

		Interpretation			
	$\exp\{\theta\}$	estimate	standard error	95%lwr	95%upr
(5.4)	$\exp\{\theta_0+\theta_1+\theta_2+\theta_3\}$	1.2015	0.0662	1.0718	1.3312
	$\exp\{\theta_0+\theta_1\}$	0.7652	0.0796	0.6093	0.9211
	$\exp\{\theta_0+\theta_3\}$	0.7384	0.2893	0.1714	1.3054
	$\exp\{\theta_0\}$	1.2402	0.0991	1.0459	1.4345

Figure 8: Cardiac/infectious hospitalizations for example patients. Plot (a): patient A has cardiac hospitalizations at $s = (1.79, 5.48, 5.56)$ and infectious ones at $t = (4.75, 4.82)$. The unique (s, t) pairs are (1.79, 4.75), (1.79, 4.82), (5.48, 4.75), (5.48, 4.82), (5.56, 4.75) and (5.56, 4.82). Plot (b): similarly, we plot the pair-wise event time points of patient A, C, and D with numbers of pairs followed in the parentheses. Plot (c)-(f): boundary defined by $|s - t| = 0.5$, 1, 1.5 and 2 (years) in plot (c), (d), (e) and (f); points fall inside boundary are 12, 19, 20 and 24; within boundary density (number of joint events over time length) equals to 12, 9.5, 6.7 and 6. Joint events clustered around diagonal line $t = s$.

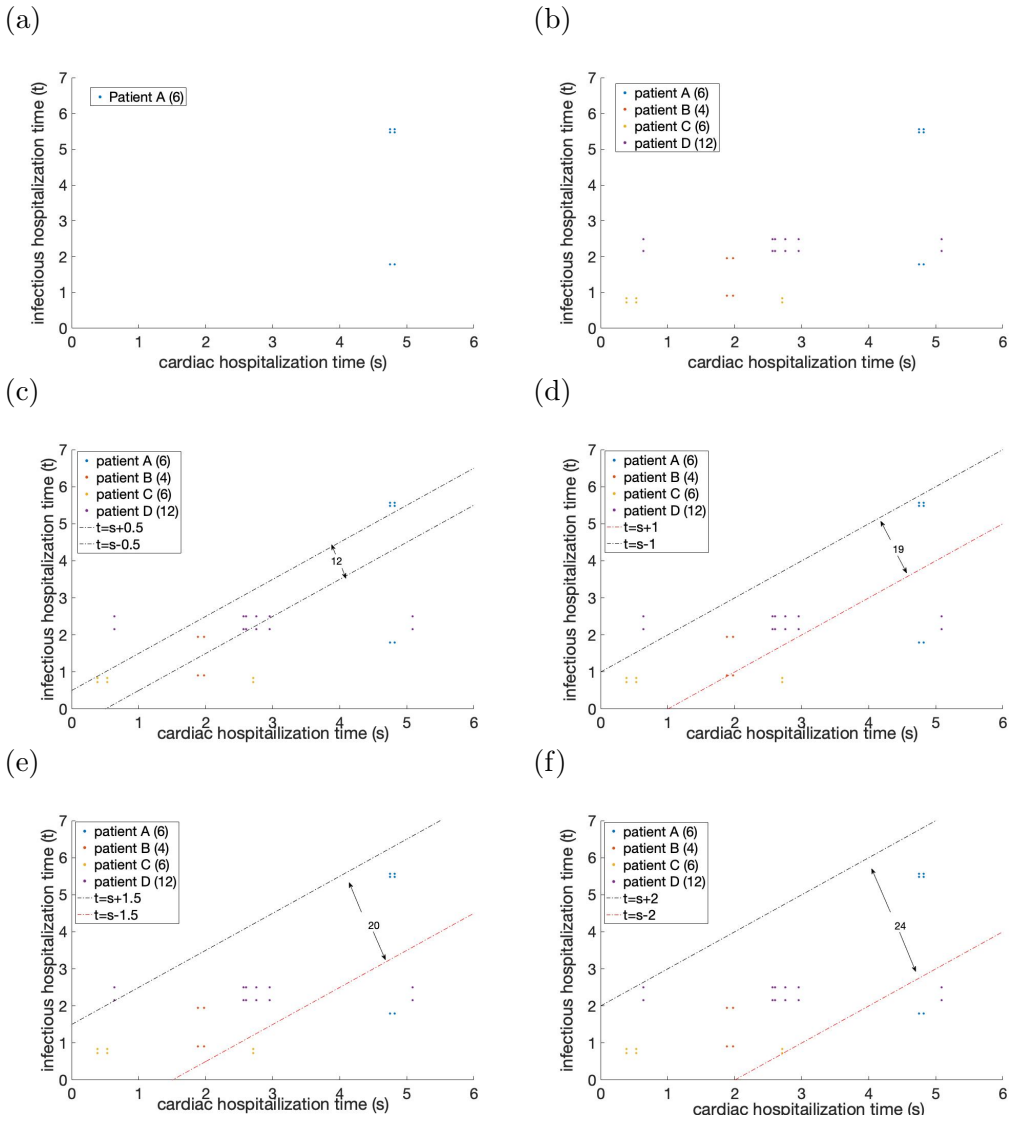

Figure 9: Cardiac/infectious hospitalizations for all patients (N=1502). Plot(a): 2259 joint events observed within the region defined by $|t - s| \leq 0.5$, which gives us the event density (joint event count over interval length) 2259. Similarly,the density of joint events fall within boundary region in plot (b) is 1254.5 and the density dropped to 898.3 and 703.8 in plot(c) and (d).

(a) Solid lines: $|t - s| \leq 0.5$

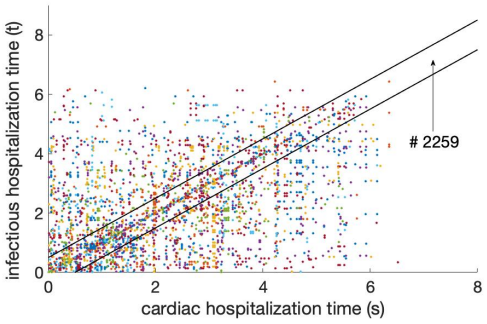

(b) Solid lines: $|t - s| \leq 1$

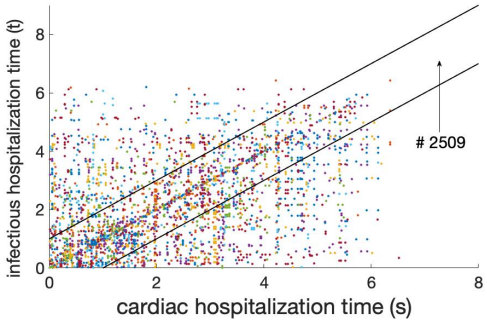

(c) Solid lines: $|t - s| \leq 1.5$

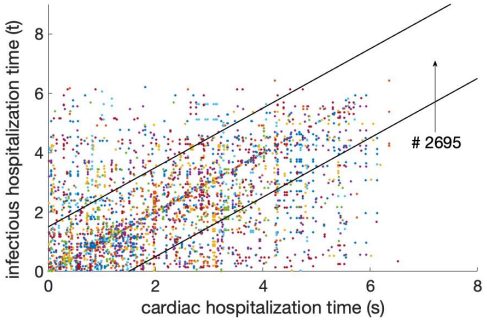

(d) Solid lines: $|t - s| \leq 2$

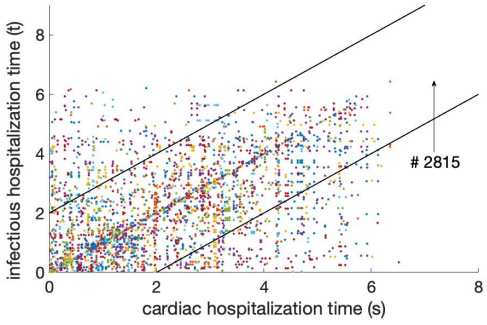

5.3 Application 2: the rate ratio of composite cardiac hospitalizations

Cardiac disease is a common cause of death in chronic hemodialysis patients. We observe that 53.79% of patients experienced a total of 1762 hospitalizations attributed to cardiac diseases. It is critical for us to understand the progression of cardiac diseases to prevent, predict and reduce the fatality among dialysis patients. Existing literature focuses on detecting the dose or flux effect on the cardiac hospitalization and cardiac deaths (Alfred K. Cheung and et al., 2000; Cheung et al., 2004; Jennifer E. Flythe and Brunelli, 2011), while the dependence at different recurrence times has not been studied yet.

First, we want to investigate if patients who had cardiac hospitalization in the past are more vulnerable and more likely to experience similar hospitalization than those who did not have. We slightly modify the rate ratio by defining

$$\rho(s,t,\theta) = \frac{\mu_{2|1}(t|s)}{\mu_2(t)}, \tag{5.6}$$

with $t > s \geq 0$ and utilizing the composite cardiac hospitalization data to fit the constant rate ratio model in equation (5.7)

$$\rho(s,t,\theta) = \theta_0. \tag{5.7}$$

Table 26 shows strong dependence between past and future cardiac events. The interpretation of the estimated rate ratio equal: a multiplicative increase of 1.7287 risk in cardiac hospitalizations for patients who had cardiac hospitalizations in the past compared to those who did not. The 95% confidence interval (1.4300, 2.0274)

shows this increasing risk is significant.

The global dependence structure specified by the model in (5.7) is significant but ignored the possible local dependence. To check the goodness of fit for model (5.7), we applied the Gaussian multiplier method and got a p-value=0.000 based on 1000 re-samplings. We would like to reject $H_0 : \rho(s,t,\theta) = \theta_0$ and the global association model is not enough to describe the dependence structure between past and future cardiac events. Here we consider the log-distance model which allows the rate ratio to vary continuously with the difference between current and past cardiac hospitalization times,

$$log\{\rho(s,t,\theta)\} = \theta_0 + \theta_1(t-s), \quad \text{for} \quad t > s \geq 0. \tag{5.8}$$

From the results of model (5.8) in Table 26, we observe significant time difference effect. Thus the dependence between the current and past cardiac event decays with the time difference. If the past cardiac event is far away from the current event in a time scale, then they are less associated.

On the other hand, the rate ratio is the ratio of event rates, and a positive association entails an elevated event rate, which suggests a high event density - event count per unit time. If the model (5.8) is reasonable, we would expect to the density in region $(t-s) < r_1$ would be higher than that of in region $(t-s) < r_2$ if $r_1 < r_2$.

To demonstrate the idea, we first consider patient B, who had cardiac hospitalizations at time 0.11, 0.16, 0.33, 0.34 years during the follow-up. The 6 pairs of (s,t)-(0.11,0.16), (0.11, 0.33), (0.11, 0.34), (0.16, 0.33), (0.16, 0.34) and (0.33, 0.34) are shown in the first plot of Figure 10. In the same way, we have the past-current event

time points for patients A, C, and D.

In Figure 11 plot (a), there are 9 points in region $s < t < s + 0.5$, which gives us a density value 18. When the distance between s and t is enlarged, the event density is decreasing to 11, 10 and 8.5 in the regions defined in plot(b), (c) and (d) respectively. Figure 12 shows the scatter plot for 1502 patients, each point stands for a event time pair (s, t). We observe higher density and more clustered points when the distance between s and t are smaller; when $t - s$ increases, the density decreases. Therefore it is reasonable to assume that if event times are close, the association is stronger, which is reflected by a higher relative conditional rate.

Table 26: The estimate, standard error and the 95% confidence interval of parameters in the rate ratio model (5.7) and (5.8).

model	θ	estimate	standard error	95%lwr	95%upr
(5.7)	θ_0	1.7287	0.1524	1.4300	2.0274
(5.8)	θ_0	1.0779	0.3138	0.4629	1.6930
	θ_1	-0.4469	0.1964	-0.8319	-0.0618

Figure 10: Cardiac hospitalizations for example patients: Patient B has hospitalization time set 0.11, 0.16, 0.33 and 0.34. Let t be the current event time, and s be the past time (i.e $t > s$). For t=0.16, past event time is s=0.11; for t=0.33, s would be 0.11 or 0.16; while for t=0.34 (the most recent records), previous events occurred at s=0.11, 0.16 and 0.33. Therefore, in total we have 6 pairs of unique (s,t) under the assumption ($t > s$). Using the same technique, we plot the current-past event time pairs of patient A, C, and D.

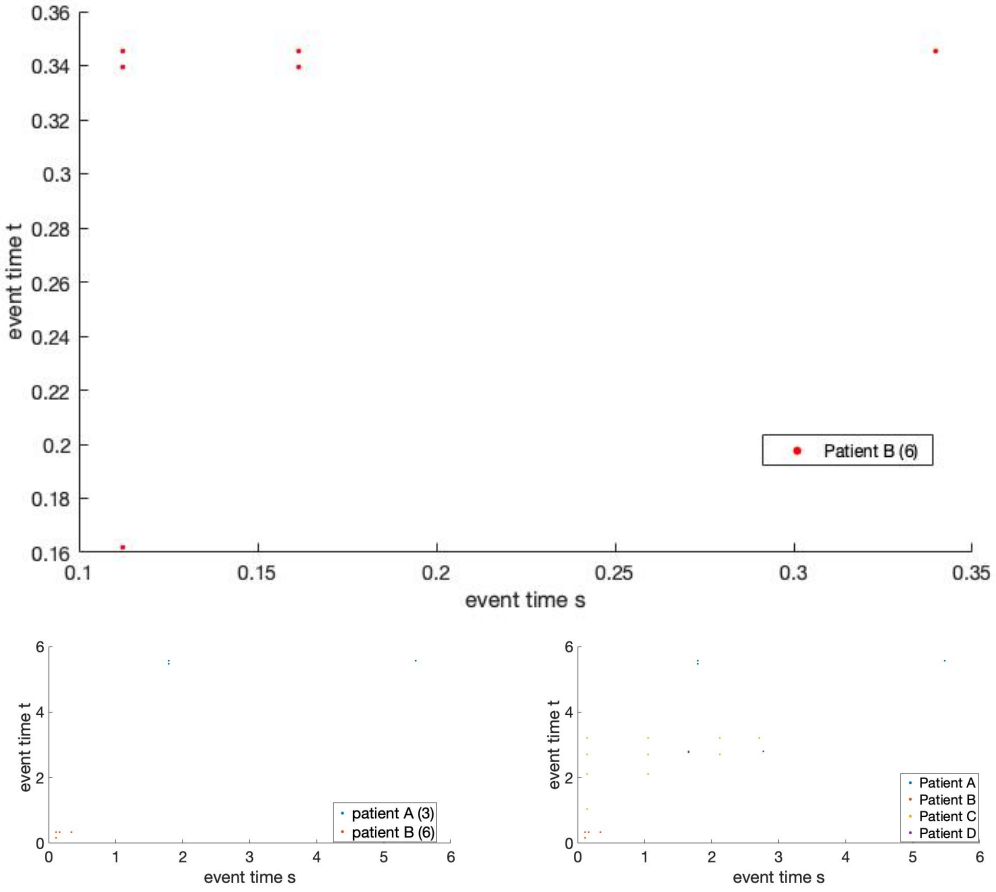

Figure 11: Clustering in hospitalizations : (s, t) pairs have higher density in when $t - s$ is small. We define the density as the number of pairs over the corresponding distance. In plot(a), there are 9 pairs of events occurred within distance 0.5, therefore the density for $t - s \leq 0.5$ is 18. Using the same technique, for region $t - s \leq 1$ the density is 11; for region $t - s \leq 1.5$ the density is 5 and for $t - s \leq 2$ is reduced to 4.25.

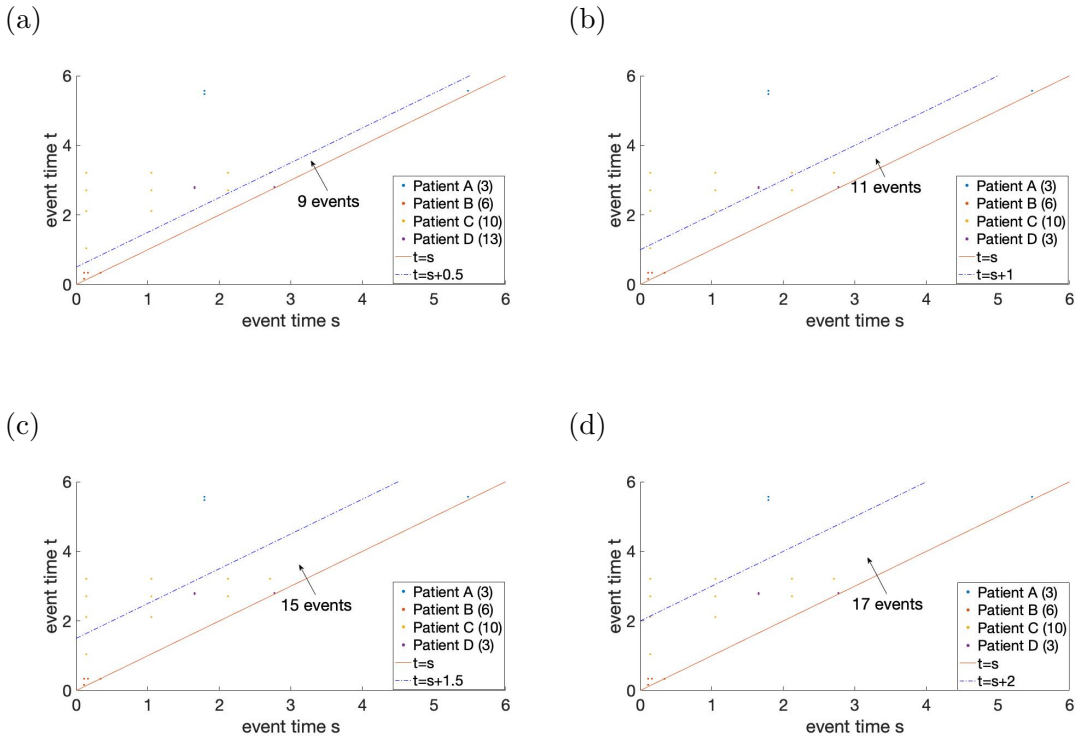

Figure 12: Clustering in hospitalizations (N=1502) : (s,t) pairs have higher density in when $t-s$ is small. We define the density as the number of pairs over the corresponding distance. In plot(a), there are 707 pairs of events occurred within distance 0.5, therefore the density for $t-s \leq 0.5$ is 1414.Using the same technique, for region $t-s \leq 1$ the density is 1113; for region $t-s \leq 1.5$ the density is 919 and for $t-s \leq 2$ is reduced to 764.

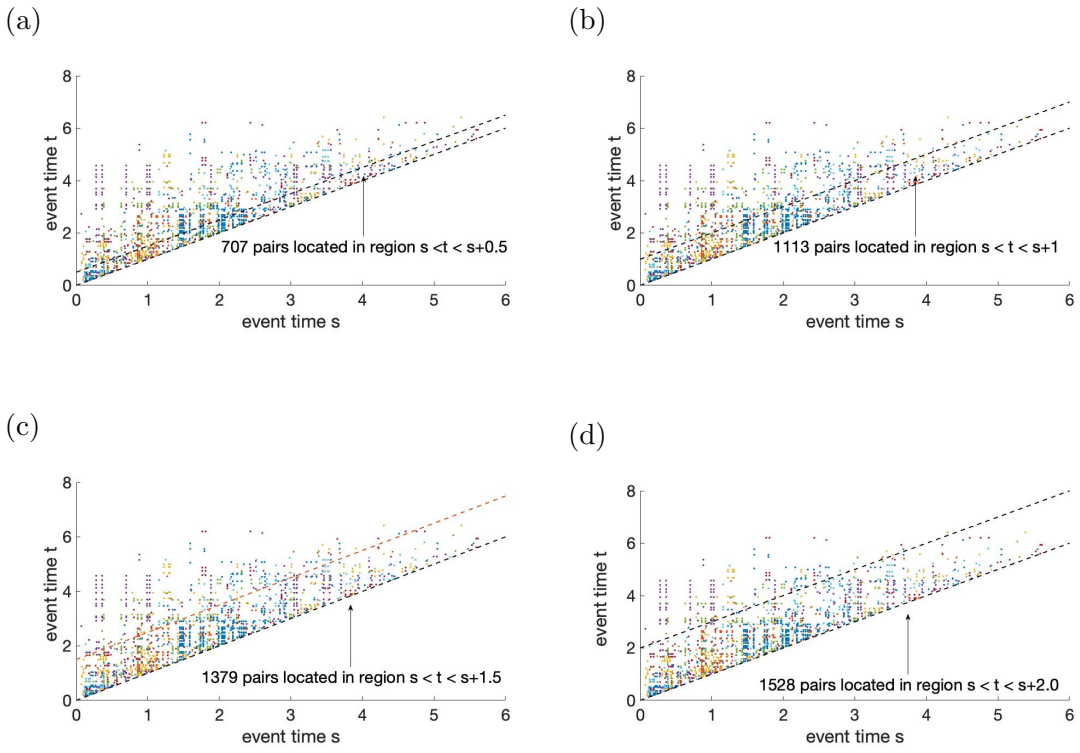

REFERENCES

O. Aalen. Nonparametric inference for a family of counting processes. *The Annals of Statistics*, 6(4):701–726, 1978.

O. Aalen. A model for nonparametric regression analysis of counting processes. In W. Klonecki, A. Kozek, and J. Rosiński, editors, *Mathematical Statistics and Probability Theory*, pages 1–25, New York, NY, 1980. Springer New York.

H. Abu-Libdeh, B. W. Turnbull, and L. C. Clark. Analysis of multi-type recurrent events in longitudinal studies; application to a skin cancer prevention trial. *Biometrics*, 46(4):1017–1034, 1990.

G. Y. Alfred K. Cheung, Mark J. Sarnak and et al. Atherosclerotic cardiovascular disease risks in chronic hemodialysis patients. *Kidney International*, 58:353–362, 2000.

P. K. Andersen and R. D. Gill. Cox's regression model for counting processes: A large sample study. *The Annals of Statistics*, 10(4):1100–1120, 1982.

J. E. Anderson, T. A. Louis, N. V. Holm, and B. Harvald. Time-dependent association measures for bivariate survival distributions. *Journal of the American Statistical Association*, 87(419):641–650, 1992.

A. K. Cheung, G. Y. Mark J. Sarnak, and et al. Cardiac diseases in maintenance hemodialysis patients : Results of the HEMO Study. *Kidney International*, 65: 2380–2389, 2004.

D. G. Clayton. A model for association in bivariate life tables and its application in epidemiological studies of familial tendency in chronic disease incidence. *Biometrika*, 65(1):141–151, 1978.

R. J. Cook and J. Lawless. *The Statistical Analysis of Recurrent Events*. Springer, 2007.

D. R. Cox. Regression models and life-tables. *Journal of the Royal Statistical Society. Series B (Methodological)*, 34(2):187–220, 1972.

M. H. Gail, T. J. Santner, and C. C. Brown. An analysis of comparative carcinogenesis experiments based on multiple times to tumor. *Biometrics*, 36(2):255–266, 1980.

P. B. Gilbert, S. Yanqing, and L. Mei. HHS Public Access. pages 348–358, 2017.

T. Greene, G. J. Beck, J. Gassman, F. Gotch, J. W. Kusek, A. S. Levey, N. Levin, G. Schulman, and G. Eknoyan. Design and statistical issues of the hemodialysis (hemo) study. *Controlled Clinical Trials*, 21:502–525, 11 2000.

T. H Scheike. The additive nonparametric and semiparametric aalen model as the rate function for a counting process. *Lifetime Data Analysis*, 8(3):247–262, Sep 2002.

T. H Scheike and Y. Sun. On cross-odds ratio for multivariate competing risks data. *Biostatistics (Oxford, England)*, 13:680–94, 06 2012.

S. E. K. Jennifer E. Flythe and S. M. Brunelli. Rapid fluid removal during dialysis is associated with cardiovascular morbidity and mortality Jennifer. *Kidney International*, 79(2):250–257, 2011.

G. A. Kaysen. Serum albumin concentration in dialysis patients : Why does it remain resistant to therapy ? Beyond inadequate nutrient. *Kidney International*, 64:92–98, 2003.

J. F. Lawless. Regression methods for poisson process data. *Journal of The American Statistical Association*, 82:808–815, 1987a.

J. F. Lawless. Negative binomial and mixed poisson regression. *Canad.J.Statist.*, 15 (3):209–225, 1987b.

J. F. Lawless and C. Nadeau. Some simple robust methods for the analysis of recurrent events. *Technometrics*, 37(2):158–168, 1995.

D. Y. Lin, L. J. Wei, I. Yang, and Z. Ying. Semiparametric regression for the rate and mean function of recurrent events. *J Royal Statistical Society B*, 62, 2000.

T. Martinussen and T. Scheike. A semiparametric additive regression model for longitudinal data. *Biometrika*, 86(3):691–702, 09 1999.

W. Nelson. Graphical analysis of system repair data. *Journal of Quality Technology*, 20(1):24–35, 1988.

W. Nelson. Confidence limits for recurrence data: Applied to cost or number of product repairs. *Technometrics*, 37(2):147–157, 1995.

E. T. M. Ng and R. J. Cook. Robust inference for bivariate point processes. *The Canadian Journal of Statistics / La Revue Canadienne de Statistique*, 27(3):509–524, 1999.

J. Ning, Y. Chen, C. Cai, X. Huang, and M. C. Wang. On the dependence structure of bivariate recurrent event processes: Inference and estimation. *Biometrika*, 102 (2):345–358, 2015.

D. Oakes. Bivariate survival models induced by frailties. *Journal of the American Statistical Association*, 84(406):487–493, 1989.

M. S. Pepe and J. Cai. Some graphical displays and marginal regression analyses for recurrent failure times and time dependent covariates. *Journal of the American Statistical Association*, 88(423):811–820, 1993.

D. Pollard. *Empirical Processes: Theory and Applications*, volume 2 of *NSF-CBMS Regional Conference Series in Probability and Statistics*. Institute of Mathematical Statistics, Hayward, CA, 1990.

M. V. Rocco, G. Yan, J. Gassman, J. B. Lewis, D. Ornt, B. Weiss, and A. S. Levey. Comparison of causes of death using HEMO study and HCFA end-stage renal disease death notification classification systems. *American Journal of Kidney Diseases*, 39(1):146–153, Jan 2002.

D. E. Schaubel and J. Cai. Regression methods for gap time hazard functions of sequentially ordered multivariate failure time data. *Biometrika*, 91(2):291–303, 2004.

D. E. Schaubel and J. Cai. Analysis of clustered recurrent event data with application to hospitalization rates among renal failure patients. *Biostatistics*, 6(3):404–419, 2005.

P. Thall. Mixed poisson likelihood regression models for longitudinal interval count data. *Biometrics*, 44:197–209, 04 1988.

P. F. Thall and J. M. Lachin. Analysis of recurrent events: Nonparametric methods for random-interval count data. *Journal of the American Statistical Association*, 83(402):339–347, 1988.

APPENDIX A: PROOFS OF THE PROPOSITIONS IN CHAPTER 3

Proof of Proposition 1

By the conditional expectation property and the conditional independent increment of N_{k1}, N_{k2}, we have :

$$\begin{aligned}
&E\{dN_{k1}(s)dN_{k2}(t)|Z_{k1}(s), Z_{k2}(t)\} \\
&= E\Big\{E\{dN_{k1}(s)dN_{k2}(t)|Z_{k1}(s), Z_{k2}(t), R_k\}\Big\} \\
&= E\Big\{E\{dN_{k1}(s)|Z_{k1}(s), R_k\}E\{dN_{k2}(t)|Z_{k2}(t), R_k\}\Big\} \\
&= E\Big\{R_k\{d\mu_{01}(s) + \beta_1^T Z_{k1}(s)\, ds\}R_k\{d\mu_{02}(t) + \beta_2^T Z_{k2}(t)\, dt\}\Big\} \\
&= E\{R_k^2\}\{d\mu_{01}(s) + \beta_1^T Z_{k1}(s)\, ds\}\{d\mu_{02}(t) + \beta_2^T Z_{k2}(t)\, dt\} \qquad \text{(A.1)}
\end{aligned}$$

and

$$E\{dN_{k1}(s)\,|\,Z_{k1}(s)\} = E\Big\{E\{dN_{k1}(s)\,|\,Z_{k1}(s), R_k\}\Big\} = E\{R_k\}\{d\mu_{01}(s) + \beta_1^T Z_{k1}(s)\, ds\},$$

$$E\{dN_{k2}(t)\,|\,Z_{k2}(t)\} = E\Big\{E\{dN_{k2}(t)\,|\,Z_{k2}(t), R_k\}\Big\} = E\{R_k\}\{d\mu_{02}(t) + \beta_2^T Z_{k2}(t)\, dt\}.$$

Therefore, follows from the definition of the rate ratio in (2.1),

$$\rho = \frac{E\{dN_{k1}(s)dN_{k2}(t)\,|\,Z_{k1}(s), Z_{k2}(t)\}}{E\{dN_{k1}(s)\,|\,Z_{k1}(s)\}E\{dN_{k2}(t)\,|\,Z_{k2}(t)\}} = \frac{E\{R_k^2\}}{E\{R_k\}E\{R_k\}} = \frac{\mu^2 + \sigma^2}{\mu^2} = 1 + \frac{\sigma^2}{\mu^2} \qquad \text{(A.2)}$$

□

Proof of Proposition 2

Similar to the proof of Proposition 1,

$$\begin{aligned}
&E\{dN_{k1}(s)dN_{k2}(t)|Z_{k1}(s), Z_{k2}(t)\} \\
&= E\Big\{E\{dN_{k1}(s)|Z_{k1}(s), R_k\}E\{dN_{k2}(t)|Z_{k2}(t), R_k\}\Big\} \\
&= E\{R_k(s)R_k(t)\} \cdot \{d\mu_{01}(s) + \beta_1^T Z_{k1}(s)\, ds\}\{d\mu_{02}(t) + \beta_2^T Z_{k2}(t)\, dt\} \qquad \text{(A.3)}
\end{aligned}$$

and

$$\begin{aligned}
E\{dN_{k1}(s) \mid Z_{k1}(s)\} &= E\{R_k(s)\}\{d\mu_{01}(s) + \beta_1^T Z_{k1}(s)\, ds\} \\
E\{dN_{k2}(t) \mid Z_{k2}(t)\} &= E\{R_k(t)\}\{d\mu_{02}(t) + \beta_2^T Z_{k2}(t)\, dt\}. \qquad \text{(A.4)}
\end{aligned}$$

Since $R_k(u)$ is piecewise constant, we have

$$E\{R_k(s)R_k(t)\} = \begin{cases} E(R_{k0}R_{k0}) = (a_0b_0 + \delta_0)^2 + a_0b_0^2 & \text{if } s,t \in (0, c_0] \\ E(R_{k1}R_{k1}) = (a_1b_1 + \delta_1)^2 + a_1b_1^2 & \text{if } s,t \in (c_0, \tau] \\ E(R_{k0}R_{k1}) = (a_0b_0 + \delta_0)(a_1b_1 + \delta_1) & \text{otherwise} \end{cases} \qquad \text{(A.5)}$$

$$E\{R_k(s)\}E\{R_k(t)\} = \begin{cases} E(R_{k0})E(R_{k0}) = (a_0b_0 + \delta_0)^2 & \text{if } s,t \in (0, c_0] \\ E(R_{k1})E(R_{k1}) = (a_1b_1 + \delta_1)^2 & \text{if } s,t \in (c_0, \tau] \\ E(R_{k0})E(R_{k1}) = (a_0b_0 + \delta_0)(a_1b_1 + \delta_1) & \text{otherwise} \end{cases} \qquad \text{(A.6)}$$

This yields the piecewise constant rate ratio below :

$$\rho(\theta, s, t) = \frac{E\{R_k(s)R_k(t)\}}{E\{R_k(s)\}E\{R_k(t)\}} = \begin{cases} 1 + \frac{a_0 b_0^2}{(a_0 b_0 + \delta_0)^2} & \text{if } s, t \in (0, c_0] \\ 1 + \frac{a_1 b_1^2}{a_1 b_1 + \delta_1)^2} & \text{if } s, t \in (c_0, \tau] \\ 1 & \text{otherwise} \end{cases} \tag{A.7}$$

□

Proof of Proposition 3

By the definition of mean event rate

$$
\begin{aligned}
&E[\, dN_1(s)\, dN_2(t) \,|z_1, z_2] \\
&= P\{\, dN_1(s) = 1,\, dN_2(t) = 1 \,|Z_1(s) = z_1, Z_2(t) = z_2\} \\
&= P\{\, d\tilde{N}_1(s) + dN_0(s) = 1,\, d\tilde{N}_2(t) + dN_0(t) = 1 \,|\, z_1, z_2\}
\end{aligned}
$$

since $\{\tilde{N}_j(\cdot)\}$ and $\{N_0(\cdot)\}$ are conditional independent to each other, we have

$$
\begin{aligned}
&P\{\, d\tilde{N}_1(s) + dN_0(s) = 1,\, d\tilde{N}_2(t) + dN_0(t) = 1 \,|\, z_1, z_2\} \\
&= P\{d\tilde{N}_1(s) = 1,\, dN_0(s) = 0,\, d\tilde{N}_2(t) + dN_0(t) = 1 \,|\, z_1, z_2\} \\
&\quad + P\{d\tilde{N}_1(s) = 0,\, dN_0(s) = 1,\, d\tilde{N}_2(t) + dN_0(t) = 1 \,|\, z_1, z_2\} \qquad \text{(A.8)}
\end{aligned}
$$

On the right hand side of (A.8),

$$
\begin{aligned}
&P\{d\tilde{N}_1(s) = 1, dN_0(s) = 0,\, d\tilde{N}_2(t) + dN_0(t) = 1 | z_1, z_2\} \\
&= P\{d\tilde{N}_1(s) = 1 \,|\, z_1\} \cdot P\{dN_0(s) = 0,\, d\tilde{N}_2(t) = 0,\, dN_0(t) = 1 | z_1, z_2\} \\
&\quad + P\{d\tilde{N}_1(s) = 1 \,|\, z_1\} \cdot P\{dN_0(s) = 0,\, d\tilde{N}_2(t) = 1,\, dN_0(t) = 0 | z_1, z_2\} \\
&= \tilde{\lambda}_1(s \,|\, z_1)\, ds \cdot \lambda_0(t \,|\, z_2)\, dt + \tilde{\lambda}_1(s \,|\, z_1)\, ds \cdot \tilde{\lambda}_2(t \,|\, z_2)\, dt \qquad \text{(A.9)}
\end{aligned}
$$

Similarly,

$$
\begin{aligned}
&P\{d\tilde{N}_1(s)=0, dN_0(s)=1,\, d\tilde{N}_2(t)+dN_0(t)=1|\, z_1, z_2\} \\
&= P\{d\tilde{N}_1(s)=0\,|\,z_1\}\cdot P\{dN_0(s)=1,\, d\tilde{N}_2(t)=0,\, dN_0(t)=1|\, z_1, z_2\} \\
&\quad + P\{d\tilde{N}_1(s)=0\,|\,z_1\}\cdot P\{dN_0(s)=1,\, d\tilde{N}_2(t)=1,\, dN_0(t)=0|\, z_1, z_2\} \\
&= 1\cdot\rho_0(\theta,s,t|\, z_1,z_2)\lambda_0(s\,|\,z_1)\,ds\cdot\ \lambda_0(t\,|\,z_2)\,dt + 1\cdot\tilde{\lambda}_2(t\,|\,z_2)\,dt\,\lambda_0(s\,|\,z_1)\,ds \qquad \text{(A.10)}
\end{aligned}
$$

Combine equation (A.9) and (A.10) allows us to represent equation (A.8) as below

$$
\begin{aligned}
&E[\,dN_1(s)\,dN_2(t)\,|z_1,z_2] \\
&= P\{\,d\tilde{N}_1(s)+dN_0(s)=1,\, d\tilde{N}_2(t)+dN_0(t)=1\,|\,z_1,z_2\} \\
&= \tilde{\lambda}_1(s\,|\,z_1)\,ds\cdot\lambda_0(t\,|\,z_2)\,dt + \tilde{\lambda}_1(s\,|\,z_1)\,ds\cdot\tilde{\lambda}_2(t\,|\,z_2)\,dt \\
&\quad + 1\cdot\rho_0(\theta,s,t|\, z_1,z_2)\lambda_0(s\,|\,z_1)\,ds\cdot\ \lambda_0(t\,|\,z_2)\,dt + \cdot\tilde{\lambda}_2(t\,|\,z_2)\,dt\cdot\ \lambda_0(s\,|\,z_1)\,ds \\
&= \{\tilde{\lambda}_1(s\,|\,z_1)+\lambda_0(s\,|\,z_1)\}\{\tilde{\lambda}_0(t\,|\,z_2)+\lambda_0(t\,|\,z_2)\}\,ds\,dt \\
&\quad + \{\rho_0(\theta,s,t|\, z_1,z_2)-1\}\lambda_0(s\,|\,z_1)\lambda_0(t\,|\,z_2)\,ds\,dt \\
&= \lambda_1(s\,|\,z_1)\lambda_2(t\,|\,z_2)\,ds\,dt + \{\rho_0(\theta,s,t|\, z_1,z_2)-1\}\lambda_0(s\,|\,z_1)\lambda_0(t\,|\,z_2)\,ds\,dt \qquad \text{(A.11)}
\end{aligned}
$$

and

$$
E[\,dN_1(s)\,|\,z_1]\,E[\,dN_2(t)\,|\,z_2] = \lambda_1(s\,|\,z_1)\lambda_2(t\,|\,z_2)\,ds\,dt. \qquad \text{(A.12)}
$$

By definition the rate ratio of bivariate counting processes $\{N_1(s), N_2(t)\}$ is

$$
\rho(\theta,s,t|\, z_1,z_2) = \frac{E[\,dN_1(s)\,dN_2(t)|\, z_1,z_2]}{E[\,dN_1(s)|\, z_1]E[\,dN_2(t)|\, z_2]} \qquad \text{(A.13)}
$$

and substituting equations (A.11) and (A.12) into the (A.13) gives us

$$\rho(\theta, s, t|\, z_1, z_2) = 1 + \{\rho_0(\theta, s, t|\, z_1, z_2) - 1\}\frac{\lambda_0(s|z_1)\lambda_0(t|\, z2)}{\lambda_1(s|\, z_2)\lambda_2(t|\, z_2)}$$

The rate ratio of $N_1(s)$ and $N_2(t)$ depends on that of $N_0(s)$ and $N_0(t)$. If $N_0(s)$ and $N_0(t)$ are independent, $\rho_0(\theta, s, t|z_1, z_2)$ would be 1, which leads to $\rho(\theta, s, t|z_1, z_2) = 1$ as well. If the occurrence of events at time s, t are positively correlated, $\rho_0(\theta, s, t|z_1, z_2)$ will be greater than 1 and therefore $\rho(\theta, s, t|z_1, z_2) > 1$. For negatively associated event occurrence, both $\rho_0(\theta, s, t|z_1, z_2)$ and $\rho(\theta, s, t|z_1, z_2)$ will be both less than 1.

□

APPENDIX B: PROOFS OF THE THEOREMS IN CHAPTER 3

Condition I.

Adapting from H Scheike (2002), we show the asymptotic properties of the first-stage estimators in our proposed method. The following regularity conditions are assumed for $j = 1, 2$:

C.1. $\{N^*_{kj}(\cdot), C_{kj}, Z_{kj}(\cdot)\}$ are independent and identically distributed for $k = 1, 2, ..., N$.

C.2. $Pr(C_{kj} > \tau) > 0$, where τ is predetermined constant; $N_{kj}(\tau) < \eta < \infty$ are bounded by a constant almost surely

C.3. $N_{kj}(\tau)$ are bounded by a constant;

C.4. $|Z_{kj}(0)| + \int_0^\tau |\, dZ_{kj}(s)| < c_Z < \infty$, almost surely, where $c_Z > 0$ is a constant.

C.5. Denote the positive-definiteness matrix A_j as

$$A_j = E\{\int_0^\tau \{Z_{kj}(u) - \bar{z}_j(\beta_j, u)\}^{\otimes 2}\, ds\},$$

where $\bar{z}_j(t) = \lim_{N\to\infty} \bar{Z}_j(t)$ and $\bar{Z}_j(t) = \frac{\sum_{k=1}^N Z_{kj}(t) Y_{kj}(t)}{\sum_{k=1}^N Y_{kj}(t)}$.

Proof of Theorem 3.1

Denote the likelihood function as

$$L_j(\beta_j) = \sum_{k=1}^N \int_0^\tau \{Z_{kj}(u) - \bar{Z}_j(u)\}\, dM_{kj}(u, \beta_j), \tag{A.14}$$

and with the first order Taylor expansion with respect to β_j gives us

$$(\hat{\beta}_j - \beta_j) = \hat{A}_j^{-1}(\beta^*)N^{-1}\int_0^\tau \{Z_{kj}(u) - \bar{Z}_j(u)\}\, dM_{kj}(u, \beta_j), \tag{A.15}$$

where

$$dM_{kj}(t;\beta_j) = dN_{kj}(t) - Y_{kj}(t)\{d\mu_{0j}(t) + \beta_j^T Z_{kj}(t)\, dt\}$$
$$\hat{A}_j(\beta_j) = -N^{-1}\sum_{k=1}^{N}\int_0^\tau \{Z_{kj}(u) - \bar{Z}_j(\hat{\beta}_j, u)\}^{\otimes 2}\, du,$$

with β^* a value falls between $\hat{\beta}_j$ and β_j.

By (C.4) and the strong law of large numbers (SLLN), $\hat{\beta}_j$ converges almost surely to β_j. From the Slutsky's theorem and (A.15), $\sqrt{N}(\hat{\beta}_j - \beta_j)$ is asymptotically normal with mean zero and covariance matrix $A_j^{-1}\Sigma_j A_j^{-1}$, where

$$\Sigma_j = E[\int_0^\tau \{Z_{1j}(u) - \bar{Z}_j(u)\} dM_{1j}(u, \beta_j) \int_0^\tau \{Z_{1j}(v) - \bar{Z}_j(v)\}\, dM_{1j}(v, \beta_j)].$$

From (A.15) it is straight forward to show

$$\sqrt{N}\{\hat{\beta}_j - \beta_j\} = A_j^{-1}N^{-1/2}\sum_{k=1}^{N}\xi_{kj} + o_p(1). \tag{A.16}$$

where

$$\xi_{kj} = \int_0^\tau \{Z_{kj}(u) - \bar{z}_j(u)\}\, dM_{kj}(u, \beta_j). \tag{A.17}$$

The asymptotic covariance matrix of $\sqrt{N}(\hat{\beta}_j - \beta_j)$ can be consistently estimated by

$\hat{A}_j^{-1}\hat{\Sigma}_j\hat{A}_j^{-1}$, with the corresponding estimators

$$
\begin{aligned}
d\hat{M}_{kj}(t;\hat{\beta}_j) &= dN_{kj}(t) - Y_{kj}(t)\{d\hat{\mu}_{0j}(t) + \hat{\beta}_j^T Z_{kj}(t)\,dt\},\\
\hat{\xi}_{kj} &= \int_0^\tau \{Z_{kj}(u) - \bar{Z}_j(u)\}\,d\hat{M}_{kj}(u;\hat{\beta}_j),\\
\hat{\Sigma}_j &= N^{-1}\sum_{k=1}^{N}\hat{\xi}_{kj}^{\otimes 2}.
\end{aligned}
$$

□

Proof of Theorem 3.2

Consider

$$\hat{\mu}_{0j}(t) - \mu_{0j}(t) = \{\hat{\mu}_{0j}(t;\hat{\beta}_j) - \hat{\mu}_{0j}(t;\beta_j)\} + \{\hat{\mu}_{0j}(t;\beta_j) - \mu_{0j}(t)\} \tag{A.18}$$

By the first order Taylor approximation, we have

$$\hat{\mu}_{0j}(t;\hat{\beta}_j) - \hat{\mu}_{0j}(t;\beta_j) = -(\hat{\beta}_j - \beta_j)\int_0^t \bar{Z}_j^T(u)\,du + o_p(N^{-1}), \tag{A.19}$$

$$\hat{\mu}_{0j}(t;\beta_j) - \mu_{0j}(t) = N^{-1}\sum_{k=1}^{N}\int_0^t \frac{dM_{kj}(u;\beta_j)}{\hat{\pi}_j(u)} + o_p(N^{-1}). \tag{A.20}$$

Using the strong convergence of β_j in Theorem 3.1 and the Uniform SLLN (Pollard 1990), $\{\hat{\mu}_{0j}(t;\hat{\beta}_j) - \hat{\mu}_{0j}(t;\beta_j)\}$ converges almost surely to 0 uniformly in $t \in [0,\tau]$. Similarly, $\mu_{0j}(t;\beta_j)$ converges strongly to $\mu_{0j}(t)$ uniformly.

By the Triangle Inequality,

$$|\hat{\mu}_{0j}(t) - \mu_{0j}(t)| \le |\hat{\mu}_{0j}(t;\hat{\beta}_j) - \hat{\mu}_{0j}(t;\beta_j)| + |\hat{\mu}_{0j}(t;\beta_j) - \mu_{0j}(t)|.$$

Therefore, $\hat{\mu}_{0j}(t)$ converges almost surely to $\mu_{0j}(t)$ uniformly in $t \in [0,\tau]$ as well.

Substituting (A.19), (A.20) into (A.18) and multiplying both sides by $\sqrt{N}$ gives,

$$\sqrt{N}\{\hat{\mu}_{0j}(t) - \mu_{0j}(t)\} = N^{-1/2}\sum_{k=1}^{N}\phi_{kj}(t) + o_p(1), \tag{A.21}$$

where

$$\phi_{kj}(t;\beta_j) = \int_0^t \frac{dM_{kj}(u;\beta_j)}{\pi_j(u)} - H^T(t)A_j^{-1}\int_0^\tau \{Z_{kj}(u) - \bar{z}_j(u)\}\,dM_{kj}(u,\beta_j), \tag{A.22}$$

with $H(t) = \int_0^t \bar{z}_j(u)\,du$.

Thus $\sqrt{N}\{\hat{\mu}_{0j}(t) - \mu_{0j}(t)\}$ converges weakly to a mean-zero Gaussian process with

covariance function $\Gamma_j(s,t) = E[\phi_{1j}(s;\beta_j)\phi_{1j}(t;\beta_j)]$, which can be consistently approximated by

$$\hat{\Gamma}_j(s,t) = N^{-1}\sum_{k=1}^{N}\hat{\phi}_{kj}(s;\hat{\beta}_j)\hat{\phi}_{kj}(t;\hat{\beta}_j),$$

where

$$\hat{\phi}_{kj}(t;\hat{\beta}_j) = \int_0^t \frac{d\hat{M}_{kj}(u;\hat{\beta}_j)}{\hat{\pi}_j(u)} - \hat{H}^T(t)\hat{A}_j^{-1}\int_0^\tau \{Z_{kj}(u) - \bar{Z}_j(u)\}\, d\hat{M}_{kj}(u;\hat{\beta}_j),$$

with

$$\hat{\pi}_j(t) = N^{-1}\sum_{k=1}^{N} Y_{kj}(t),$$
$$\hat{H}^T(t) = \int_0^t \bar{Z}_j^T(u)\, du.$$

□

Proof of Theorem 3.3

To prove the asymptotic of $\Big\{U(\theta,\hat{\beta}_1,\hat{\mu}_1(\cdot),\hat{\beta}_2,\hat{\mu}_2(\cdot)) - U(\theta,\beta_1,\mu_{01}(\cdot),\beta_2,\mu_{02}(\cdot))\Big\}$ where $U(\theta,\hat{\beta}_1,\hat{\mu}_{01}(\cdot),\hat{\beta}_2,\hat{\mu}_{02}(\cdot)) = \sum_{k=1}^{N} U_k(\theta,\hat{\beta}_1,\hat{\mu}_{01}(\cdot),\hat{\beta}_2,\hat{\mu}_{02}(\cdot))$, we consider the following decomposition:

$$
\begin{aligned}
&U_k(\theta,\hat{\beta}_1,\hat{\mu}_{01}(\cdot),\hat{\beta}_2,\hat{\mu}_{02}(\cdot)) \\
&= U_k(\theta,\beta_1,\mu_{01}(\cdot),\beta_2,\mu_{02}(\cdot)) \\
&+ \{U_k(\theta,\hat{\beta}_1,\hat{\mu}_{01}(\cdot),\hat{\beta}_2,\hat{\mu}_{02}(\cdot)) - U_k(\theta,\beta_1,\mu_{01}(\cdot),\hat{\beta}_2,\hat{\mu}_{02}(\cdot))\} \\
&+ \{U_k(\theta,\beta_1,\mu_{01}(\cdot),\hat{\beta}_2,\hat{\mu}_{02}(\cdot)) - U_k(\theta,\beta_1,\mu_{01}(\cdot),\beta_2,\mu_{02}(\cdot))\} \qquad \text{(A.23)}
\end{aligned}
$$

The third term in (A.23) can be further expressed as

$$
\begin{aligned}
\int_0^\tau \int_0^\tau -\frac{\partial\rho(s,t,\theta)}{\partial\theta}\rho(s,t,\theta)\cdot\Big\{&Y_{k2}(t)\{d\hat{\mu}_{02}(t) + \hat{\beta}_2^T Z_{k2}(t)\,dt \\
&- d\mu_{02}(t) - \beta_2^T Z_{k2}(t)\,dt\}Y_{k1}(s)\{d\mu_{01}(s) + \beta_1^T Z_{k1}(s)\,ds\}\Big\},
\end{aligned}
$$

by replacing $(\hat{\beta}_2 - \beta_2)$ and $\hat{\mu}_{0j}(t) - \mu_{0j}(t)$ with (A.16) and (A.21) respectively, we have

$$
\begin{aligned}
&U_k(\theta,\beta_1,\mu_{01}(s),\hat{\beta}_2,\hat{\mu}_{02}(t)) - U_k(\theta,\beta_1,d\mu_{01}(s),\beta_2,d\mu_{02}(t)) \\
&= \int_0^\tau \int_0^\tau -\frac{\partial\rho(s,t,\theta)}{\partial\theta}\rho(s,t,\theta)Y_{k1}(s)\{d\mu_{01}(s) + \beta_1^T Z_{k1}(s)\,ds\} \\
&\quad Y_{k2}(t)\Big\{Z_{k2}^T(t)dt\,A_2^{-1}N^{-1}\sum_{l=1}^{N}\xi_{l2} + N^{-1}\sum_{l=1}^{N} d\phi_{l2}(t;\beta_2)\Big\} + o_p(N^{-1}) \qquad \text{(A.24)}
\end{aligned}
$$

Similarly $\{U_k(\theta,\hat{\beta}_1,\hat{\mu}_{01}(s),\hat{\beta}_2,\hat{\mu}_{02}(t)) - U_k(\theta,\beta_1,\mu_{01}(s),\hat{\beta}_2,\hat{\mu}_{02}(t))\}$ in (A.23) is equiv-

alent to

$$\int_0^\tau \int_0^\tau -\frac{\partial \rho(s,t,\theta)}{\theta}\rho(s,t,\theta)Y_{k1}(s)Y_{k2}(t)[\, d\mu_{02}(t) + \beta_2^T Z_{k2}(t)dt\,] \\ \Big\{\, Z_{k1}^T(s)\, ds\, A_1^{-1} N^{-1} \sum_{l=1}^N \xi_{l1} + N^{-1} \sum_{l=1}^N d\phi_{l1}(s;\beta_1)\Big\} + o_p(N^{-1}) \tag{A.25}$$

It follows from (A.24), (A.25) and the definition in (3.9) that

$$N^{-1/2}\Big\{U(\theta,\hat\beta_1,\hat\mu_{01}(\cdot),\hat\beta_2,\hat\mu_{02}(\cdot)) - U(\theta,\beta_1,\mu_{01}(\cdot),\beta_2,\mu_{02}(\cdot))\Big\} \\ = N^{-1/2}\sum_{k=1}^N \Big\{h_{1,N}\xi_{k1}A_1^{-1} + g_{1,N,k} + h_{2,N}\xi_{k2}A_2^{-1} + g_{2,N,k}\Big\} + o_p(N^{-1/2}) \tag{A.26}$$

where the terms are denoted by

$$q_l(s,t) = -\frac{\partial \rho(s,t,\theta)}{\partial\theta}\rho(s,t,\theta)Y_{l1}(s)Y_{l2}(t),$$

$$h_{1,N} = N^{-1}\sum_{l=1}^N \int_0^\tau \int_0^\tau q_l(s,t)\{d\mu_{02}(t) + \beta_2^T Z_{l2}(t)\, dt\} Z_{l1}^T(s)\, ds,$$

$$h_{2,N} = N^{-1}\sum_{l=1}^N \int_0^\tau \int_0^\tau q_l(s,t)\{d\mu_{01}(s) + \beta_1^T Z_{l1}(s)\, ds\} Z_{l2}^T(t)\, dt,$$

$$g_{1,N,k} = N^{-1}\sum_{l=1}^N \int_0^\tau \int_0^\tau q_l(s,t)\{d\mu_{02}(t) + \beta_2^T Z_{l2}(t)\, dt\}\, d\phi_{k1}(s;\beta_1),$$

$$g_{2,N,k} = N^{-1}\sum_{l=1}^N \int_0^\tau \int_0^\tau q_l(s,t)\{d\mu_{01}(s) + \beta_1^T Z_{l1}(s)\, ds\}\, d\phi_{k2}(t;\beta_2).$$

Deriving from (A.26) the covariance matrix can be estimated by

$$\hat\Omega = N^{-1}\sum_{k=1}^N \Big\{\hat h_{1,N}\hat\xi_{k1}\hat A_1^{-1} + \hat g_{1,N,k} + \hat h_{2,N}\hat\xi_{k2}\hat A_2^{-1} + \hat g_{2,N,k}\Big\}^{\otimes 2}, \tag{A.27}$$

with

$$
\begin{aligned}
\hat{q}_l(s,t) &= -\frac{\partial \rho(s,t,\theta)}{\partial \theta}\rho(s,t,\theta)Y_{l1}(s)Y_{l2}(t) \\
\hat{h}_{1,N} &= N^{-1}\sum_{l=1}^{N}\int_0^\tau\int_0^\tau q_l(s,t)\{d\hat{\mu}_{02}(t) + \hat{\beta}_2^T Z_{l2}(t)\,dt\}Z_{l1}^T(s)\,ds, \\
\hat{h}_{2,N} &= N^{-1}\sum_{l=1}^{N}\int_0^\tau\int_0^\tau q_l(s,t)\{d\hat{\mu}_{01}(s) + \hat{\beta}_1^T Z_{l1}(s)\,ds\}Z_{l2}^T(t)\,dt, \\
\hat{g}_{1,N,k} &= N^{-1}\sum_{l=1}^{N}\int_0^\tau\int_0^\tau q_l(s,t)\{d\hat{\mu}_{02}(t) + \hat{\beta}_2^T Z_{l2}(t)\,dt\}\,d\hat{\phi}_{k1}(s;\hat{\beta}_1), \\
\hat{g}_{2,N,k} &= N^{-1}\sum_{l=1}^{N}\int_0^\tau\int_0^\tau q_l(s,t)\{d\hat{\mu}_{01}(s) + \hat{\beta}_1^T Z_{l1}(s)\,ds\}\,d\hat{\phi}_{k2}(t;\hat{\beta}_2).
\end{aligned}
\tag{A.28}
$$

□

Proof of Theorem 3.4

Denote

$$W_k(\theta, \beta_1, \mu_{01}(\cdot), \beta_2, \mu_{02}(\cdot))$$
$$= U_k(\theta, \beta_1, \mu_{01}(\cdot), \beta_2, \mu_{02}(\cdot)) + \Big\{h_{1,N}\xi_{k1}A_1^{-1} + g_{1,N,k} + h_{2,N}\xi_{k2}A_2^{-1} + g_{2,N,k}\Big\}, \quad \text{(A.29)}$$

which follows from equation (A.26) and let

$$\mathcal{I}(\theta, \beta_1, \mu_{01}(\cdot), \beta_2, \mu_{02}(\cdot)) = -N^{-1}\sum_{k=1}^{N}\Big(\frac{\partial U_k(\theta, \beta_1, \mu_{01}(\cdot), \beta_2, \mu_{02}(\cdot))}{\partial\theta}\Big)^T. \quad \text{(A.30)}$$

The First-order Taylor expansion of the estimation equation around the true values gives us,

$$\sqrt{N}(\hat{\theta} - \theta)$$
$$= N^{-1/2}\{\mathcal{I}(\theta, \beta_1, \mu_{01}(\cdot), \beta_2, \mu_{02}(\cdot))\}^{-1}\sum_{k=1}^{N} W_k(\theta, \beta_1, \mu_{01}(\cdot), \beta_2, \mu_{02}(\cdot)) + o_p(1). \quad \text{(A.31)}$$

By the central limit theorem that $\sqrt{N}(\hat{\theta} - \theta)$ is asymptotically normal with mean 0 and its variance that can be estimated by $\hat{\Phi} = N^{-1}(\hat{\mathcal{I}})^{-1}\sum_{k=1}^{N}(\hat{W}_k)^{\otimes 2}(\hat{\mathcal{I}}^T)^{-1}$, with

$$\hat{\mathcal{I}} = \mathcal{I}\big(\hat{\theta}, \hat{\beta}_1, \hat{\mu}_{01}(\cdot), \hat{\beta}_2, \hat{\mu}_{02}(\cdot)\big),$$
$$\hat{W}_k = W_k(\hat{\theta}, \hat{\beta}_1, \hat{\mu}_{01}(\cdot), \hat{\beta}_2, \hat{\mu}_{02}(\cdot)),$$

obtained with the plugged in estimators $\hat{\theta}, \hat{\beta}_1, \hat{\mu}_{01}(\cdot), \hat{\beta}_1, \hat{\mu}_{02}(\cdot), \hat{\xi}_{k1}$ and $\hat{\xi}_{k2}$.

□

APPENDIX C: PROOFS OF THE MODEL CHECKING PROCEDURE IN CHAPTER 3

Recall (3.25)

$$
\begin{aligned}
&V(s,t,\hat{\theta},\hat{\mu}_1(\cdot;Z_{k1}),\hat{\mu}_2(\cdot;Z_{k2}))\\
&= V\Big(s,t,\theta,\hat{\mu}_1(\cdot;Z_{k1}),\hat{\mu}_2(\cdot;Z_{k2})\Big)\\
&\quad + N^{-1/2}\frac{\partial V\Big(s,t,\theta,\hat{\mu}_1(\cdot;Z_{k1}),\hat{\mu}_2(\cdot;Z_{k2})\Big)}{\partial\theta}N^{1/2}(\hat{\theta}-\theta)+o_p(1),
\end{aligned}
$$

Note that $V\Big(s,t,\theta,\hat{\mu}_1(\cdot;Z_{k1}),\hat{\mu}_2(\cdot;Z_{k2})\Big)$ can be further decomposed by

$$
\begin{aligned}
&V\Big(s,t,\theta,\hat{\mu}_1(\cdot;Z_{k1}),\hat{\mu}_2(\cdot;Z_{k2})\Big)\\
&= V\Big(s,t,\theta,\mu_1(\cdot;Z_{k1}),\mu_2(\cdot;Z_{k2})\Big)\\
&\quad + V\Big(s,t,\theta,\hat{\mu}_1(\cdot;Z_{k1}),\hat{\mu}_2(\cdot;Z_{k2})\Big) - V\Big(s,t,\theta,\mu_1(\cdot;Z_{k1}),\hat{\mu}_2(\cdot;Z_{k2})\Big)\\
&\quad + V\Big(s,t,\theta,\mu_1(\cdot;Z_{k1}),\hat{\mu}_2(\cdot;Z_{k2})\Big) - V\Big(s,t,\theta,\mu_1(\cdot;Z_{k1}),\mu_2(\cdot;Z_{k2})\Big). \qquad \text{(A.32)}
\end{aligned}
$$

Applying the same techniques in the proof of Theorem 3.3, the third and forth lines in equation (A.32) are

$$
\begin{aligned}
&\sqrt{N}\Big\{V\Big(s,t,\theta,\hat{\mu}_1(\cdot;Z_{k1}),\hat{\mu}_2(\cdot;Z_{k2})\Big) - V\Big(s,t,\theta,\mu_1(\cdot;Z_{k1}),\hat{\mu}_2(\cdot;Z_{k2})\Big)\Big\}\\
&= \sum_{k=1}^{N}\int_0^t\int_0^s \frac{\partial\rho(u,v,\theta;Z_{k1},Z_{k2})}{\theta}\rho(u,v,\theta;Z_{k1},Z_{k2})\\
&\qquad Y_{k1}(u)Y_{k2}(v)[\,d\mu_{02}(v)+\beta_2^T Z_{k2}(v)dv\,]\Big\{Z_{k1}^T(s)\,ds\,A_1^{-1}N^{-1}\sum_{l=1}^{N}\xi_{l1}+N^{-1}\sum_{l=1}^{N}d\phi_{l1}\Big\}\\
&\qquad + o_p(N^{-1}), \qquad \text{(A.33)}
\end{aligned}
$$

and

$$\sqrt{N}\Big\{V\Big(s,t,\theta,\mu_1(\cdot;Z_{k1}),\hat{\mu}_2(\cdot;Z_{k2})\Big)-V\Big(s,t,\theta,\mu_1(\cdot;Z_{k1}),\mu_2(\cdot;Z_{k2})\Big)\Big\}$$
$$=\sum_{k=1}^{N}\int_0^t\int_0^s \frac{\partial\rho(u,v,\theta;Z_{k1},Z_{k2})}{\partial\theta}\rho(u,v,\theta;Z_{k1},Z_{k2})$$
$$Y_{k2}(v)Y_{k1}(u)\{\mu_{01}(u)+\beta_1^T Z_{k1}(u)\,du\}\Big\{Z_{k2}^T(v)\,dv\,A_2^{-1}N^{-1}\sum_{l=1}^{N}\xi_{l2}+N^{-1}\sum_{l=1}^{N}d\phi_{l2}\Big\}$$
$$+o_p(N^{-1}). \tag{A.34}$$

Combine (A.33) and (A.34), and rewrite (A.32) as

$$V\Big(s,t,\theta,\hat{\mu}_1(\cdot;Z_{k1}),\hat{\mu}_2(\cdot;Z_{k2})\Big)$$
$$=V\Big(s,t,\theta,\mu_1(\cdot;Z_{k1}),\mu_2(\cdot;Z_{k2})\Big)$$
$$+N^{-1/2}\sum_{k=1}^{N}\Big\{h_{1,N}(s,t)\xi_{k1}A_1^{-1}+g_{1,N,k}(s,t)+h_{2,N}(s,t)\xi_{k2}A_2^{-1}+g_{2,N,k}(s,t)\Big\},$$
$$+o_p(N^{-1}) \tag{A.35}$$

where

$$q_l(u,v)=-\frac{\partial\rho(u,v,\theta)}{\partial\theta}\rho(u,v,\theta)Y_{l1}(u)Y_{l2}(v)$$
$$h_{2,N}(s,t)=N^{-1}\sum_{l=1}^{N}\int_0^t\int_0^s w(u,v)q_l(u,v)\{d\mu_{01}(u)+\beta_1^T Z_{l1}(u)\,du\}Z_{l2}^T(u)\,dv$$
$$g_{2,N,k}(s,t)=N^{-1}\sum_{l=1}^{N}\int_0^t\int_0^s w(u,v)q_l(u,v)\{d\mu_{01}(u)+\beta_1^T Z_{l1}(u)\,du\}\,d\phi_{k2}(v)$$
$$h_{1,N}(s,t)=N^{-1}\sum_{l=1}^{N}\int_0^t\int_0^s w(u,v)q_l(u,v)\{d\mu_{02}(v)+\beta_2^T Z_{l2}(v)\,dv\}Z_{l1}^T(u)\,du$$
$$g_{1,N,k}(s,t)=N^{-1}\sum_{l=1}^{N}\int_0^t\int_0^s w(u,v)q_l(u,v)\{d\mu_{02}(v)+\beta_2^T Z_{l2}(v)\,dv\}\,d\phi_{k1}(u) \tag{A.36}$$

To simplify the notation, we define

$$\Upsilon_{k1}(s,t,\theta) = \Big\{ h_{1,N}(s,t)\xi_{k1}A_1^{-1} + g_{1,N,k}(s,t) \Big\} + o_p(N^{-1}),$$
$$\Upsilon_{k2}(s,t,\theta) = \Big\{ h_{2,N}(s,t)\xi_{k2}A_2^{-1} + g_{2,N,k}(s,t) \Big\} + o_p(N^{-1}),$$
$$V\big(s,t,\hat{\theta},\hat{\mu}_1(\cdot;z_{k1}),\hat{\mu}_2(\cdot;z_{k2})\big) = N^{-1/2}\sum_{k=1}^{N} V_k\big(s,t,\hat{\theta},\hat{\mu}_1(\cdot;z_{k1}),\hat{\mu}_2(\cdot;z_{k2})\big),$$

so that (A.35) can be rewritten as

$$\begin{aligned} &V\Big(s,t,\theta,\hat{\mu}_1(\cdot;Z_{k1}),\hat{\mu}_2(\cdot;Z_{k2})\Big) \\ &= N^{-1/2}\sum_{k=1}^{N}\big\{V_k(s,t,\theta,\mu_1(\cdot;Z_{k1}),\mu_2(\cdot;Z_{k2})) + \Upsilon_{k1}(s,t,\theta) + \Upsilon_{k2}(s,t,\theta)\big\} + o_p(1). \end{aligned} \tag{A.37}$$

Following the empirical approximation of $\sqrt{N}(\hat{\theta}-\theta)$ in equation (A.31),

$$\begin{aligned} &N^{-1/2}\frac{\partial V(s,t,\theta,\hat{\mu}_1(\cdot;Z_{k1}),\hat{\mu}_2(\cdot;Z_{k2}))}{\partial\theta}N^{1/2}(\hat{\theta}-\theta) \\ &= \Psi_\theta(s,t)\Big\{N^{-1/2}\{\mathcal{I}(\theta,\beta_1,\mu_{01}(\cdot),\beta_2,\mu_{02}(\cdot))\}^{-1}\sum_{k=1}^{N}W_k(\theta,\beta_1,\mu_{01}(\cdot),\beta_2,\mu_{02}(\cdot))\Big\} \\ &\quad + o_p(1) \\ &= N^{-1/2}\Psi_\theta(s,t)\{\mathcal{I}(\theta,\beta_1,\mu_{01}(\cdot),\beta_2,\mu_{02}(\cdot))\}^{-1}\sum_{k=1}^{N}\big\{h_{1,N}\xi_{k1}A_1^{-1} + g_{1,N,k} + h_{2,N}\xi_{k2}A_2^{-1} \\ &\quad + g_{2,N,k}\big\} + o_p(1), \end{aligned} \tag{A.38}$$

where $\Psi_\theta(s,t) = \lim_{N\to\infty} N^{-1/2}\frac{\partial\hat{V}(s,t,\theta)}{\partial\theta}$. We reform (A.38) as

$$N^{-1/2}\frac{\partial V\Big(s,t,\theta,\hat{\beta}_1,\hat{\mu}_{01}(\cdot),\hat{\beta}_2,\hat{\mu}_{02}(\cdot)\Big)}{\partial\theta}N^{1/2}(\hat{\theta}-\theta) = N^{-1/2}\{\zeta_{k1}(s,t,\theta)+\zeta_{k2}(s,t,\theta)\} \tag{A.39}$$

by letting

$$\zeta_{k1}(s,t,\theta) = \Psi_\theta(s,t)\{\mathcal{I}(\theta,\beta_1,\mu_{01}(\cdot),\beta_2,\mu_{02}(\cdot))\}^{-1}\Big\{h_{1,N}\xi_{k1}A_1^{-1} + g_{1,N,k}\Big\},$$
$$\zeta_{k2}(s,t,\theta) = \Psi_\theta(s,t)\{\mathcal{I}(\theta,\beta_1,\mu_{01}(\cdot),\beta_2,\mu_{02}(\cdot))\}^{-1}\Big\{h_{2,N}\xi_{k2}A_2^{-1} + g_{2,N,k}\Big\}. \quad \text{(A.40)}$$

Plugging (A.37) and (A.39) back into equation (3.25) gives us (3.26)

$$\begin{aligned} &V\Big(s,t,\hat{\theta},\hat{\mu}_1(\cdot;Z_{k1}),\hat{\mu}_2(\cdot;Z_{k2})\Big) \\ &= N^{-1/2}\sum_{k=1}^{N}\Big\{V_k(s,t,\theta,\mu_1(\cdot;Z_{k1}),\mu_2(\cdot;Z_{k2})) \\ &\quad + \Upsilon_{k1}(s,t,\theta) + \Upsilon_{k2}(s,t,\theta) + \zeta_{k1}(s,t,\theta) + \zeta_{k2}(s,t,\theta)\Big\} + o_p(1). \end{aligned}$$

□

APPENDIX D: THE PROOFS OF THEOREMS IN CHAPTER 4

Condition II.

In this section, we investigate the asymptotic properties of $\hat{\theta}^c$ under the independent censoring assumption and that the distribution functions of the censoring times are independent from covariates. Following regularity conditions in Lin et al. (2000):

(C*.1) $\{N_{kj}(\cdot), Y_{kj}(\cdot), Z_{kj}(\cdot)\}(k = 1, 2, ..., N;)(j = 1, 2)$ are independent and identically distributed;

(C*.2) $Pr(C_{kj} > \tau) > 0$, where τ is predetermined constant;

(C*.3)$N_{kj}(\tau)$ are bounded by a constant;

(C*.4)$Z_{kj}(\cdot)$ has bounded total variation, i.e. $|Z_{kjl}(0)| + \int_0 \tau |dZ_{kjl}(t)| \leq C_z$ for all $j = 1, 2$ and $k = 1, 2, ..., N$, where Z_{kjl} is the lth component of dZ_{kj} and C_z is a constant.

(C*.5) $A_j^c \equiv E\Big[\int_0^\tau \{Z_{kj}(u) - \bar{z}_j(\beta_j, u)\}^{\otimes 2} Y_{kj}(u) e^{\beta_j^T Z_{kj}(u)} \, d\mu_{0j}(u)\Big]$ is positive definite, where E is the expectation.

We summarize the asymptotic properties of $\hat{\beta}_j^c$ in the following theorem, where the subscription c denote that the estimator is derived when the marginal model is multiplicative.

Proof of Theorem 4.1

Adapting A.2 in Lin et al. (2000), the partial likelihood score function for β_j is $L_j(\beta_j, \tau)$, where

$$L_j^c(\beta_j, \tau) = \sum_{k=1}^{N} \int_0^\tau \{Z_{kj}(u) - \tilde{Z}_j(\beta_j, u)\} \, dM_{kj}^c(u; \beta_j),$$

with $M_{kj}^c(t; \beta_j) = N_{kj}(t) - \int_0^t Y_{kj}(u) e^{\beta_j^T Z_{kj}(u)}$.

It is shown that $N^{-1/2}L_j^c(\beta_j, t)(0 \leq t \leq \tau)$ converges weakly to a continuous zero-mean Gaussian process with covariance function

$$\Sigma_j^c(s,t) = E[\int_0^s \{Z_{1j}(u) - \tilde{z}_j(\beta_j, u)\} dM_{1j}^c(u) \int_0^t \{Z_{1j}(v) - \tilde{z}_j(\beta_j, v)\} \, dM_{1j}^c(v)],$$

$$0 \leq s, t \leq \tau,$$

between time points s and t.

By Taylor series expansion,

$$\sqrt{N}(\tilde{\beta}_j - \beta_j) = \tilde{A}_j^{-1}(\beta^*) N^{-1/2} \sum_{k=1}^{N} \{Z_{kj}(u) - \tilde{Z}_j(\beta_j, u)\} \, dM_{kj}^c(u), \tag{A.41}$$

where $\tilde{A}_j(\beta_j) = -N^{-1}\partial L_j^c(\beta_j, \tau)/\partial\beta_j$, and β^* is on the line segment between $\tilde{\beta}_j$ and β_j, with $\tilde{\beta}_j$ is the solution to $L_j^c(\beta_j, \tau) = 0$.

The almost sure convergence of $\tilde{\beta}_j$ and $\tilde{A}_j(\beta_j)$ for β_j and A_j^c imply that $\sqrt{N}(\tilde{\beta}_j - \beta_j)$ converges in distribution to a mean-zero normal random vector with covariance matrix $(A_j^c)^{-1}\Sigma_j^c(A_j^c)^{-1}$ and $\Sigma_j^c = \Sigma_j^c(\tau, \tau)$. For future reference, we denote the asymptotic approximation as

$$\sqrt{N}(\tilde{\beta}_j - \beta_j) = (A_j^c)^{-1} N^{-1/2} \sum_{k=1}^{N} \xi_{kj}^c(u; \beta_j) + o_p(1). \tag{A.42}$$

where

$$\xi_{kj}^c(u; \beta_j) = \int_0^\tau \{Z_{kj}(u) - \tilde{z}_j(u; \beta_j)\} \, dM_{kj}^c(u; \beta_j).$$

The consistency estimators of A_j and Σ_j are denoted by

$$\tilde{A}_j = N^{-1} \int_0^\tau \{Z_{kj}(u) - \tilde{Z}_j(\tilde{\beta}_j, u)\}^{\otimes 2} Y_{kj}(u) e^{\tilde{\beta}_j^T Z_{kj}(u)} \, d\tilde{\mu}_{0j}(u),$$
$$\tilde{\Sigma}_j = N^{-1} \sum_{k=1}^{N} \tilde{\xi}_{kj}^{\otimes 2},$$

with

$$\tilde{\xi}_{kj} = N^{-1} \sum_{k=1}^{N} \int_0^\tau \{Z_{kj}(u) - \tilde{Z}_{kj}(u, \tilde{\beta}_j)\} \, d\tilde{M}_{kj}(u; \tilde{\beta}_j),$$
$$\tilde{M}_{kj}(t; \tilde{\beta}_j) = N_{kj}(t) - \int_0^t Y_{kj}(u) e^{\tilde{\beta}_j^T Z_{kj}(u)} \, d\tilde{\mu}_{0j}(u). \tag{A.43}$$

□

Proof of Theorem 4.2

Let $\tilde{\mu}_{0j}(t) \equiv \tilde{\mu}_{0j}(t, \tilde{\beta}_j) = \int_0^t \frac{d\bar{N}_j(u)}{NS_j^0(u,\tilde{\beta}_j)}$ and decompose $\tilde{\mu}_{0j}(t)$ as

$$\tilde{\mu}_{0j}(t) - \mu_{0j}(t) = \big\{\tilde{\mu}_{0j}(t, \tilde{\beta}_j) - \tilde{\mu}_{0j}(t, \beta_j)\big\} + \big\{\tilde{\mu}_{0j}(t, \beta_j) - \mu_{0j}(t)\big\}. \tag{A.44}$$

The uniform strong law of large numbers (Pollard, 1990) implies $S_j^0(\beta_j, t) \to s_j^0(\beta_j, t)$ and $\bar{N}_j(t)/N \to E[N_j(t)]$ uniformly in t and β_j, and hence the uniform convergence of $\tilde{\mu}_{0j}(t, \beta_j) = \int_0^t \frac{d\bar{N}_j(u)}{NS_j^0(u,\beta_j)}$ to $\mu_{0j}(t) = \int_0^t \frac{s_j^0(u,\beta_j)}{s_j^0(u,\beta_j)} d\mu_{0j}(u)$. Furthermore, we can represent the second term in (A.44) as

$$\begin{aligned}
\tilde{\mu}_{0j}(t, \beta_j) - \mu_{0j}(t) &= \int_0^t \frac{d\bar{N}_j(u)}{NS_j^0(u, \beta_j)} - d\mu_{0j}(u) \\
&= N^{-1} \int_0^t \frac{\sum_{k=1}^N dM_{kj}^c(u; \beta_j)}{S_j^0(u, \beta_j)}, \\
&= N^{-1} \int_0^t \frac{\sum_{k=1}^N dM_{kj}^c(u; \beta_j)}{s_j^0(u, \beta_j)} + o_p(N^{-1}).
\end{aligned} \tag{A.45}$$

The first term in (A.44) can be rewritten as

$$\begin{aligned}
\tilde{\mu}_{0j}(t, \tilde{\beta}_j) - \tilde{\mu}_{0j}(t, \beta_j) &= \int_0^t \frac{d\bar{N}_j(u)}{NS_j^0(u, \tilde{\beta}_j)} - \frac{d\bar{N}_j(u)}{NS_j^0(u, \beta_j)}, \\
&= \int_0^t -\tilde{Z}_j^T(u, \beta_j) \frac{d\bar{N}_j(u)}{NS_j^0(u, \beta_j)} (\tilde{\beta}_j - \beta_j) + o_p(N^{-1}), \\
&= -\int_0^t \tilde{z}_j(u, \beta_j)\, d\mu_{0j}(t, \beta_j)(\tilde{\beta}_j - \beta_j) + o_p(N^{-1}).
\end{aligned}$$

The asymptotic approximation of $\{\tilde{\beta}_j - \beta_j\}$ in (A.42) entails

$$\begin{aligned}
&\tilde{\mu}_{0j}(t, \tilde{\beta}_j) - \tilde{\mu}_{0j}(t, \beta_j) \\
&= [H^c(t; \beta_j)]^T (A_j^c)^{-1} N^{-1} \sum_{k=1}^N \int_0^\tau \{Z_{kj}(u) - \tilde{z}_j(u, \beta_j)\}\, dM_{kj}^c(u; \beta_j) + o_p(N^{-1}),
\end{aligned} \tag{A.46}$$

with $H^c(t;\beta_j) = \int_0^t \tilde{z}_j(u,\beta_j)\, d\mu_{0j}(u,\beta_j)$. Plugging (A.46), (A.45) into equation (A.44) and multiplying both sides by $\sqrt{N}$ yield

$$\sqrt{N}\Big\{\tilde{\mu}_{0j}(t) - \mu_{0j}(t)\Big\} = N^{-1/2}\sum_{k=1}^{N}\phi_{kj}^c(t;\beta_j) + o_p(1), \tag{A.47}$$

where

$$\begin{aligned}&\phi_{kj}^c(t;\beta_j)\\ &= \int_0^t \frac{dM_{kj}^c(u;\beta_j)}{s_j^0(u,\beta_j)} - [H^c(t;\beta_j)]^T(A_j^c)^{-1}\sum_{k=1}^{N}\int_0^\tau \{Z_{kj}(u) - \tilde{z}_j(u,\beta_j)\}\, dM_{kj}^c(u;\beta_j).\end{aligned} \tag{A.48}$$

Since $\phi_{kj}(t)$ is independent mean-zero normal random variable, $\sqrt{N}\Big\{\hat{\mu}_{0j}(t) - \mu_{0j}(t)\Big\}$ converges to a zero-mean Gaussian process with covariance function at (s,t) as

$$\Gamma_j(s,t) \equiv E[\phi_{kj}^c(s;\beta_j)\phi_{kj}^c(t;\beta_j)], \tag{A.49}$$

which can be approached by its consistent estimator

$$\tilde{\Gamma}_j(s,t) = N^{-1}\sum_{k=1}^{N}\tilde{\phi}_{kj}(s;\beta_j)\tilde{\phi}_{kj}(t;\beta_j),$$

where

$$\tilde{\phi}_{kj}(t) = \int_0^t \frac{d\tilde{M}_{kj}(u)}{S_j^0(\tilde{\beta}_j,u)} - [\tilde{H}(t)]^T\tilde{A}_j^{-1}\sum_{k=1}^{N}\int_0^\tau \{Z_{kj}(u) - \tilde{Z}_{kj}(u,\tilde{\beta}_j)\}\, d\tilde{M}_{kj}(u;\tilde{\beta}_j),$$

and

$$\tilde{H}(t) = \int_0^t \tilde{Z}_j(u,\tilde{\beta}_j)\, d\tilde{\mu}_{0j}(t,\tilde{\beta}_j). \tag{A.50}$$

□

Proof of Theorem 4.3

Considering the decomposition:

$$
\begin{aligned}
&U_k^c(\theta, \tilde{\beta}_1, \tilde{\mu}_{01}(\cdot), \tilde{\beta}_2, \tilde{\mu}_{02}(\cdot)) - U_k(\theta, \beta_1, \mu_{01}(\cdot), \beta_2, \mu_{02}(\cdot)) \\
&= \Big\{ U_k(\theta, \tilde{\beta}_1, \tilde{\mu}_{01}(s), \tilde{\beta}_2, \tilde{\mu}_{02}(\cdot)) - U_k(\theta, \beta_1, \mu_{01}(\cdot), \tilde{\beta}_2, d\tilde{\mu}_{02}(t)) \Big\} \\
&\quad + \Big\{ U_k(\theta, \beta_1, \mu_{01}(\cdot), \tilde{\beta}_2, \tilde{\mu}_{02}(\cdot)) - U_k(\theta, \beta_1, \mu_{01}(\cdot), \beta_2, \mu_{02}(\cdot)) \Big\} \qquad \text{(A.51)}
\end{aligned}
$$

The first term on the right hand side of (A.51) is equivalent to

$$
\begin{aligned}
&\int_0^\tau \int_0^\tau -\rho(\theta, s, t) \frac{\partial \rho(\theta, s, t)}{\partial \theta} Y_{k2}(t) e^{\tilde{\beta}_2^T Z_{k2}(t)} \, d\tilde{\mu}_{02}(t) \\
&\Big\{ Y_{k1}(s) e^{\tilde{\beta}_1^T Z_{k1}(s)} \, d\tilde{\mu}_{01}(s) - Y_{k1}(s) e^{\beta_1^T Z_{k1}(s)} \, d\mu_{01}(s) \Big\} \qquad \text{(A.52)}
\end{aligned}
$$

In (A.52), $Y_{k1}(s) e^{\tilde{\beta}_1^T Z_{k1}(s)} \, d\tilde{\mu}_{01}(s) - Y_{k1}(s) e^{\beta_1^T Z_{k1}(s)} \, d\mu_{01}(s)$ can be further rewritten as

$$
\begin{aligned}
&Y_{k1}(s) \Big\{ e^{\tilde{\beta}_1^T Z_{k1}(s)} \, d\tilde{\mu}_{01}(s) - e^{\beta_1^T Z_{k1}(s)} \, d\tilde{\mu}_{01}(s) + e^{\beta_1^T Z_{k1}(s)} \, d\tilde{\mu}_{01}(s) - e^{\beta_1^T Z_{k1}(s)} \, d\mu_{01}(s) \Big\} \\
&= Y_{k1}(s) \Big\{ e^{\beta_1^T Z_{k1}(s)} Z_{k1}^T(s) \, d\tilde{\mu}_{01}(s) (\hat{\beta}_1 - \beta_1) + e^{\beta_1^T Z_{k1}} (d\tilde{\mu}_{01}(s) - d\mu_{01}(s)) \Big\} \\
&\quad + o_p(\tilde{\beta}_1 - \beta_1)^{\otimes 2}
\end{aligned}
$$

Applying the asymptotic properties of the first-stage estimators from (A.42) and (A.47) gives

$$
\begin{aligned}
&Y_{k1}(s) e^{\tilde{\beta}_1^T Z_{k1}(s)} \, d\tilde{\mu}_{01}(s) - Y_{k1}(s) e^{\beta_1^T Z_{k1}(s)} \, d\mu_{01}(s) \\
&= Y_{k1}(s) \Big\{ e^{\beta_1^T Z_{k1}(s)} Z_{k1}^T(s) \, d\mu_{01}(s) (A_1^c)^{-1} N^{-1} \sum_{l=1}^{N} \xi_{l1}^c + e^{\beta_1^T Z_{k1}(s)} N^{-1} \sum_{l=1}^{N} d\phi_{l1}^c(s) \Big\} \\
&\quad + o_p(N^{-1}). \qquad \text{(A.53)}
\end{aligned}
$$

By Combining (A.52) (A.53), and (A.55) we have

$$\begin{aligned}
&\Big\{U_k^c(\theta,\tilde{\beta}_1,\tilde{\mu}_{01}(s),\tilde{\beta}_2,\tilde{\mu}_{02}(\cdot)) - U_k^c(\theta,\beta_1,\mu_{01}(\cdot),\tilde{\beta}_2,d\tilde{\mu}_{02}(t))\Big\} \\
&= \int_0^\tau \int_0^\tau -\rho(\theta,s,t)\frac{\partial\rho(\theta,s,t)}{\partial\theta} Y_{k1}(s)e^{\beta_1^T Z_{k1}(s)} \cdot Y_{k2}(t)e^{\beta_2^T Z_{k2}(t)} \\
&\quad \cdot N^{-1}\sum_{l=1}^{N}\Big\{Z_{k1}^T(s)\,d\mu_{01}(s)\,d\mu_{02}(t)A_1^{-1}\xi_{l1}^c + d\phi_{l1}^c(s)\,d\mu_{02}(t)\Big\} + o_p(1) \qquad \text{(A.54)}
\end{aligned}$$

In a similar fashion,

$$\begin{aligned}
&Y_{k2}(t)e^{\tilde{\beta}_2^T Z_{k2}(t)}\,d\tilde{\mu}_{02}(t) - Y_{k2}(t)e^{\beta_2^T Z_{k2}(t)}\,d\mu_{02}(t) \\
&= Y_{k2}(t)\{e^{\beta_2^T Z_{k2}(t)}Z_{k2}^T(t)\,d\mu_{02}(t)(A_2^c)^{-1}N^{-1}\sum_{l=1}^{N}\xi_{l2}^c + e^{\beta_2^T Z_{k2}(t)}N^{-1}\sum_{l=1}^{N}d\phi_{l2}^c(t)\} \\
&\quad + o_p(N^{-1}). \qquad \text{(A.55)}
\end{aligned}$$

Since the $Y_{k2}(t)e^{\tilde{\beta}_2^T Z_{k2}(t)}\,d\tilde{\mu}_{02}(t)$ and $Y_{k1}(s)e^{\tilde{\beta}_1^T Z_{k1}(s)}\,d\tilde{\mu}_{01}(s)$ only have $o_p(N^{-1})$ difference compared to their true values, the product term has negligible difference of even higher orders.

The second part of (A.51) via a similar technique can be proved as

$$\begin{aligned}
&\Big\{U_k^c(\theta,\beta_1,d\mu_{01}(s),\tilde{\beta}_2,d\tilde{\mu}_{02}(t)) - U_k^c(\theta,\beta_1,d\mu_{01}(s),\beta_2,d\mu_{02}(t))\Big\} \\
&= \int_0^\tau \int_0^\tau -\rho(\theta,s,t)\frac{\partial\rho(\theta,s,t)}{\partial\theta} Y_{k1}(s)e^{\beta_1^T Z_{k1}(s)} \cdot Y_{k2}(t)e^{\beta_2^T Z_{k2}(t)} \\
&\quad \cdot N^{-1}\sum_{l=1}^{N}\Big\{Z_{k2}^T(t)\,d\mu_{01}(s)\,d\mu_{02}(t)(A_2^c)^{-1}\xi_{l2}^c + e^{\beta_2^T Z_{l2}(t)}\,d\mu_{01}(s)\,d\phi_{l2}^c(t)\Big\} + o_p(1)
\end{aligned} \qquad \text{(A.56)}$$

Since

$$
\begin{aligned}
&U^c(\theta, \tilde{\beta}_1, \tilde{\mu}_{01}(\cdot), \tilde{\beta}_2, \tilde{\mu}_{02}(\cdot)) - U^c(\theta, \beta_1, \mu_{01}(\cdot), \beta_2, \mu_{02}(\cdot)) \\
&= \sum_{k=1}^{N} \Big\{ U_k^c(\theta, \tilde{\beta}_1, \tilde{\mu}_{01}(\cdot), \tilde{\beta}_2, \tilde{\mu}_{02}(\cdot)) - U_k^c(\theta, \beta_1, \mu_{01}(\cdot), \beta_2, \mu_{02}(\cdot)) \Big\}
\end{aligned}
$$

by exchanging the order of the double summations, as well as switching the notations between l and k, it can be shown that

$$
\begin{aligned}
&N^{-1/2}\{U^c(\theta, \tilde{\beta}_1, \tilde{\mu}_{01}(s), \tilde{\beta}_2, \tilde{\mu}_{02}(t)) - U^c(\theta, \beta_1, \mu_{01}(\cdot), \beta_2, \mu_{02}(\cdot))\} \\
&= N^{-1/2} \sum_{k=1}^{N} \Big\{ h_{1,N}^c (A_1^c)^{-1} \xi_{k1}^c + g_{1,N}^c + h_{2,N} (A_2^c)^{-1} \xi_{k2}^c + g_{2,N}^c \Big\} + o_p(1). \qquad \text{(A.57)}
\end{aligned}
$$

where

$$
\begin{aligned}
q_l^c(\theta, s, t) &= -\rho(\theta, s, t) \frac{\partial \rho(\theta, s, t)}{\partial \theta} Y_{l1}(s) e^{\beta_1^T Z_{l1}(s)} Y_{l2}(t) e^{\beta_2^T Z_{l2}(t)}, \\
h_{1,N}^c &= N^{-1} \sum_{l=1}^{N} \int_0^\tau \int_0^\tau q_l^c(\theta, s, t) Z_{l1}^T(s)\, d\mu_{01}(s) d\mu_{02}(t), \\
g_{1,N}^c &= N^{-1} \sum_{l=1}^{N} \int_0^\tau \int_0^\tau q_l^c(\theta, s, t)\, d\mu_{02}(t)\, d\phi_{k1}^c(s), \\
h_{2,N}^c &= N^{-1} \sum_{l=1}^{N} \int_0^\tau \int_0^\tau q_l^c(\theta, s, t) Z_{l2}^T(t)\, d\mu_{02}(t) d\mu_{01}(s), \\
g_{2,N}^c &= N^{-1} \sum_{l=1}^{N} \int_0^\tau \int_0^\tau q_l^c(\theta, s, t) d\mu_{01}(s)\, d\phi_{k2}^c(t). \qquad \text{(A.58)}
\end{aligned}
$$

□

Proof of Theorem 4.4

By the first order Taylor expansion of the estimation equation,

$$\begin{aligned}
&\sqrt{N}(\tilde{\theta}-\theta) \\
&= \{-N^{-1}\frac{\partial U^c(\theta,\beta_1,d\mu_{01}(\cdot),\beta_2,d\mu_{02}(\cdot))}{\partial\theta}\}^{-1}N^{-1/2}U^c(\theta,\hat{\beta}_1,\hat{\mu}_{01}(\cdot),\hat{\beta}_2,\hat{\mu}_{02}(\cdot)) \\
&\quad + o_p(N^{-1/2})
\end{aligned} \tag{A.59}$$

Denote

$$\mathcal{I}^c(\theta,\beta_1,\mu_{01}(\cdot),\beta_2,\mu_{02}(\cdot)) = -N^{-1}\sum_{k=1}^{N}\big(\frac{\partial U_k^c(\theta,\beta_1,\mu_{01}(\cdot),\beta_2,\mu_{02}(\cdot))}{\partial\theta}\big)^T \tag{A.60}$$

and applying (A.57) and (A.60), (A.59) can be rewritten as

$$\begin{aligned}
&\sqrt{N}(\tilde{\theta}-\theta) \\
&= N^{-1/2}\{\mathcal{I}^c(\theta,\beta_1,\mu_{01}(\cdot),\beta_2,\mu_{02}(\cdot))\}^{-1}\sum_{k=1}^{N}W_k^c(\theta,\beta_1,\mu_{01}(\cdot),\beta_2,\mu_{02}(\cdot)) + o_p(1),
\end{aligned} \tag{A.61}$$

where

$$\begin{aligned}
&W_k^c(\theta,\beta_1,\mu_{01}(\cdot),\beta_2,\mu_{02}(\cdot)) \\
&= \Big\{U_k^c(\theta,\beta_1,\mu_{01}(\cdot),\beta_2,\mu_{02}(\cdot)) + h_{1,N}^c(A_1^c)^{-1}\xi_{k1}^c + g_{1,N}^c + h_{2,N}^c(A_2^c)^{-1}\xi_{k2}^c + g_{2,N}^c\Big\}.
\end{aligned} \tag{A.62}$$

By the central limit theorem that $\sqrt{N}(\tilde{\theta}-\theta)$ is asymptotically normal with mean zero and variance Φ that can be approximated by $\tilde{\Phi} = N^{-1}\tilde{\mathcal{I}}^{-1}(\sum_{k=1}^{N}\tilde{W}_k^{\otimes 2})(\tilde{\mathcal{I}}^T)^{-1}$, where $\tilde{\mathcal{I}}$ and $\tilde{W}_k$ are the empirical counterparts of

$$\mathcal{I}^c(\theta,\beta_1,\mu_{01}(\cdot),\beta_2,\mu_{02}(\cdot))$$

and

$$W_k^c(\theta, \beta_1, \mu_{01}(\cdot), \beta_2, \mu_{02}(\cdot))$$

respectively, which are obtained by replacing θ, β_1, $\mu_{01}(\cdot)$, β_1, $\mu_{02}(\cdot)$ in equations (A.62) and (A.60) with their estimates $\tilde{\theta}$, $\tilde{\beta}_1$, $\tilde{\mu}_{01}(\cdot)$, $\tilde{\beta}_1$, $\tilde{\mu}_{02}(\cdot)$.

□

APPENDIX E: PROOFS OF THE MODEL CHECKING PROCEDURE IN CHAPTER 4

Recall (4.24)

$$
\begin{aligned}
&V^c(s,t,\tilde{\theta},\hat{\mu}_1(\cdot;Z_{k1}),\hat{\mu}_2(\cdot;Z_{k2}))\\
&= V^c\Big(s,t,\theta,\hat{\mu}_1(\cdot;Z_{k1}),\hat{\mu}_2(\cdot;Z_{k2})\Big)\\
&\quad + N^{-1/2}\frac{\partial V^c\Big(s,t,\theta,\hat{\mu}_1(\cdot;Z_{k1}),\hat{\mu}_2(\cdot;Z_{k2})\Big)}{\partial\theta}N^{1/2}(\tilde{\theta}-\theta)+o_p(1)
\end{aligned}
\tag{A.63}
$$

We decompose $V^c\Big(s,t,\theta,\hat{\mu}_1(\cdot;Z_{k1}),\hat{\mu}_2(\cdot;Z_{k2})\Big)$ by letting

$$
\begin{aligned}
&V^c\Big(s,t,\theta,\hat{\mu}_1(\cdot;Z_{k1}),\hat{\mu}_2(\cdot;Z_{k2})\Big)\\
&= V^c\Big(s,t,\theta,\mu_1(\cdot;Z_{k1}),\mu_2(\cdot;Z_{k2})\Big)\\
&\quad + V^c\Big(s,t,\theta,\hat{\mu}_1(\cdot;Z_{k1}),\hat{\mu}_2(\cdot;Z_{k2})\Big) - V^c\Big(s,t,\theta,\mu_1(\cdot;Z_{k1}),\hat{\mu}_2(\cdot;Z_{k2})\Big)\\
&\quad + V^c\Big(s,t,\theta,\mu_1(\cdot;Z_{k1}),\hat{\mu}_2(\cdot;Z_{k2})\Big) - V^c\Big(s,t,\theta,\mu_1(\cdot;Z_{k1}),\mu_2(\cdot;Z_{k2})\Big).
\end{aligned}
\tag{A.64}
$$

By definition in equation (4.21), the first term on the right hand side of equation A.64 can be written as

$$
V^c\Big(s,t,\theta,\mu_1(\cdot;Z_{k1}),\mu_2(\cdot;Z_{k2})\Big)=\sum_{k=1}^{N}V_k^c\Big(s,t,\theta,\mu_1(\cdot;Z_{k1}),\mu_2(\cdot;Z_{k2})\Big)
\tag{A.65}
$$

with

$$
\begin{aligned}
&V_k^c(s,t,\tilde{\theta},\hat{\mu}_1(\cdot;z_{k1}),\hat{\mu}_2(\cdot;z_{k2}))\\
&=\int_0^t\int_0^s\frac{\partial\rho(u,v,\theta)}{\partial\theta}\Big|_{\theta=\tilde{\theta}}\Big\{\,dN_{k1}(u)dN_{k2}(v)\\
&-\rho(u,v,\tilde{\theta})Y_{k1}(u)d\mu_{01}(u)e^{\beta_1^TZ_{k1}(u)}\cdot Y_{k2}(v)d\mu_{02}(v)e^{\beta_2^TZ_{k2}(v)}\Big\}.
\end{aligned}
$$

The second term on the right hand side of equation (A.32), analogous to equation (A.54) follows

$$\begin{aligned}
&\sqrt{N}\Big\{V^c\Big(s,t,\theta,\hat{\mu}_1(\cdot;Z_{k1}),\hat{\mu}_2(\cdot;Z_{k2})\Big)-V^c\Big(s,t,\theta,\mu_1(\cdot;Z_{k1}),\hat{\mu}_2(\cdot;Z_{k2})\Big)\Big\}\\
&=\sum_{k=1}^{N}\int_0^t\int_0^s -\frac{\partial\rho(u,v,\theta;Z_{k1},Z_{k2})}{\theta}\rho(u,v,\theta;Z_{k1},Z_{k2})Y_{k1}(s)e^{\beta_1^T Z_{k1}(s)}\cdot Y_{k2}(t)e^{\beta_2^T Z_{k2}(t)}\\
&\quad\cdot N^{-1}\sum_{l=1}^{N}\Big\{Z_{k1}^T(s)\,d\mu_{01}(s)\,d\mu_{02}(t)(A_1^c)^{-1}\xi_{l1}^c+\,d\phi_{l1}^c(s)\,d\mu_{02}(t)\Big\}+o_p(1),
\end{aligned}\tag{A.66}$$

and the last term in equation (A.64) has the expansion below

$$\begin{aligned}
&\sqrt{N}\Big\{V^c\Big(\theta,\hat{\mu}_1(\cdot;Z_{k1}),\hat{\mu}_2(\cdot;Z_{k2})\Big)-V^c\Big(\theta,\hat{\mu}_1(\cdot;Z_{k1}),\mu_2(\cdot;Z_{k2})\Big)\Big\}\\
&=\sum_{k=1}^{N}\int_0^t\int_0^s -\frac{\partial\rho(\theta,s,t;Z_{k1},Z_{k2})}{\partial\theta}\rho(\theta,s,t;Z_{k1},Z_{k2})Y_{k1}(s)e^{\beta_1^T Z_{k1}(s)}\cdot Y_{k2}(t)e^{\beta_2^T Z_{k2}(t)}\\
&\quad\cdot N^{-1}\sum_{l=1}^{N}\Big\{Z_{k2}^T(t)\,d\mu_{01}(s)\,d\mu_{02}(t)(A_2^c)^{-1}\xi_{l2}^c+e^{\beta_2^T Z_{l2}(t)}\,d\mu_{01}(s)\,d\phi_{l2}^c(t)\Big\}+o_p(1).
\end{aligned}\tag{A.67}$$

Combining (A.66) and (A.67) together gives us the i.i.d summation form of equation (A.64) as

$$\begin{aligned}
&V^c\Big(s,t,\theta,\hat{\mu}_1(\cdot;Z_{k1}),\hat{\mu}_2(\cdot;Z_{k2})\Big)\\
&=N^{-1/2}\sum_{k=1}^{N}\Big\{V_k^c\Big(s,t,\theta,\mu_1(\cdot;Z_{k1}),\mu_2(\cdot;Z_{k2})\Big)\\
&\quad+h_{1,N}^c(s,t)\xi_{k1}^c(A_1^c)^{-1}+g_{1,N,k}^c(s,t)+h_{2,N}^c(s,t)\xi_{k2}^c(A_2^c)^{-1}+g_{2,N,k}^c(s,t)\Big\},\\
&\quad+o_p(N^{-1})
\end{aligned}\tag{A.68}$$

where

$$
\begin{aligned}
q_l^c(u,v) &= -\rho(\theta,u,v)\frac{\partial\rho(\theta,u,v)}{\partial\theta}Y_{l1}(u)e^{\beta_1^T Z_{l1}(u)}Y_{l2}(v)e^{\beta_2^T Z_{l2}(v)},\\
h_{1,N}^c(s,t) &= N^{-1}\sum_{l=1}^{N}\int_0^t\int_0^s q_l^c(\theta,u,v)Z_{l1}^T(u)\,d\mu_{01}(u)d\mu_{02}(v),\\
g_{1,N,k}^c(s,t) &= N^{-1}\sum_{l=1}^{N}\int_0^t\int_0^s q_l^c(\theta,s,t)\,d\mu_{02}(t)\,d\phi_{k1}^c(s),\\
h_{2,N}^c(,s,t) &= N^{-1}\sum_{l=1}^{N}\int_0^t\int_0^s q_l^c(\theta,s,t)Z_{l2}^T(t)\,d\mu_{02}(t)d\mu_{01}(s),\\
g_{2,N,k}^c(s,t) &= N^{-1}\sum_{l=1}^{N}\int_0^t\int_0^s q_l^c(\theta,s,t)d\mu_{01}(s)\,d\phi_{k2}^c(t).
\end{aligned}
\tag{A.69}
$$

To simplify the notation, we define

$$
\begin{aligned}
\Upsilon_{k1}^c(s,t,\theta) &= \Big\{h_{1,N}^c(s,t)\xi_{k1}^c(A_1^c)^{-1} + g_{1,N,k}^c(s,t)\Big\} + o_p(N^{-1}),\\
\Upsilon_{k2}^c(s,t,\theta) &= \Big\{h_{2,N}^c(s,t)\xi_{k2}^c(A_2^c)^{-1} + g_{2,N,k}^c(s,t)\Big\} + o_p(N^{-1}),
\end{aligned}
$$

so that (A.68) can be rewritten as

$$
\begin{aligned}
&V^c\Big(s,t,\theta,\hat\mu_1(\cdot;Z_{k1}),\hat\mu_2(\cdot;Z_{k2})\Big)\\
&= N^{-1/2}\sum_{k=1}^{N}\big\{V_k^c(s,t,\theta,\mu_1(\cdot;Z_{k1}),\mu_2(\cdot;Z_{k2})) + \Upsilon_{k1}^c(s,t,\theta) + \Upsilon_{k2}^c(s,t,\theta)\big\} + o_p(1).
\end{aligned}
\tag{A.70}
$$

Following the empirical approximation of $\sqrt{N}(\tilde\theta-\theta)$ in equation (4.13),

$$
\begin{aligned}
&N^{-1/2}\frac{\partial V^c(s,t,\theta,\hat\mu_1(\cdot;Z_{k1}),\hat\mu_2(\cdot;Z_{k2}))}{\partial\theta}N^{1/2}(\tilde\theta-\theta)\\
&= \Psi_\theta^c(s,t)\Big\{N^{-1/2}\{\mathcal{I}^c(\theta,\beta_1,\mu_{01}(\cdot),\beta_2,\mu_{02}(\cdot))\}^{-1}\sum_{k=1}^{N}W_k^c(\theta,\beta_1,\mu_{01}(\cdot),\beta_2,\mu_{02}(\cdot))\Big\}\\
&\quad + o_p(1),
\end{aligned}
\tag{A.71}
$$

where $\Psi^c_\theta(s,t) = \lim_{N\to\infty} N^{-1/2}\frac{\partial V^c(s,t,\theta)}{\partial\theta}$. We reform equation (A.71) as

$$N^{-1/2}\frac{\partial V^c\Big(s,t,\theta,\hat{\beta}_1,\hat{\mu}_{01}(\cdot),\hat{\beta}_2,\hat{\mu}_{02}(\cdot)\Big)}{\partial\theta}N^{1/2}(\tilde{\theta}-\theta) = N^{-1/2}\{\zeta^c_{k1}(s,t,\theta)+\zeta^c_{k2}(s,t,\theta)\} \tag{A.72}$$

where

$$\begin{aligned}
\zeta^c_{k1}(s,t,\theta) &= \Psi^c_\theta(s,t)\{\mathcal{I}^c(\theta,\beta_1,\mu_{01}(\cdot),\beta_2,\mu_{02}(\cdot))\}^{-1}\Big\{h_{1,N}\xi^c_{k1}(A^c_1)^{-1}+g^c_{1,N,k}\Big\},\\
\zeta^c_{k2}(s,t,\theta) &= \Psi^c_\theta(s,t)\{\mathcal{I}^c(\theta,\beta_1,\mu_{01}(\cdot),\beta_2,\mu_{02}(\cdot))\}^{-1}\Big\{h^c_{2,N}\xi_{k2}(A^c_2)^{-1}+g^c_{2,N,k}\Big\}.
\end{aligned} \tag{A.73}$$

Substituting (A.70) and (A.72) back into equation (A.64) gives us (4.26)

$$\begin{aligned}
&V^c\Big(s,t,\tilde{\theta},\hat{\mu}_1(\cdot;Z_{k1}),\hat{\mu}_2(\cdot;Z_{k2})\Big)\\
&= N^{-1/2}\sum_{k=1}^{N}\Big\{V^c_k(s,t,\theta,\mu_1(\cdot;Z_{k1}),\mu_2(\cdot;Z_{k2}))\\
&\quad+\Upsilon^c_{k1}(s,t,\theta)+\Upsilon^c_{k2}(s,t,\theta)+\zeta^c_{k1}(s,t,\theta)+\zeta^c_{k2}(s,t,\theta)\Big\}+o_p(1).
\end{aligned}$$

□